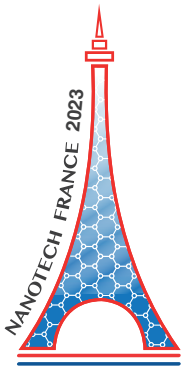

NanoMatEn 2023

NanoMetrology 2023

GAMS 2023

NANOTECH FRANCE \ NANOMATEN \ GAMS \ NANOMETROLOGY 2023 INTERNATIONAL JOINT CONFERENCES

28 - 30 June 2023, Paris , France

Book of Abstracts

Organizer

SETCOR
Conferences & Exhibitions

Nanotech France 2023 / NanoMatEn 2023 / NanoMetrology 2023 / GAMS 2023
Joint Conferences Program
28 - 30 June 2023, Paris, France

June 28, 2023		
08:00 - 12:00	**Onsite Participant registration**	
08:00 - 10:30	**Morning Coffee Break**	
Nanotech / GAMS Joint Plenary session		
Amphithéâtre		
Session's Chairs: **Prof. Pablo Taboada Antelo, University of Santiago de Compostela, Spain** **Prof. Rodrigo Ferrão de Paiva Martins, Nova Univ. of Lisbon, Portugal**		
10:30 - 11:00	Bio-nano-technologies for cardiac regenerative medicine **C. Giachino**, R. Rastaldo, D. Rossin, S. Perveen, R. Vanni, D. Fusco, A. Marsano, R. Pires, R. Reis, N. Barbani and C. Cristallini	**Prof. Claudia Giachino**, University of Torino, **Italy**
11:00 - 11:30	Stability of fibrillated nanocellulose suspension in the presence of AgNPs, AuNPs, Rhamnolipid and inorganic surfactants **Z. Sadowski** and A. Wirwis	**Prof. Zygmunt Sadowski**, Wroclaw University of Science and Technology, **Poland**
11:30- 11:45	Laser ablation synthesis of fresh Te nanoparticles for MALDI MS applications **K. Novotný**, I. Krempl, L. Pečinka, P. Vaňhara and J. Havel	**Prof. Karel Novotný**, Masaryk University, **Czech Rep**
11:45 - 12:00	Facile Fabrication of Reduced Graphene Oxide-Carbon Nanotubes-Silicon Composites for High Current Density Anode Materials **H.D. Jang**, S.K. Kim and K.M. Roh	**Prof. Hee Dong Jang**, Korea Institute of Geoscience & Mineral Resources, **Rep. of Korea.**
12:00 - 14:00	**Lunch Break**	
Nanotech / GAMS Joint Session I.A: **Nanomaterials Fabrication / Synthesis / properties**		
Amphithéâtre		
Session's Chairs: **Prof. Karel Novotný, Masaryk University, Czech Rep** **Prof. Zygmunt Sadowski, Wroclaw University of Science and Technology, Poland**		
14:00 - 14:30	An enhanced generation of singlet oxygen through the use of Au bi-pyramids/SiO2 core-shell nanoparticles for photocatalysis C. Mendoza, D. Chateau, A. Desert, C.A. Páez, N.Emmanuel, L. Khrouz, C. Monnereau, L. Dreesen, J-C. M. Monbaliu, S. Parola and **B. Heinrichs**	**Prof. Benoit Heinrichs**, University Liège, **Belgium**
14:30 – 15:00	Piezoelectric III-Nitride nanowires based energy harvesters: Towards the development of wireless micro-devices **N. Gogneau**	**Dr. Noelle Gogneau**, Paris Saclay University, **France**
15:00 - 15:15	Metal Oxide Aerogels: Porous Matrices for Curcumin Entrapment W. Hamd, D. Patra and **H. El-Rassy**	**Prof. Houssam Rassy**, American University of Beirut, **Lebanon**
15:15- 15:30	Keratin/Halloysite binary nanohybrids for bio-polymer nanocomposites **G-M. Teodorescu**, A. Ioniță, Z. Vuluga, C-A. Nicolae, M. Ghiurea and V. A. Faraon	**Mr. George Mihail Teodorescu**, INCDCP-ICECHIM- Bucharest, **Romania**
15:30 - 15:45	Nanocomposite derived from Local Ilmenite and Monazite for Solid Oxide Fuel Cell Cathode Material **M.Z. Ahmad** and S. Ahmad	**Mr. Muhammad Zaid Ahmad**, National University of Malaysia, **Malaysia**
15:45 - 16:00	Development of Nanocatalysts Derived from Ferrocene/Ferrocenium **E. Somsook**	**Prof. Ekasith Somsook,** Mahidol University, **Thailand**

16:00 - 16:30	Afternoon Coffee Break	
	Session's Chairs: **Prof. Benoit Heinrichs, University Liège, Belgium** **Prof. Houssam Rassy, American University of Beirut, Lebanon**	
16:30 - 16:45	Green synthesis of WO3 nanomaterial and their gas sensing properties **H. Pakdel,** V. Galstyan and E. Comini 1	**Ms. Hakimeh Pakdel**, University of Brescia, **Italy**
16:45 - 17:00	Nanosensor Fabrication with Silicon Nanowires M. Aleem, S. Kundu and **B. Kim**	**Prof. Bruce Kim**, City University of New York, **USA**
17:00 - 17:15	Delamination Mechanics and Electrical Performance of Transferred Vertically Aligned Carbon Nanotube Arrays **L. Lum**, Y.M. Zhai, R.T. Jiang, C.W. Tan and B.K. Tay	**Mr. Lucas Lum**, Nanyang Technological University, **Singapore**
17:15 - 17:30	Multifunctional, bicontinuously phase separated comb copolymer ionogel electrolyte for solid-state supercapacitors **W. Jin Mun** and J. Hak Kim	**Mr. Woo Jin Mun**, Yonsei University, **Rep. of Korea**
17:30 - 17:45	Fabrication of solid flexible supercapacitors based on adhesively, mechanically strong partially fluorinated comb copolymer electrolyte films **S. Jae Moon** and J. Hak Kim	**Mr. Seung Jae Moon**, Yonsei University, **Rep. of Korea**
17:45 - 18:00	MoS2 Nanowormes in-situ sputtered with Molybdenum Nitride Nanoflakes for high-performance Na-ion Supercapacitive Electrodes **B. Ranjan** and D. Kaur	**Mr. Bhanu Ranjan**, Indian Institute of Technology Roorkee, **India**

June 28, 2023		
Nanotech / NanoMetrolgy joint session I.B: Nanomaterials Modelling and Characterisation/ Nanosafety		
Conference Room Derain 1+2		
Session's Chairs: Prof. Jacques Jupille, Institut des Nanosciences de Paris, France Prof Juan Francisco Sánchez Royo, University of Valencia, Spain		
14:00 - 14:30	Evidence of the release of metals into the environment by the alteration of microplastics and focus on the potential contamination by Cr(VI) **D. Vantelon**, I. Khatib, C. Rivard, C. Catrouillet, J. Gigault and M. Davranche	**Dr. Delphine Vantelon**, LUCIA beamline Synchrotron SOLEIL, **France**
14:30 - 14:45	A Verified and Validated Finite Element Solution of a Nano-Calibration Problem in Near-Field Scanning Microwave Microscopy **J. T. Fong**, P. V. Marcal, N. A. Heckert, S. Berweger,T. M. Wallis, K. Genter and P. Kabos	**Dr. Jeffrey Fong**, U.S. National Inst. of Standards & Tech, **USA**
14:45 - 15:00	Towards time- and energy-resolved tabletop XUV photoelectron spectroscopy of solvated nanoparticle systems **J.Trester**, P. Zhang and H. Jakob Wörner	**Mr. Joel Trester**, ETH Zürich, **Switzerland**
15:00 - 15:15	Contact Force in Current-Detecting Atomic Force Microscopy-Moving Towards C-AFM Tomography in Photovoltaic Research **M. Hývl**, M. Ledinský and A. Fejfar	**Dr. Matěj Hývl**, Institute of Physics, Academy of Sciences, **Czech Rep.**
15:15 - 15:30	Effect of Gaussian and Bessel laser beams on linear and nonlinear optical properties of vertically coupled cylindrical quantum dots **D.B. Hayrapetyan**	**Prof. David Hayrapetyan**, Russian-Armenian University, **Armenia**
15:30 - 15:45	Talbot effect in InAs/GaAs coupled cylindrical quantum dots ensemble **P. Mantashyan**, G. Mantashian and D. Hayrapetyan	**Dr. Paytsar Mantashyan**, A.B Nalbandyan Institute of Chemical Physics, **Armenia**
15:45 - 16:00	Wrinkling and crumpling in twisted few and multilayer CVD graphene: High density of edge modes influencing Raman spectra D. Nikolaievskyi, M. Torregrosa, A. Merlen, S. Clair, O. Chuzel, J.-L. Parrain, T. Neisus, A. Campos, M. Cabie, C. Martin and **C. Pardanaud**	**Dr. Cedric Pardanaud**, Aix Marseille Univ, **France**
16:00 - 16:30	**Afternoon Coffee Break**	
Session's Chairs: Prof. Jacques Jupille, Institut des Nanosciences de Paris, France Prof. David Hayrapetyan, Russian-Armenian University, Armenia		
16:30 - 16:45	Degradation processes in two-dimensional lead iodide perovskites studied by Photoemission M. Krecmarova, J. Rodríguez-Romero, I. Mora-Seró, J.P. Martínez-Pastor, M.C. Asensio and **J.F. Sánchez-Royo**	**Prof. Juan Francisco Sánchez Royo**, University of Valencia, **Spain.**
16:45 - 17:00	Is the Surface of Hofmann-like Spin-Crossover {Fe(pz)[Pt(CN)4]} Same as its Bulk? **A. Martínez Serra**, A. Dhingra, M. C. Asensio, J. A. Real, and J. F. Sánchez Royo	**Mr. Alejandro Martínez Serra**, University of Valencia, **Spain.**
17:00 - 17:15	Surface Stabilisation of the High-Spin State of Fe(II) Spin-Crossover Complexes **A. Dhingra**, A. Martínez Serra, M. C. Asensio, J. A. Real, and J. F. Sánchez Royo	**Dr. Archit Dhingra**, University of Valencia, **Spain**
17:15 - 17:30	Machine Learning-based Prediction and Inverse Design of 2D Met-amaterial Structures with Tunable Deformation-Dependent Poisson's Ratio **X. Wang**, J. Tian and K. Tang	**Prof. Xianqiao Wang**, University of Georgia, **USA**

17:30 - 17:45	Determination of Diazonium Compounds For Modification Silver Nanoparticles in Estrogen Detection using DFT calculation **S. Srisung**, S. Nilrattanakoon and N. Wasukan	**Dr. Sujittra Srisung**, Srinakharinwirot University, **Thailand**
17:45 - 18:00	MetamaterialFinder: A Software Framework for Discovering and Analyzing Mechanical Metamaterials Based on Simple Closed Curves **M. Fleisch**, A. Thalhamer, G. Pinter, S. Schlögl and M. Berer	**Mr. Mathias Fleisch**, Polymer Competence Center Leoben GmbH, **Austria**
18:00 - 18:15	In Operando Spectroscopic Ellipsometry Investigation of MOF Thin Films for the Selective Capture of Acetic Acid **S.Dasgupta**, S.Biswas, K.Dedecker, E. Dumas1, N. Menguy, B. Berini, B. Lavedrine, C. Serre, C. Boissière and N. Steunou	**Dr. Sanchari Dasgupta**, ILV, UVSQ, University Paris Saclay, **France**

June 29, 2023		
Nanotech / GAMS 2023 - Joint Session II.A - Nanocoatings/ Thin films and nanostructured surfaces		
Amphithéâtre		
Session's Chairs: **Prof. Jacques Jupille, Institut des Nanosciences de Paris, France** **Prof. Sankara S. Tatiparti, Indian Institute of Technology Bombay, India** **Prof. Houssam Rassy, American University of Beirut, Lebanon**		
09:00 - 09:30	Liquid crystals, topological defects and nanoparticles **E. Lacaze**	**Prof. Emmanuelle Lacaze,** Institut des NanoSciences de Paris- CNRS, **France**
09:30 - 10:00	Ultrathin NiFe nanoalloyed films as low-cost and stable oxygen evolution reaction catalysts L. Ciambriello and **L. Gavioli**	**Prof. Luca Gavioli**, Università Cattolica del Sacro Cuore, **Italy**
10:00 - 10:30	Fabrication of a nanoporous filter for disposable facemasks out of biodegradable Polyesteramide through electrospinning: PublicMask **S. Hengsberger**, R. Marti and J. Charmet	**Prof. Stefan Hengsberger**, University of Applied Sciences and Arts Western Switzerland, **Switzerland**
10:30 - 11:00	**Morning Coffee Break**	
Session's Chairs: **Prof. Jacques Jupille, Institut des Nanosciences de Paris, France** **Prof. Luca Gavioli, Università Cattolica del Sacro Cuore, Italy**		
11:00 - 11:15	Highly TCO-Zn0.99B0.01O nanostructured thin films achieved by coupling rf magnetron sputtering and sol gel process K. Medjnoun, **A-R. Moussa Tankari**, K. Djessas and M. Nouiri	**Mr. Moussa Tankari Abdoulrazak**, PROMES-CNRS, **France**
11:15 - 11:30	Influence of ion bombardment on nanostructured DLC:N films deposited by RF magnetron sputtering. **A. Lousa**, M. Punset, J. Caro, C. Díaz, G. García-Fuentes, R. Bonet, E. Rupérez and J. Esteve	**Mr. Arturo Lousa**, University of Barcelona, **Spain**
11:30 - 11:45	Growth of luminescent rare-earth doped LaNbO compounds thin films by magnetron sputtering for the improvement of solar cells E. Salas-Colera, M. Tardío, E. García-Tabarés, B. Perea, M.L. Crespillo, J.E. Muñoz-Santiuste and **B. Galiana**	**Dr. Beatriz Galiana**, University Carlos III de Madrid, **Spain**
11:45 - 12:00	Modular UV Curing Sol-Gel Coating for Levelling and Easy to Clean Multi-layer Systems. **L. Florentino**	**Mrs. Lucia Florentino**, Idonial Foundation, **Spain**
12:00 - 14:00	**Lunch Break**	
NanoMatEn / GAMS Joint Session II.B: **Materials and Nanomaterials for Energy / Nanoelectronics/ Nanophotonics**		
Amphithéâtre		
Session's Chairs: **Prof Stefan Hengsberger, University of Applied Sciences and Arts Western Switzerland, Switzerland** **Prof Juan Francisco Sánchez Royo, University of Valencia, Spain** **Prof. Sasha Omanovic, McGill University, Canada**		
14:00 - 14:30	Nanogenerator: A Horizon of Green Power **R. Martins**, E. Fortunato and S. Nandy	**Prof. Rodrigo Ferrão de Paiva Martins**, Nova University of Lisbon, **Portugal**
14:30 - 15:00	Exploring Memristive Squaraine Microtubes: Programmable Multi-Level Memory Behaviour for Neuromorphic Applications **G. Redmond**	**Prof. Gareth Redmond**, University College Dublin, **Ireland**
15:00 - 15:15	Fractional-Order Fast Integral Terminal Sliding Mode Control for A Piezoelectric Feeding Tool Holder System K-M. Chang, J-M. Chen, W-L. Li and **Y-T. Liu**	**Prof. Yung-Tien Liu**, National Kaohsiung University of Science and Technology, **Taiwan**
15:15 - 15:30	Spatially-assisted electron-hole pair separation in core/shell quantum dots for energy conversion **D. Barba**, C. Wang, G. Singh Selopal, H. Zhao and F. Rosei	**Dr. David Barba**, INRS, **Canada**

15:30 - 15:45	Spectrally Selective Multilayer Coating System to Improve the Thermo-Optical Properties of New-Designed Particle Receiver for Concentrated Solar Power Plant. **E. Salas-Colera**, E. García-Tabarés, M.R. Rodríguez-Sánchez, A. Acosta-Iborra and F. Hernández-Jiménez	**Dr. Eduardo Salas Colera**,, University Carlos III de Madrid, **Spain**
15:45 - 16:00	Up-Converting NaY(Gd)F4:Yb3+,Er3+ β-phase Nanorods with Enhanced Red Emission for Perovskite Solar Cells **A. Gonzalo**, E. García-Tabarés, B. Serrano, J. E. Muñoz Santiuste and B. Galiana	**Dr. Alicia Gonzalo**, University Carlos III de Madrid, **Spain**
16:00 - 16:30	**Afternoon Coffee Break**	
Session's Chairs: **Prof. Luca Gavioli, Università Cattolica del Sacro Cuore, Italy** **Prof. Rodrigo Ferrão de Paiva Martins, Nova University of Lisbon, Portugal**		
16:30 - 16:45	The influence of material synthesis parameters on the electrocatalytic activity of NiMo-oxide nanostructures as anode electrocatalysts in alkaline water splitting towards green hydrogen production M.Rammal and **S.Omanovic**	**Prof. Sasha Omanovic**, McGill University, **Canada**
16:45 - 17:00	Anomaly in potential-composition-temperature isotherms during electrochemical hydrogenation of Pd thin films in an alkaline medium M. T. Pise, A. Chatterjee, B.P. Kashyap, R.N. Singh and **S.S.V. Tatiparti**	**Prof. Sankara S. Tatiparti**, Indian Institute of Technology Bombay, **India**
17:00 - 17:15	Hydrogen storage capacity of titanium, zirconium and TixZr1-x thin films **I. Zukerman**, M. Buzaglo and S. Hayun	**Mr. Ido Zukerman**, NRC-Negev, **Israel**
17:15 - 17:30	Concrete modules for energy harvesting **R. Campos**, R. Pedroso, D. Esteves, J. Gonçalves, J.Serafim, D. Correia, D. Gaspar and Â. Nunes	**Mr. Ricardo M. Campos**, CeNT- Centre of Nanotechnology and Smart Materials, **Portugal**
17:30 - 17:45	Sustainability of Expanded Polystyrene as a Preferred Thermal Insulation Material **C. Martins**, J. Araújo, J. Coutinho, D. Rodrigues, A. Moreira, P.F. Teixeira, N.O. Ferreira, D. Queiroz and N.B Pereira	**Mrs. Cíntia Martins**, CeNTI - Centre for Nanotechnology and Smart Materials, **Portugal**
17:45 - 18:00	Metal oxides composite electrodes for the oxygen evolution reaction **C.M. Pereira**, J.L. Chen, A.T. S. C. Brandão, R. Costa and M. J. Sottomayor	**Dr. Carlos M. Pereira**, Porto University - FCUP, **Portugal**
18:00 - 18:15	Investigation of the Physical Properties of New Binary Mixed Oxide Nanocomposites for Environmental Applications **M. Alzaid.**	**Dr. Meshal Alzaid**, Jouf University, **Saudi Arabia.**

June 29, 2023		
Nanotech France / GAMS Joint Session II.C - Nano for life science and Medicine		
Conference Room Derain 1+2		
Session's Chairs: **Prof. Claudia Giachino, University of Torino, Italy** **Prof. Xavier Fernandez Busquets, University of Barcelona/ IBEC, Spain**		
09:00 - 09:30	Carbon nano-onions for biomedical applications **S. Giordani**	**Prof. Silvia Giordani,** Dublin City University, **Ireland**
09:30 - 10:00	Motile micro- and nanorobotics: System integration, autonomy and biomedical applications **O.G. Schmidt**	**Prof. Oliver G. Schmidt**, Chemnitz University of Technology, **Germany**
10:00 - 10:30	Genetically Encoded Biosensor Development and Its Application in Regulating Microbial Biosynthesis T Jia.ng, C. Li, Y. Zou, J. Zhang, Q. Gan and **Y. Yan**	**Prof. Yajun Yan**, University of Georgia, **USA**
10:30 - 11:00	**Morning Coffee Break**	
11:00 - 11:30	Macrophage-targeted nanotherapies for hard-to-treat malignancies in females **B. Godin**	**Prof. Biana Godin**, Houston Methodist Research Institute, **USA**
11:30 - 11:45	Boosting translation in nano-enabled medical technologies: Lessons learned in the H2020 OITB Project Safe-N-Medtech **A. del Pozo**	**Mr. Angel del Pozo,** Biokeralty Research Institute AIE, **Spain**
11:45 - 12:00	Nanotechnological Approaches against Leishmaniasis: Aerosol Therapy with Pentamidine-loaded Liposomes and Discovery of New β-sheet Intercalator Drugs **L. Román-Álamo**, M. Allaw, Y. Avalos-Padilla, M.L. Manca, M. Manconi, J.A. Vázquez, J.E. Peris, X. Roca-Geronès, S. Poonlaphdecha, M.M. Alcover, R. Fisa, C. Riera, E.M. Arce, D. Muñoz-Torrero and X. Fernàndez-Busquets	**Ms. Lucia Roman Alamo**, University of Barcelona/ IBEC, **Spain**
12:00 - 14:00	**Lunch Break**	
Session's Chairs: **Prof. Silvia Giordani, Dublin City University, Ireland** **Prof. Biana Godin, Houston Methodist Research Institute, USA** **Prof. Pablo Taboada Antelo, University of Santiago de Compostela, Spain**		
14:00 - 14:30	Fabricating Quantum Dots for Technological Applications **K. Critchley**	**Prof. Kevin Critchley**, University of Leeds, **UK**
14:30 - 15:00	Hybrid nanostructures for combined therapeutics and tissue repair **P.Taboada Antelo**	**Prof. Pablo Taboada Antelo**, Univ; of Santiago de Compostela, **Spain**
15:00 - 15:30	Combination Therapy at the Nanoscale for the Targeted Delivery of New β-sheet Intercalator Antimalarial Drugs I. Bouzón-Arnáiz, Y. Avalos-Padilla, V. Iglesias, O. Cuspinera-Darnaculleta, L. Román-Álamo, C. Camarero-Hoyos, M. Ramírez, M. Rawat, R. Coyle, M. Lee, E.M. Arce, D. Muñoz-Torrero and **X. Fernàndez-Busquets**	**Prof. Xavier Fernandez Busquets**, University of Barcelona/ IBEC, **Spain**
15:30 - 16:00	Erythrocytes derived vesicles as platform for therapeutic nucleic acid delivery **G. Della Pelle**, T. Božič, B. Markelc, J. Šribar, K. Žagar Soderžnik, M. Erdani-Kreft, S. Hu-doklin and N. Kostevšek	**Mrs. Giulia Della Pelle**, Jožef Stefan Institute, **Slovenija**
15:45 - 16:00	Use of nanostructured MOX sensors to detect colorectal cancer by measuring blood samples and post-surgical follow-up **M. Astolfi**, G. Rispoli, G. Anania, G. Zonta and C. Malagù	**Dr. Michele Astolfi**, University of Ferrara, **Italy**
16:00 - 16:15	High-fidelity heart valve biomodel for aortic root and mitral valve surgery simulation training applications D. Varghese, K. Stoklosa , A. Joshi, W. Awad, P. Curry, A. Shahidi and **R. Arm**	**Mr. Richard Arm**, Nottingham Trent University, **UK**
16:00 - 16:30	**Afternoon Coffee Break**	

June 30, 2023		
NanoMatEn - Session III. **Nanotechnology for Environmental Application / Water treatment**		
Session's Chairs: **Prof. Sankara S. Tatiparti, Indian Institute of Technology Bombay, India** **Prof. Zygmunt Sadowski, Wroclaw University of Science and Technology, Poland**		
Conference Room Derain 1+2		
09:00 - 09:30	Labs and Organs on Chip for Health and Climate **A.Van Den Berg**	**Prof. Albert van den Berg,** BIOS-Lab on Chip Group/Scientific Director MESA+, Institute University of Twente, **The Netherlands**
09:30 - 10:00	From the Atomic Structure to the Optoelectronic Properties Studies of Low Dimensional Inorganic NanoMaterials via TEM **R. Arenal**	**Dr. Raul Arenal**, Zaragoza University, **Spain**
10:00 - 10:30	**Morning Coffee Break**	
10:30 - 11:00	2D Nanostructures at Atomic Scale: From Energy and Environmental Applications to Quantum Devices **J. Arbiol**	**Prof. Jordi Arbiol,** ICREA and Catalan Institute of Nanoscience and Nanotechnology, CSIC and BIST, **Spain**
11:00- 11:15	Metalorganic Copolymers From Iron(II) Clathrochelates: Versa-tile Materials and Conspicuous Adsorbents of Lithium Ions, Io-dine, and Organic Dyes S. Shetty, N. Baig and **B. Alameddine**	**Prof. Bassam Alameddine**, Gulf University for Science and Technology, **Kuwait**
11:15 - 11:30	Naphthyridine-based Luminophores for Highly Efficient Thermally Activated Delayed Fluorescence Organic Light-Emitting Diodes **R. Keruckiene**, E. Vijaikis, C.-H. Chen, B.-Y. Lin, J.-X. Huang, C.-C.Chu, Y.-C. Dzeng, C. Chen, .J.-H. Lee, T.-L. Chiu, S. Macionis, J. Keruckas, R. Butkute, J. V. Grazulevicius and E. Skuodis	**Dr. Rasa Keruckienė**, Kaunas University of Technology, **Lithuania**
11:30 - 11:45	Nanostructured thin films of manganese oxide coupled with electro-chemistry: an innovative eco-friendly water depollution process **C. Boillereau** and S. Peulon	**Ms. Charlène Boillereau**, University Paris-Saclay, CEA, CNRS/ NIMBE, **France**
11:45 - 12:00	Enhanced adsorption and Photo-Fenton degradation of 2, 4-Dichlorophenoxyacetic acid using nanomagnetite/alginate nanocomposite based on brown algae: kinetic and thermodynamic studies **L. M. Alshandoudi**	**Dr. Laila M. Alshandoudi**, University of Technology and Applied Sciences, **Sultanate of Oman**
12:00 - 12:15	A new approach towards the realization of specific and label-free biological sensing based on field-effect devices S. Samanta, V.S. Tiwari, S. Sadhujan, S. Harilal, A. Eisenberg-Lerner, Z. Rotfogel, E. Pikhay, R. Shima-Edelstein, D. Greental, M.Y. Bashouti, B. Akabayov, I. Ron, Y. Roizin, O. Erez and **G. Shalev**	**Dr. Gil Shalev**, Ben-Gurion University of the Negev, **Israel**

Posters Session
June 28 - 29, 2023

N.	Title	Author / Affiliation / Country
1.	Targeted synthesis and tailoring of gold nanorods **D.G. Schauer**, J. Bredehoeft and H. Jakob Wörner	**Mr. David G. Schauer**, ETH Zurich, **Switzerland**
2.	High-Speed Die Attachment by Transient Liquid Phase Bonding Using a Preform of 5 µm Cu@Sn Core-Shell Particles for High-Temperature Applications Y. Kim, B. Jo Han and **J-H. Lee**	**Prof. Jong-Hyun Lee**, University of Seoul, **Rep. of Korea**
3.	Analysis of B-rich B-Te Ovonic Threshold Switching Materials and Devices with Various Compositions **H. Kwon**, K. Jeong, Y. Seong, H. Kim and M-H. Cho	**Mr. Hoedon Kwon**, Yonsei University, **Rep. of Korea**
4.	The Effects of Gold Nanorods with Wavelength Irradiation **T. Román**, E. Morales-Narváez and Y. Montelogo	**Ms.Tatiana Román**, Centro de Investigaciones en Óptica, **México**
5.	Effect of ZnO particle size on the activity in the photoreduction of CO2 **I. Pełech**, A.W. Morawski, K. Ćmielewska, E. Kusiak-Nejman and U. Narkiewicz	**Prof. Iwona Pełech**, West Pomeranian University of Technology in Szczecin, **Poland**
6.	Nitrates on Ceria: Effects of Morphology and Zr Doping **E. Ivanova**, M. Mihaylov, K. Chakarova, H. Aleksandrov, P. Petkov, G. Vayssilov and K. Hadjiivanov	**Dr. Elena Ivanova**, Bulgarian Academy of Sciences, **Bulgaria**
7.	CO Adsorption on Ni-MFI Zeolite **M. Mihaylov**, E. Ivanova, N. Drenchev and K. Hadjiivanov	**Prof. Mihail Mihaylov**, Bulgarian Academy of Sciences, **Bulgaria**
8.	Fabrication of highly permselective, mechanically robust block copolymer/ionic liquid membranes for CO2 separation **Y. Jun Kim** and J. Hak Kim	**Mr. Young Jun Kim, Yonsei University, Rep.of Korea**
9.	Comparing submicron-thick mixed-matrix membranes with metal organic frameworks of MIL-140C and UiO-67 for CO2 separation **H. Jin Roh**, M. Kang and J. Hak Kim	**Mr. Hyuk Jin Roh**, Yonsei University, **Rep. of Korea**
10.	Structure-Property Relationship of Aramid Nanofiber-Reinforced Thermotropic Liquid Crystalline Polyester Nanocomposites T-G. Eom, Y-G. Song, S-J. Kim, M. Seo, J-H. Park, and **Y. Gyu Jeong**	**Prof. Young Gyu Jeong**, Chungnam National University, **Rep. of Korea**
11.	Synthesis and characterization of silica/phytic acid binary nanofillers **M. Wysokowski**, J. Stachowiak and P. Bartczak	**Dr. Marcin Wysokowski**, Poznan University of Technology, **Poland**
12.	Polymer Based Nanocomposites filled with Graphitic Materials and Metalic Oxides Applied to X-ray Shielding in Interventional Radiology Procedures **L. O. Faria** and L. A. Silva	**Prof. Luiz Oliveira de Faria**, Centro de Desenvolvimento da Tecnologia Nuclear, **Brazil**
13.	Vanadium aluminum carbide nanoparticles as a storable absorber to generate mode-locked pulses from Yb fiber laser **F. Fadhil** and A. H. Al-Janabi	**Dr. Fay Fadhil**, University of Baghdad, **Iraq**
14.	Iron(III)-Polyphenol Nanocoating for Black Hair-Dyeing **E.K. Kang** and I.S. Choi	**Ms. Eunhye Kang**, KAIST-Daejeon, **Rep. of Korea**
15.	A study of cardanol-based phosphoric flame retardant to improve the flame retardancy of epoxy material **D-H. Kim**	**Dr. Do-Hyun Kim**, Korea Institute of Civil Engineering and Building Technology, **Rep. of Korea**
16.	Optimizing Ge film adhesion on polycarbonate: unraveling the impact of O2/Ar plasma exposure J. Peralta, **J. Esteve** and A.Lousa	**Prof. Joan Esteve**, University of Barcelona, **Spain**
17.	Synthesis of Ag/Fe2O3 nanocomposite from essential oil of ginger via green method and its bactericidal activity **F.A. M. Al Zahrani**, N. A. AL Zahrani, S. N. Al Ghamdi, · L. Lin, S.S. Salem and R. M. El Shishtawy	**Dr. Fatimah A. M. Al Zahrani**, King Khalid University, **Saudi Arabia**
18.	Organic-Inorganic Hybridgel: new food packaging material **F. Trodtfeld**, T. Tölke and C. Wiegand	**Ms. Franziska Trodtfeld,** INNOVENT e.V- Jena, **Germany**
19.	Molecular dynamics study of self-diffusion pathways in alkali metals **Y. Kondratyeva** and A.V. Sergeev	**Ms. Yevgeniya Kondratyeva**, N.N. Semenov Federal Research Center for Chemical Physics, **Russia**
20.	Autophagy enhancer-Trehalose coated implant is available for the inflammed and infected bone S-Y. Park, K-J. Seong, S. Kim, M-S. Kook, M-Y. Park, H-J. Song, S-G. Park, J-Y. Jung and **W-J. Kim**	**Prof. Won-Jae Kim**, Chonnam National University, **Rep. of Korea**

21.	Carbon composites for biomedical application **P. Tzvetkov**, B. Tsyntsarski, I Stoycheva, G. Georgiev, B. Petrova, E. Grigorova and P. Markov	**Dr. Peter Tzvetkov**, Bulgarian Academy of Sciences, **Bulgaria**
22.	Bio-inspired formation of protein-nanoparticle complexes mimicking ocular environment **J. Hun Kim** and T. Geol Lee	**Prof. Jeong Hun Kim**, Seoul National University Hospital, **Rep. of Korea**
23.	Efficient in vitro and in vivo DNA Delivery by Multicomponent Lipid Nanoparticles **S. Renzi**, E. Quagliarini, L. Digiacomo, J. Wang, L. Cui, G. Ferri, L. Pesce, V. De Lorenzi, G. Matteoli, H. Amenitsch, L. Masuelli, R. Bei, F. Cardarelli, A. Amici, C. Marchini, D. Pozzi and G. Caracciolo	**Mrs. Serena Renzi,** Sapienza University of Rome, **Italy**
24.	Magnetic levitation of nanoparticle-protein corona as an effective tool for cancer diagnosis **E. Quagliarini**, L. Digiacomo, D. Caputo, A. Coppola, H. Amenitsch, G. Caracciolo and D. Pozzi	**Dr. Erica Quagliarini**, Sapienza University of Rome, **Italy**
25.	Transdermal site-specific delivery of CD38-peptide-modified extracellular vesicles by microneedles for targeted therapy of extramedullary plasmacytoma **Y. Cao**, D. Wu and Q. Li	**Ms. Yulin Cao**, Huazhong University of Science and Technology, **China**
26.	A role of Bi2Se3 topological insulator as electrodes in high-performance WSe2 photodetector **D. Kim**, J. Chae, S-B. Hong, J. Kim, G. Kwon, H. Kwon, K. Jeong and M-H. Cho	**Ms. Dajeong Kim**, Yonsei University, **Rep. of Korea**
27.	Analysis on the Electro-Optical Properties of Quantum-Dot Light-Emitting Diodes based on Charge Transport Simulation **Y. Kim**, S. Jung, J. Jo, S. Lee, J. Yang, S. Zhan, and J. M. Kim	**Mr. Yoonwoo Kim**, University of Cambridge, **UK**
28.	Homogeneous Elongation of N-Doped CNTs on Nano-Fibrillated Hollow Carbon Nanofiber: Resolving Mass and Charge Imbalance in Asymmetric Supercapacitors **T. Kim**, T. Hoon Ko, K. Chhetri and H. Yong Kim	**Dr. Taewoo Kim**, Jeonnbuk National University, **Rep. of Korea**
29.	Cobalt Sulfide Hollow Spheres with Partial Selenium Surface Modification as an Efficient Bifunctional Oxygen Electrocatalyst for Rechargeable Zinc-Air Batteries **T. Hoon Ko**, T. Woo Kim and H. Yong Kim	**Dr. Tae Hoon Ko**, Jeonbuk National University, **Rep. of Korea**
30.	Phenothiazine-S,S-dioxide as a versatile compound in the synthesis of organic emitters **R. Butkute**, F. Khan, M. Guzauskas, A. Dabulienė, M. Mahmoudi, D. Volyniuk, L. Skhirtladze, M. Stanitska, R. Misra and J. V. Grazulevicius	**Dr. Rita Butkutė**, Kaunas University of Technology, **Lithuania**
31.	Modular Infrared Heater with Nanofluid Thermal Accumulation Collector - Unsteady Entropy Analysis **F. Alic**	**Prof. Fikret Alic,** University of Tuzla, **Bosnia and Herzegovina**
32.	Nanocarbons as additives to Mg-based hydrogen storage materials **E. Grigorova**, B. Tsyntsarski, P. Markov, P. Tzvetkov and I. Stoycheva	**Dr. Eli Grigorova**, Bulgarian Academy of Sciences, **Bulgaria**
33.	Green Hydrogen from Sunlight via Plasmon Enhanced Photocatalysis **L. Steinmüller** and T. Walter	**Mrs. Lucie Steinmüller,** Innovent e.V- Jena, **Germany**
34.	Enhancement of Electric Field Intensity by Plasmon Coupling between Ag Film and Gold Nanoparticles **J. -H. Jang**, H. Y. Lee, J. -H. Ryu, J. -Y. Lee, S. -H. Kim, S. -L. Hwang, H. S. Ahn, Y. T. Chun and S. N. Yi	**Mr. Jun-Hyeon Jang**, Korea Maritime & Ocean University, **Rep. of Korea**
35.	Evaluation of quality of patterns for printed electronics by measuring printability **C-H. Kim** and H. K. Park	**Prof. Chung-Hwan Kim**, Chungnam National University, **Rep. of Korea**
36.	Polymeric Enhanced Membranes for Photocatalytic Degradation of Organic Contaminants A.C.W.E. Santo, L.L.S. Silva, A.M.F. Linhares, C.P.Borges and **F.V. Fonseca**	**Prof. Fabiana V. Fonseca**, Federal University of Rio de Janeiro, **Brazil**
37.	Design of Metal-Organic Frameworks-based composites for visible-light-driven heterogeneous photocatalysis **K. Dassouki**, S.Dasgupta, E. Dumas and N. Steunou	**Mr. Khaled Dassouki**, Versailles St Quentin en Yvelines University, **France**

Nanotech / GAMS Joint Plenary session

Bio-nano-technologies for cardiac regenerative medicine

Claudia Giachino[1], Raffaella Rastaldo[1], Daniela Rossin[1], Sadia Perveen[1], Roberto Vanni[1], Debora Fusco[2], Anna Marsano[2], Ricardo Pires[3], Rui Reis[3], Niccoletta Barbani[4], Caterina Cristallini[4].

[1] Department of Clinical & Biological Sciences, University of Turin, Italy
[2]Department of Biomedicine, University of Basel, Switzerland
[3] University of Minho – 3B's Research Group (UMINHO), Portugal
[4] CNR-IPCF, Institute for Chemical and Physical Processes, Pisa, Italy

Abstract:
Cardiovascular diseases represent the main cause of death worldwide. Myocardial infarction (MI) results in a substantial loss of cardiomyocytes in the infarcted area followed by the formation of a dense collagenous scar due to fibroblast and endothelial cell proliferation. Nowadays, pharmacological approaches are only able to delay the progression toward heart failure. Cell-based regenerative medicine and tissue engineering have emerged as promising alternatives to develop novel clinical approaches to treat MI.
Human mesenchymal stem cell (hMSC)-based therapies have shown some beneficial effects in regenerating injured myocardium. However, their therapeutic effect is limited by their poor engraftment capacity. I will present data showing that, upon both *in vitro* static and dynamic cultures, silica nanoparticle (SiO_2NP) internalization affects the area and maturation of hMSC focal adhesion complexes, thus increasing their adhesion capacity in infarcted isolated rat hearts. SiO_2NP internalization also enhances Connexin-43 expression, favouring hMSC interaction with co-cultured cardiac myoblasts and positively impacting on chemotactic ability of hMSCs through the SDF1α/CXCR4 axis. These findings suggest a high potential for SiO_2NPs to improve hMSC engraftment at sites of injury and, in turn, therapeutic efficacy upon cell injection in vivo.
The use of tissue-engineered scaffolds, resembling the characteristics of the native heart tissue, has emerged as another possible effective therapeutic approach for ischemia-induced MI. In the second part of my talk, I will present *in vitro, ex vivo* and *in vivo* results of a multicenter project aimed at developing innovative bio-artificial scaffolds with the potential to serve as acellular patches for *in vivo* cardiac regeneration.

Stability of fibrillated nanocellulose suspension in the presence of AgNPs, AuNPs, Rhamnolipid and inorganic surfactants

Z. Sadowski [1,*], A. Wirwis[1]
[1] Department of Chemistry, Wroclaw University of Science and Technology
Wybrzeze Wyspianskiego 27, 50-370 Wroclaw, Poland

Abstract:
Excenssive production of plastic packaging for food storage creates a need to replace it with paper-base packaging materials [1]. Cellulose together with mineral filler are the main components of paper. Metal nanoparticles especially silver, gold and copper have a strong bactricidal effect. In our study, we used a fibrous nanocellulose produced by ITENE (Spain). Silver and gold nanoparticles were synthesized using extracts from green tea or olive tree leaves. The aim of the study was to investigated the adhesion of nanoparticles to the surface of nanocellulose fibers by tracking changes in stability of aquous nanocellulose suspensions. In addition, surfactants and a biosurfactant (Rhamnolipid) were applied to improve the stability of the suspensions. The optical properties and morphology of both AgNPs and AuNPs were estimated using DLS and UV-vis spectroscopy. The stability of water suspension of nanocellulose was observed using TURBISCAN Lab technology. Turbiscan Stability Index (TSI) was used to characterize of the stability of nanocellulose dispersion. The zeta potential was determined by ZetaMeter 2000 from Malvered Instruments. Nanocellulose particles were dispersed in aqueos NaCl (10^{-3} M) solution. The morphology of the nanocelluose particles with silver and gold nanoparticles was examined by scanning transmission electron microscopy. It has been observed that the adhesion of gold nanoparticles significantly improve the stability of an aqueous suspension of nanocellulose fibers (Figure 1). The addition of an anionic surfactant (SDS) and a biosurfacatant (Rhamnolipid)to the aqueous suspension of nanocellulose fibers increased stability. The opposite effect was observed when a cationic surfactant (CTAB) was added to the suspension. It is notewarthy that Rhamnolipid in low concentrations is a stabilized and high concentration a destabiliser of the cellulose fiber suspension. The mechanisms of action of silver and gold nanoparticles and surfactants were attempted to be described based on colloid interactions [2].

Keywords: nanocellulose fibrils, AgNPs, AuNPs, adhesion, suspension stability, surfactants, Rhamnolipid, adsorption, packaging material.

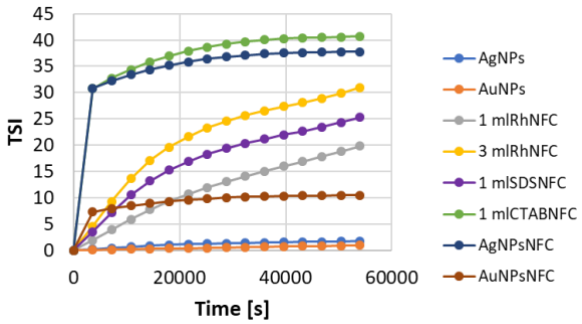

Figure 1:

References:

1. Pandey, S., Sharma, K., Gundabala, V. (2022), Antimicrobial bio-inspired active packaging materials for shelf life and safety development. A review, *Food Bioscience.*, 48, 101730.
2. Shang, Z., An, X., Seta, T.F., Ma, M., Shen, M., Dai, L., Liu, H., Ni, Y. (2019), Improving dispersion stability of hydrochloric acid hydrolyzed cellulose nano-crystal, *Carbohydrate Polymers*, 222, 115037.

Acknowledgements
The authors would like to thank the funding support provided by BioNanoPolys project under Horizon 2020 UE.

Laser ablation synthesis of fresh Te nanoparticles for MALDI MS applications

K. Novotný [1*], I. Krempl [1], L. Pečinka [1], P. Vaňhara[2,3], J. Havel[1,2]
[1] Department of Chemistry, Faculty of Science, Masaryk University, Brno, Czech Republic
[2] International Clinical Research Centre,St. Anne's University Hospital, Brno,Czech Republic
[3] Dep. of Histology and Embryology, Faculty of Medicine, Masaryk University, Brno,Czech Republic

Abstract:
Nowadays, there is high interest in replacing organic matrices in matrix assisted laser desorption ionization (MALDI-MS) for analysis of small molecules. Aromatic acids and their derivates are ordinarily used for proton transfer with investigated analyte, however, mass spectra suffer from interferences caused by fragmentation of organic acids (<1 kDa) and from ion suppression. Decomposed products of these thermal and acidity labile molecules caused the assignment of low molecular weight molecules quite difficult (overlapped peaks of matrix and investigated ions). Using NPs as a novel type of matrices is intensively studied by many research groups. NPs show clear background mass spectra with only a few interference signals. Charged adducts of NPs with analytes are easily formed.

Tellurium (Te) belongs to the chalcogens group and is a well-known p-type semiconductor with a small energy bandgap of 0.33 eV at room temperature. These exceptional properties result in strong interest to produce tellurium nanostructures and NPs.

Laser ablation is a well-known NPs preparation method. During synthesis, contamination is minimized using a pure Te target and a pure liquid or gas environment. Moreover, instrumentation can be relatively simple. Since only a small concentration of nanoparticles is needed for MALDI MS applications, sufficient quantities can be prepared in a short time. For these purposes, it is convenient to construct a simple device for preparing NPs directly in the laboratory. It is necessary to always prepare fresh nanoparticles due to their rapid agglomeration. The addition of stabilizers is undesirable because it leads to unwanted interferences in the mass spectrum.

Keywords: pulsed laser ablation, laser ablation sysnthesis, tellurium, nanoparticles, nanoparticles stability, MALDI-MS, MALDI matrices.

In this work, tellurium NPs were prepared using a novel laser ablation experimental setup and characterized by TEM and their potential in MALDI-MS was tested.

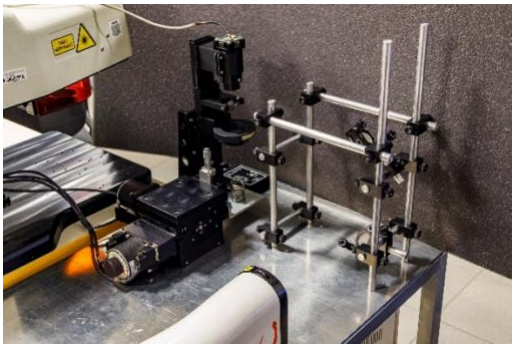

Figure 1: Modular experimental setup for generating Te NPs in liquids or gas environments. In the case laser ablation synthesis in liquid the Te target was placed in the beaker and liquid was added. In the case of synthesis in gas, the ablation cell (not pictured) was washed by helium and the Te target was placed inside.

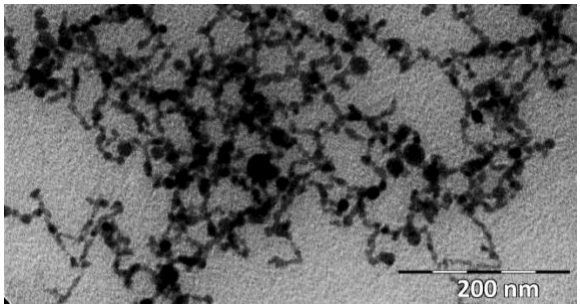

Figure 2: TEM images of tellurium nanoparticles prepared in acetone during ablation of Te target using pulsed NdYAG laser at 1064 nm.

References:

1. Semaltianos, N. G. (2010) Nanoparticles by Laser Ablation, *Critical Rewiews in Solid State and Materials Sciences, 35:105-124.*
2. Chen, Y. S., Ding, J., He, X. M., Xu, J., Feng, Y. Q. (2018) Synthesis of tellurium nanosheet for use in matrix assisted laser desorption/ionization time-of-flight mass spectrometry of small molecules, *Microchimica Acta 185: 368*

Acknowledgement: This work was supported by project no. GA22-07635S of Grant Agency of Czech Republic.

Facile Fabrication of Reduced Graphene Oxide-Carbon Nanotubes-Silicon Composites for High Current Density Anode Materials

H.D. Jang1,2, S.K. Kim1, K.M. Roh1
1 Resources & Materials Research Center, Korea Institute of Geoscience & Mineral Resources, Daejeon, Rep. of Korea.
2 Department of Nanomaterials Science and Engineering, University of Science & Technology, Daejeon, Rep. of Korea.

Abstract:
Silicon (Si) is considered a promising anode material for lithium-ion batteries (LIBs) due to its high performance. However, when Si is exposed to an electrolyte, it forms a solid electrolyte interphase (SEI) film and the following electrode decomposition results in poor performance of the LIB. Effective coverage of Si by carbon materials is an interesting potential solution to solve this problem. In this study, we prepared reduced graphene oxide-carbon nanotubes-silicon(RGO-CNTs--Si) composites and showed that it can be used as a high-performance anode material for LIBs. Fabrication of the RGO-CNTs-Si composites was composed of three steps (Figure 1). The first step was preparation of well dispersed GO-CNTs colloids by the bead milling without any chemical treatment and then co-assembly of the GO-CNT-Si composites by spray drying the colloidal mixture. Finally, the RGO-CNT-Si composites were fabricated by thermal reduction of GO in the CNTs-GO-Si composites. The morphology of the composites was generally the shape of a crumpled paper ball and the size showed a distribution of 1 to 5 µm. The highest capacitance of the CNT-RGO-Si composite was about 1634 mAhg-1 during the 100 cycles test of charge and discharge at 1 C current density. The composites exhibited coulombic efficiency of over 96% with excellent stability.

Keywords: Aerosol process; Lithium ion battery (LIB); Anode materials; Beads milling; Carbon nanotubes-reduced graphene oxide-silicon (CNTs-RGO-Si)

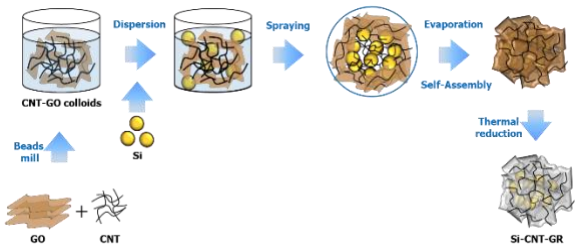

Figure 1: Schematic illustration of the formation RGO-CNTs-Si composites by beads milling, spray drying and thermal treatment.

References:

1. Luo, J. Zhao, X. Wu, J., Jang, H.D., Kung, H.H., Huang, J. (2012). Crumpled Graphene- Encapsulated Si Nanoparticles for Lithium Ion Battery Anodes. *J. Phys. Chem. Lett*. 3, 1824-1829.
2. Kim, S.K., Chang, H., Kim, C.M., Yoo, H., Kim, H., Jang, H.D. (2018). Fabrication of ternary silicon-carbon nanotubes-graphene composites by Co-assembly in evaporating droplets for enhanced electrochemical energy storage. *J. Alloys Compd*. 751, 43-48.

Nanotech / GAMS Joint Session I.A: Nanomaterials Fabrication / Synthesis / properties

An enhanced generation of singlet oxygen through the use of Au bipyramids/SiO_2 core-shell nanoparticles for photocatalysis

C. Mendoza,[1] D. Chateau[2], A. Desert[2], C.A. Páez[1], N.Emmanuel[3], L. Khrouz[2], C. Monnereau[2], L. Dreesen[4], J-C. M. Monbaliu[3], S. Parola[2], and B. Heinrichs[1]

[1] Nanomaterials,Catalysis&Electrochemistry, Department of Chemical Engineering, ULiège, Belgium
[2] Functional Materials&Photonics, Laboratoire de Chimie, Ecole Normale Supérieure de Lyon, France
[3] Center for Integrated Technology and Organic Synthesis, Department of Chemistry, ULiège, Belgium
[4] GRASP-Biophotonics, Department of Physics, ULiège, Belgium

Abstract:
Gold nanomaterials display interesting nanoplasmonic features with potential application in various fields depending on the size and shape of the metal nanoparticle (NP). Au bipyramids (AuBPs) exhibit intense and well-defined plasmon resonance, easily tunable with the aspect ratio and synergy between Au NPs and chromophores can enhance the photophysical properties of nearby molecules. In Rose Bengal (RB)-NPs systems for the production of singlet oxygen ($^1O_2$), it is now well established that the control of the dye-to-NP distance ranging from 10 to 20 nm is crucial to achieve the proper coupling between plasmon resonance and the dye[1]. We have developed AuBPs@mesoporous SiO_2 core-shell nanostructures to control the distance between metallic surface and photosensitizers in order to increase the production of $^1O_2$ through metal-enhanced fluorescence (MEF). An enhancement of $^1O_2$ generation has been shown with the obtained anisotropic AuBPs and AuBPs@mSiO_2 in presence of RB using different methods of $^1O_2$ quantification. They are of interest to the application in photooxygenation reactions *e.g.* α-terpinene to ascaridole, an anthelmintic drug.

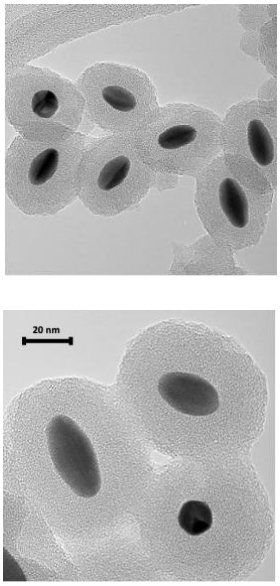

Fig. 1. TEM images of AuBPs@mSiO_2 at 280kX and 490kX

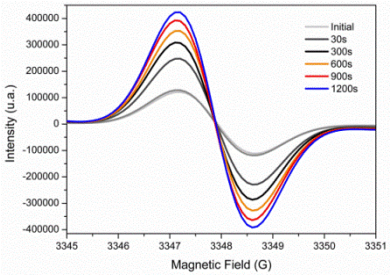

Fig. 2. EPR/TEMP spectra of AuBPs@mSiO_2 in presence of RB under visible irradiation as a function of time

References

1. H.H. Lin, I.C. Chen, *J. Phys. Chem. C.* 119 (2015) 26663–26671.

Piezoelectric III-Nitride nanowires based energy harvesters: Towards the development of wireless micro-devices

N. Gogneau [1], P. Chrétien [2], T. Sodhi [1], A. Chevillard [1], Q. C. Bui [1], L. Couraud [1], L. Leroy [1], L. Travers [1], J-C.Harmand [1], F. H. Julien [1], , F. Houzé [2], M. Tchernycheva [1]

[1] Centre de Nanosciences et Nanotechnologies, Université Paris-Saclay, Université Paris-Cité, CNRS, UMR9001, Palaiseau, France

[2] Université Paris-Saclay, CentraleSupélec, Sorbonne Université, CNRS, Laboratoire de Génie électrique et électronique de Paris, Gif sur Yvette, France, Sao Paulo, Brazil

Abstract:

The number of "Internet of Things" (IoTs) is constantly on a rise both in our daily life and in high-tech applications. Their energetic autonomy is today a key worldwide challenge, particularly for ones operating in an environment with restricted, or even absent, electrical grid infrastructure. The recent miniaturization of the electronic devices results in the reduction of their energy consumption (to mW and even µW). Combined with the progress in micro-nano-fabrication, new perspectives have opened the development of autonomous power systems based on renewable energy harvesting. Among renewable energies, the mechanical deformations and vibrations, harvested using piezoelectric materials, present the advantages to be ubiquitous and permanently available.

From now few years, GaN nanowires (NWs) are considered as promising nanomaterials to develop high-efficient and ultra-compact piezoelectric nano-generators. Thanks to their large surface-to-volume, high crystalline quality and nanoscale dimensions, NWs present unique advantages to significantly enhance the piezo-device performances. Thus, GaN NWs based piezo-nano-generators have been demonstrated delivering, under laboratory testing conditions, power densities in the µW-mW/cm3 range. To further improve the device performances and use them for real applications, it is today essential to enhance the electro-mechanical coupling properties of NWs. Here we investigate two different way for imporving the piezo-response of GaN NWs.

The first solution constists in integrating a thick In-rich InGaN insertion in the GaN NW volume in order to take advantage of the higher piezoelectric coefficients of the InGaN versus GaN [1]. Thus, we demonstrate output voltages reaching several hundreds of mV generated per GaN NW, and an improvement of about 35% of the piezo-conversion capacity (output voltage up to 470 mV/NW) by integrating a thick In-rich InGaN insertion in the GaN NW volume. These latest values largely exceed the maximum voltages generated by ZnO NWs, the widely investigated nanostructures for developing piezo-generators.

The second solution consists in considering the surface charge effects (strongly pronounced in GaN NWs) and their expression depending on the NW diameter. Thus, by using an unique nano-characterization tools, we demonstrate that the electromechanical coupling coefficient can be enhanced until to 43% by architecturing the NW dimensions [2].

Based on our developments, we propose an efficient piezo-generator design operating under compressive strain. The devices integrate NW arrays of several square millimeters in size and deliver a maximum power density up to few mW/cm^3 under mechanical inputs miming the ones used in real applications.

Keywords: Ga(In)N NWs, Piezoelectric properties, electromechanical coupling coefficient, Surface charge effects, Energy harvesters

References:

1. Jegenyes, N., Morassi, M., Chrétien, P., Travers, L., Lu, L., Julien, F.H., Tchernycheva, M., Houzé, F., Gogneau, N. (2018) High Piezoelectric Conversion Properties of Axial InGaN/GaN Nanowires *Nanomaterials*, 8, 367.
   Gogneau, N., Chrétien, P., Sodhi, T., Couraud, L., Leroy, L., Travers, L., Harmand, J-C., Julien, F. H., Tchernycheva, M., Houzé, F. (2022) Electromechanical conversion efficiency of GaN NWs: critical influence of the NW stiffness, the Schottky nano-contact and the surface charge effects *Nanoscale* 14, 4965–4976

Metal Oxide Aerogels: Porous Matrices for Curcumin Entrapment

W. Hamd, D. Patra, H. El-Rassy *
Department of Chemistry, American University of Beirut, Beirut, Lebanon

Abstract:
Metal oxide aerogels are highly porous materials with large surface areas [1]. These materials are prepared via the sol-gel technique, either through the hydrolysis and condensation route [2], by polymer crosslinking [3], or via the epoxide-assisted approach [4]. The gel formation depends on multiple critical parameters, including but not limited to the concentration of the precursors, the order of their mixing, and temperature. Several metal oxides aerogels prepared according to this technique were reported in the literature such as silica (SiO_2), titania (TiO_2), alumina (Al_2O_3), zirconia (ZrO_2), iron oxide (Fe_2O_3), cobalt-ferrite ($CoFe_2O_3$), neodymium oxide (Nd_2O_3), dysprosia (Dy_2O_3), holmia (Ho_2O_3), erbia (Er_2O_3), samaria (Sm_2O_3), and vanadia (V_2O_5).
Curcumin (IUPAC name: (*E*)- 1,7-bis(4-hydroxy-3-methoxyphenyl)hept-3-ene-1,6-dione) is a polyphenol found to benefit several medical conditions, and can be used for fluorescence probing [5] and sensing applications [6]. Several encapsulation and loading media were investigated to enhance the stability of curcumin and widen its spectrum of use.
This work reports the loading of different metal oxide aerogels with curcumin. We show how mixing curcumin with the metal precursors prior to the formation of the solid network ensures a maximum entrapment. The curcumin-network interactions stabilize the organic moiety and create hybrid aerogels to be potential vehicles for curcumin in various media. The characterization of the hybrid aerogels and the stability study revealed distinct behaviors depending on the nature of the metal oxide.

Keywords: Aerogel; Curcumin; Metal Oxide; Host-Guest interaction; Fluorescence.

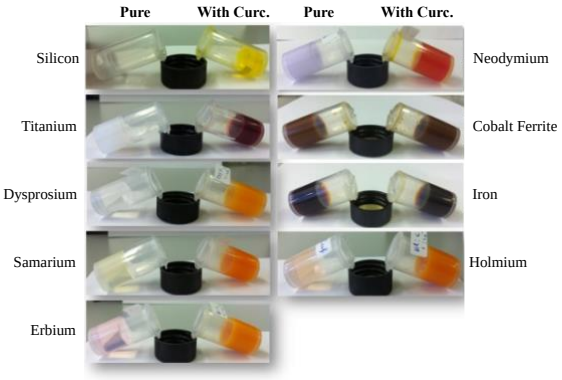

Figure 1: Wet metal oxide alcogels with and without curcumin.

References:

1. Manzocco L.; Mikkonen K. S.; García-González C. A., *Food Structure*, **2021**, *28*, 100188.
2. Al-Oweini R. and El-Rassy H., *Journal of Molecular Structure*, **2009**, *919*, 140.
3. Capadona L. A.; Meador M. A. B.; Alunni A.; Fabrizio E. F.; Vassilaras P.; Leventis N., *Polymer*, **2006**, *47*, 5754.
4. Gash A. E.; Tillotson T. M.; Satcher Jr J. H.; Hrubesh L. W.; Simpson R. L., *Journal of Non-Crystalline Solids*, **2001**, *285*, 22.
5. Patra D.; El Khoury E.; Ahmadieh D.; Darwish S.; Tafech R. M., *Photochemistry and Photobiology*, **2012**, *88*, 317.
6. Mouslmani M.; Bouhadir K. H.; Patra D., *Biosensors and Bioelectronics*, **2015**, *68*, 181.

Keratin/Halloysite binary nanohybrids for bio-polymer nanocomposites

G-M. Teodorescu[1], A. Ioniță[1], Z. Vuluga[1,*], C-A. Nicolae[1], M. Ghiurea[1], V. A. Faraon[1]
[1] Polymers and Bioproducts Departments, INCDCP-ICECHIM, Bucharest, Romania
[*]corresponding author: zvuluga@icechim.ro

Abstract:
The high mechanical properties of feather keratin, good thermal stability, as well as low cost and low density, have attracted the attention of researchers for their use as reinforcing agents in polymer composites. Compared to synthetic fibers, keratin fibers from chicken feathers are biodegradable and non-abrasive. In addition, it represents a continuously renewable resource. The main problem of natural fibers is the low thermal stability at plastic processing temperatures. This limits their use as reinforcing agent in engineering thermoplastics (e.g. polyamide). In general, the solutions developed for improving the thermal stability of natural fibers and obtaining bio-composites based on engineering polymers with high processing temperature are based on the use of expensive and dangerous chemicals and obtaining products with high costs and high impact on the environment. An environmentally friendly solution to improve the thermal stability of natural fibers in thermoplastic composites is the use of nanoparticles such as natural nanosilicates. This work presents the morphostructural and thermal properties of keratin/halloysite binary nanohybrids. Keratin extracted by hydrolysis from chicken feathers (Fig. 1), was mixed with halloysite, a natural aluminosilicate nanotubes in aqueous solution, in a ratio of 2:1, both at acidic and basic pH. The formation and properties of the keratin/halloysite hybrid were investigated by X-ray diffraction (XRD), thermogravimetric analysis (TGA) and scanning electron microscopy (SEM). The obtained results demonstrated that at basic pH the degree of interaction between keratin and halloysite is stronger, favoring obtaining the hybrid in higher concentration and with improved thermal stability by 10% compared to keratin. By uniform dispersing of binary nanohybrid in a bio-polyamide matrix, nanocomposite with improved mechanical and thermal properties was obtained. Applications in automotive industry of bio-polyamide nanocomposite are foreseen.

Keywords: feather keratin, halloysite nanotubes, binary nanohybrides, thermal stability.

Figure 1: Hidrolized keratine extracted from chicken feathers

References:

1. Zahn, M., Wool, R. P. (2011), Mechanical Properties of Chicken Feather Fibers, *Polymer Composites*, 32(6), 937 – 944.
2. Ogunsona, E. O., A Codou,. Misra, M., Mohanty, A. K. (2019), A critical review on the fabrication processes and performance of polyamide biocomposites from a biofiller perspective, *Materials Today Sustainability*, 5, 100014.
3. Franciszczak, P., Taraghi, I., Paszkiewicz, S., Burzynski, M., Meljon, A., Piesowicz, E. (2020), Efect of Halloysite Nanotube on Mechanical Properties, Thermal Stability and Morphology of Polypropylene and Polypropylene/Short Kenaf Fibers Hybrid Biocomposites, *Materials*, 13, 4459.

Acknowledgements:
This work was supported by a grant of the Ministry of Research, Innovation and Digitization, CNCS/CCCDI – UEFISCDI, project number PN-III-P2-2.1-PED-2021-0795, financing contract 701PED/2022, within PNCDI III and also through Program 1 - Development of the national research-development system, Subprogram 1.2-Institutional performance-Projects to finance excellence in RDI, Contract no. 15PFE/2021.

Nanocomposite derived from Local Ilmenite and Monazite for Solid Oxide Fuel Cell Cathode Material

M.Z. Ahmad [1], S. Ahmad [1]
[1] Department of Applied Physics, Faculty of Science and Technology, Universiti Kebangsaan Malaysia, 43600, UKM Bangi, Selangor Darul Ehsan, Malaysia

Abstract:
Solid oxide fuel cell (SOFC), which is well-known as a green energy technology, have experienced phenomenal development in recent years. However, the SOFC faces a challenge in balancing durability, reliability, and cost-effectiveness for commercialization. To overcome this issue, a cost-saving approach is to utilize abundant natural resources for material production. In Malaysia, ilmenite, an iron-based mineral, and monazite, a mineral that contain oxides of lanthanum, are abundant. Therefore, our main objectives are to develop a nanocomposite of $La_{1-x}Sr_xTi_{0.3}Fe_{0.7}$ (LSTF) for cathode materials application using the local extracted minerals from both ilmenite and monazite. Ferric oxide from local ilmenite as well as lanthanum oxide from monazite are extracted with varying degree of purity using extractive metallurgy method. The LSTF powder is prepared using a conventional solid-state reaction, and the symmetrical SOFC is developed through screen-printing with yttria-stabilized zirconia (YSZ) as the electrolyte. Although electrical performance analysis is ongoing, it is predicted that the locally sourced LSTF cathode will perform equally or better than those made from purchased materials due to the presence of impurities with electrical properties such as cerium and neodymium.

Keywords: fuel cells , solid oxide fuel cells, perovskites, electrical properties, microstructure-final, composites, rare earth element, monazite extraction, ilmenite extraction

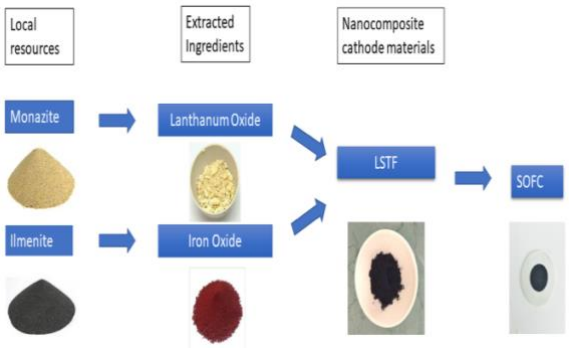

Figure 1: Figure illustrating the SOFC is constructed using LSTF as the cathode part containing both lanthanum and iron extracted from local resources.

References:

1. Che Zainul Bahri, C. N. A., M. Al- Areqi, W., Ab. Majid, A., & Mohd Ruf, M. I. F. (2016). Production Of Rare Earth Elements From Malaysian Monazite By Selective Precipitation. Malaysian Journal of Analytical Science, 20(1), 44–50.
2. Wibowo, D. (2016). Development of Extraction Method and Characterization of TiO2 Mineral from Ilmenite. International Journal of ChemTech Research, 9.
3. 18. Cao, Z., Zhang, Y., Miao, J., Wang, Z., Lü, Z., Sui, Y., Huang, X., & Jiang, W. (2015). Titanium-substituted lanthanum strontium ferrite as a novel electrode material for symmetrical solid oxide fuel cell. International Journal of Hydrogen Energy, 40(46), 16572–16577.

Development of Nanocatalysts Derived from Ferrocene/Ferrocenium

Ekasith Somsook[1]
[1] NANOCAST Laboratory, Center for Catalysis Science and Technology (CAST), Department of Chemistry and Center of Excellence for Innovation in Chemistry, Faculty of Science, Mahidol University, Bangkok, Thailand

Abstract:
Iron oxide/carbon nanocatalysts were successfully synthesized by the calcination of ferrocenium at high temperatures ranging from 500°C to 900°C. Then the synthesized nanocomposites were characterized by XRD, TEM, VSM, BET, TGA, XPS, EPR, and CHN. The prepared nanocatalysts were applied for the decomposition of methylene blue as a model for the treatment of waste water. It was unexpected to discover that the prepared nanocatalysts were highly active for the reaction with methylene blue in the dark even though no excess of hydrogen peroxide was added. The nanocatalyst calcined at 800°C exhibited the rod shape with the best catalytic activity. The nanocatalysts could be reused for 12 times without the significant loss of the catalytic activity.

Keywords: iron oxide; carbon; nanocatalyst; ferrocenium; methylene blue

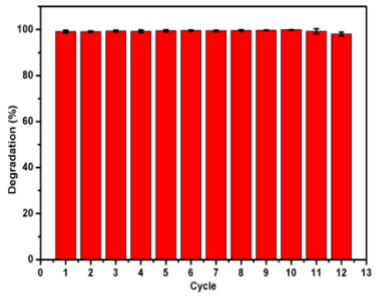

The reusability of nanocatalysts obtained from the calcination temperature at 800°C in the methylene blue degradation

References:

1. Poonsawat, T.; Techalertmanee, T.; Chumkaeo, P.; Yunita, I.; Meechai, T.; Namkajorn, M.; Pornsuwan, S.; Somsook, E. "Facile Synthesis of High Performance Iron Oxide/Carbon Nanocatalysts Derived from the Calcination of Ferrocenium for the Decomposition of Methylene Blue" *Catalysts* **2019**, *9*, 948.
2. Kumpan, N.; Poonperm, T.; Chaicharoenwimolkul, L.; Pornsuwan, S.; Somsook, E. "Ferrocenated Nanocatalysts Derived from the Decomposition of Ferrocenium in Basic Solution and their Aerobic Activities for the Rapid Decolorization of Methylene Blue and the Facile Oxidation of Phenylboronic Acid" *RSC Adv.* **2017**, *7*, 5759-5763.
3. Jinasan, A.; Poonsawat, T.; Chaicharoenwimolkul, L.; Pornsuwan, S.; Somsook*, E. "Highly Active Sustainable Ferrocenated Iron Oxide Nanocatalysts for the Decolorization of Methylene Blue." *RSC Adv.***2015**, *10*, 31324-31328.

Green synthesis of WO_3 nanomaterial and their gas sensing properties

H. Pakdel [1*], V. Galstyan [1,2], E. Comini [1]
[1] Sensor Laboratory, Department of Information Engineering (DII), University of Brescia, Brescia, Italy
[2] Department of Engineering "Enzo Ferrari", University of Modena and Reggio Emilia, Modena, Italy

Abstract:
The industrialization processes have led to the release of various pollutants into the air, which have many destructive effects on human health. Thus, chemical gas sensing devices based on semiconductors are highly required for environmental monitoring because of their low cost, simplicity, small size, and low power consumption.[1] Tungsten trioxide (WO_3), is an electrochemically stable and environmentally friendly n-type semiconductor, which has unique physical and chemical properties. It is one of the most studied materials for the fabrication of conductometric gas sensors.[2] Besides, the preparation of nanostructured materials without using any dangerous capping agent or chemical compounds is a challenging issue to minimize the effects of unsafe reagents.[3] Therefore, the green synthesis of oxide nanomaterials is important for the fabrication of gas sensing devices. In this work, we synthesized nanostructured WO_3 in the aqueous medium using ascorbic acid as a green capping and reducing agent. Furthermore, the effects of various parameters (such as reaction time and capping agent) on the fabrication of material have been studied. Figure 1(a) reports the SEM image of prepared WO_3 nanoparticles, which was prepared by using ascorbic acid. Figure 1(b) displays the XRD pattern of the WO_3 nanomaterial, which indicates that it is crystallized to the monoclinic phase. The gas sensing performance of the structure was examined toward acetone at various temperatures (Figure 1(c)). The obtained results show that the material has a maximum sensing response at 400 °C. Then, the effect of relative humidity (RH) on the functionalities of the material was investigated. The fabricated WO_3 nanoparticles exhibit good and stable responses to acetone at different levels of RH. As can be seen, The materials also showed good selelctivity to acetone compare to the interfering gases at its optimum operating temperature (Figure 1(d)). Thus, we developed an efficient green synthesis method for the preparation of WO_3 nanoparticles and the fabrication of high performance acetone sensors.

Keywords: green synthesis, nanomaterials, WO_3, gas sensing, Acetone detection.

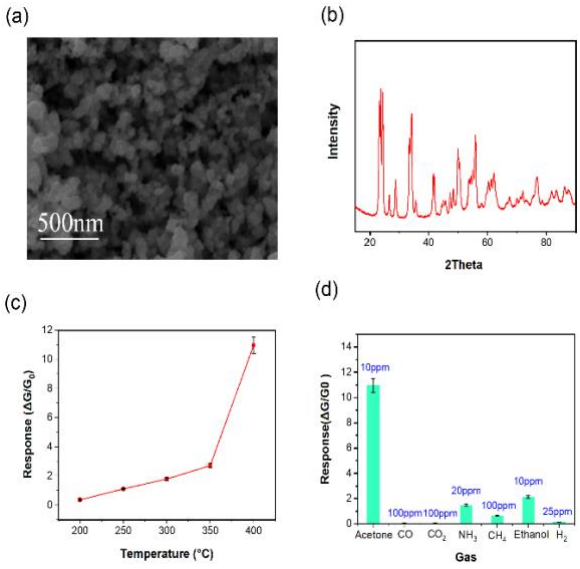

Figure 1: (a) SEM image of the prepared WO_3 nanomaterial. (b) XRD pattern of the WO_3. (c) Gas sensing response of WO_3 toward 10 ppm of acetone at various operating temperatures and 40% of relative humidity. (d) Response of WO_3 to acetone, CO, CO_2, NH_3, CH_4, ethanol, and H_2 at 400 °C.

References:

1. Das, S.; Mojumder, S.; Saha, D.; Pal, M. (2022), Influence of major parameters on the sensing mechanism of semiconductor metal oxide based chemiresistive gas sensors: A review focused on personalized healthcare. Sensors and Actuators B: Chemical, *352*, 131066.
2. Galstyan, V.; Poli, N.; D'Arco, A.; Macis, S.; Lupi, S.; Comini, E. (2020), A novel approach for green synthesis of WO_3 nanomaterials and their highly selective chemical sensing properties. *Journal of Materials Chemistry A*, *8* (39), 20373-20385.
3. Duan, H.; Wang, D.; Li, Y. (2015), Green chemistry for nanoparticle synthesis. *Chemical Society Reviews*, *44* (16), 5778-5792.

Nanosensor Fabrication with Silicon Nanowires

B. Kim, M. Aleem, S. Kundu, T. Selvarathinam[1], J. Park [2]
[1] City University of New York, CCNY, New York, U.S.A.
[2] Korea Research Institute of Ships & Ocean Engineering, South Korea

Abstract:
Silicon nanowires (SiNW) are a promising platform for the highly sensitive electrical detection of biological and chemical analytes. Compared to thin metal film-based sensors, nanowires have extremely high sensitivity to molecules of chemical analytes. Our paper discusses the progress we have made on the synthesis and functionalization of silicon nanowires on a silicon-on-insulator substrate. A fully automated chemical vapor deposition (CVD) system from FirstNano in New York was used to synthesize SiNW on a 4-inch silicon substrate. We adjusted a doping concentration of boron gas to synthesize a longer SiNW. The average length of a silicon nanowire was approximately 16μm, with an approximate width of 50nm. Figure 1 illustrates an SEM image of magnified nanowires on a silicon substrate. After a high quality SiNW was synthesized, we developed nanosensors by utilizing optical lithography and e-beam evaporation. This paper discusses mask designs, elimination of silicon substrate contamination, metal etching and IV curves for a packaged sensor chip. We present results of the UV-Vis measurements after the surface modifications of the nanosensor. The paper presents a highly labor intensive drop-cast method for nano-wires that caused some contamination issues on the nanosensors. We present different chemical agents for surface modifications on SiNWs. These different chemical modifications could be used on SiNWs to attact specific analytes of interest to nanosensors.

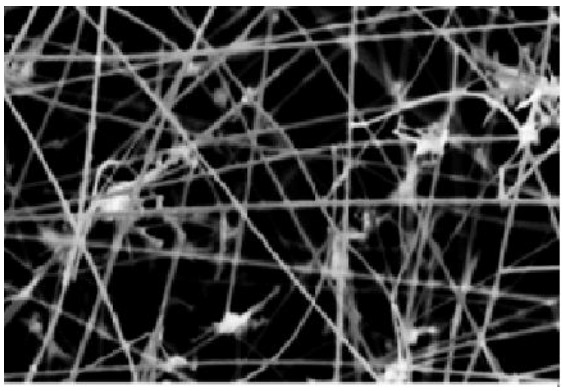

Figure 1: SEM image of silicon nanowires.

Keywords: Silicon nanowires, Surface functionalization, Nanowire synthesis, Contamination

References:

1. Fernando Patolsky, Gengfeng Zheng & Charles M Lieber, “Fabrication of silicon nanowire devices for ultrasensitive, label-free, real-time detection of biological and chemical species,” nature protocols, Vol.1 No.4 (2006) 1711.
2. Nor F. Za’bah, Kelvin S. K. Kwa, Le-on Bowen, Budhika Mendis, and Anthony O’Neill, “Top-down fabrication of single crystal silicon nanowire using optical lithography,” Journal of Applied Physics 112, 024309 (2012).
3. X.T. Vu, R. GhoshMoulick, J.F. Eschermann, R. Stockmann, A. Offenhausser, S. Ingebrandt, “Fabrication and application of silicon nanowire transistor arrays for biomolecular detection,” Sensors and Actuators B 144 (2010) 354–360.
4. B.C. Kim, A. Gupta, J.W. Park, “Development techniques for nano-biosensors,” International Journal of Biosensors & Bioelectronics, Vol. 7, Issue 1, pp. 1-3, 2021.
5. B.C. Kim and A. Gupta,” A Reliable Device Topology for ZnO Nanowire-based Gas Sensors,” Madridge Journal of Nanotechnology & Nanoscience (ISSN: 2638-2075), Volume 4, Issue 1, May 15, 2019.

Acknowledgments
This work was conducted as a part of the research projects under “Development of automatic screening and hybrid detection system for hazardous material detecting in port container” (1525013872) financially supported by the Ministry of Oceans and Fisheries, Korea.

Delamination Mechanics and Electrical Performance of Transferred Vertically Aligned Carbon Nanotube Arrays

L. Lum [1], Y.M. Zhai[1], R.T. Jiang[1], C.W. Tan[1,2], B.K. Tay [1,2]
[1] School of Electrical and Eelctronic Engineering, Nanyang Technological University, Singapore
[2] CNRS-NTU-THALES UMI 3288 CINTRA, Research Techno Plaza, Nanyang Technological University, Singapore

Abstract:
In the past years, research has delved into exploring the potential of carbon nanotubes (CNTs) as a valuable material for electronics. CNTs have been studied as a thermal interface material, interconnects, and for various other applications. Despite their promising qualities, CNTs face several challenges that hinder their extensive use in device applications. For instance, CNTs require high growth temperatures and have interfacial resistance issues. In this work, the impact of the post-growth processes used to facilitate the transfer of vertically aligned carbon nanotube (VACNT) arrays has been characterized by analysing the tensile strength of the bond formed as well as the electrical conductivity of the transferred arrays. Ex-situ grown, VACNT arrays were bonded via a gold thermocompression bonding method onto gold-plated target substrates on each end of the arrays. The I-V characteristics of the substrate-VACNT-substrate structures were then measurered with a 4-point probe to determine the impact of array compression and gold deposition on the VACNT arrays. This work then analyses the delamination mechanics of such bonded VACNT arrays by destructively testing the tensile strength of the bond. The failure analysis of the bonded substrates shows excellent adhesion between the VACNT arrays and the deposited gold layer used for in the thermocompression bonding. This study will allow for a greater understanding of the bonding mechanics of to allow for the exploration of the large-scale integration of CNTs in the electronics of the future.

Keywords: Carbon Nanotubes, Destructive Testing, Electrical Conductivity, Ex-situ Fabrication, Tensile Strength, Thermocompression Bonding

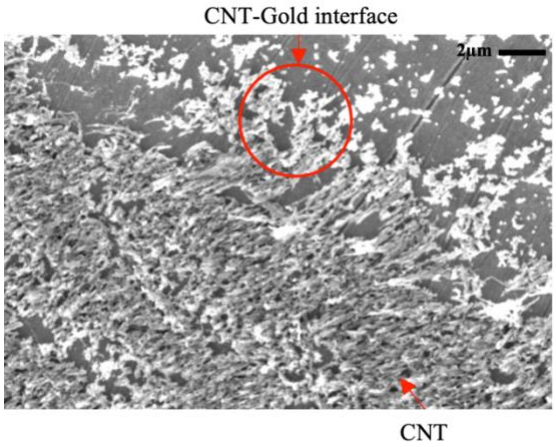

Figure 1: SEM Image of delaminated CNT-gold interface, showing adhesion between the CNTs and deposited gold layer.

References:

1. Lum, L. Y. X. et al., "Development of a CMOS-Compatible Carbon Nanotube Array Transfer Method," *Micromachines* (Basel), vol. 12, no. 1, Jan 18 2021, doi: 10.3390/mi12010095.
2. R. D. Johnson *et al.*, 'Thermocompression bonding of vertically aligned carbon nanotube turfs to metalized substrates', *Nanotechnology*, vol. 20, no. 6, p. 065703, Jan. 2009, doi: 10.1088/0957-4484/20/6/065703.

Multifunctional, bicontinuously phase separated comb copolymer ionogel electrolyte for solid-state supercapacitors

Woo Jin Mun [1], Jong Hak Kim [1,*]
[1] Department of Chemical and Biomolecular Engineering, Yonsei University, Seoul, South Korea

Abstract:
Solid-state electrolytes with high safety and good mechanical property have attracted significant interest as alternatives to conventional liquid electrolytes, which have the risks of flammability and leakage. Herein, we report a high-performance polymer ionogel electrolyte comprising a poly(isobornyl methacrylate)-co-poly(ethylene glycol) methyl ether methacrylate (PIBM-*co*-PEGMA) (PIBEG) amphiphilic comb copolymer for solid-state supercapacitors (SCs). The PIBEG comb copolymer was synthesized *via* facile, cheap, and scalable free radical polymerization, followed by the incorporation of an ionic liquid (IL) to fabricate ion-conducting flexible comb copolymer ionogel electrolytes. The PIBEG/IL electrolytes had a bicontinuously phase separated nanostructure with an ionic conductivity of 4.35 mS cm^{-1}. The solid SC with PIBEG/IL electrolytes exhibited a specific capacitance of 48.6 F g^{-1} and an energy density of 37.12 Wh kg^{-1} at a power density of 1174 W kg^{-1}. Furthermore, SCs could be fabricated without the use of separators or adhesives due to the multifunctional properties of PIBEG/IL electrolytes, including strong adhesion, high conductivity, and good mechanical strength.

Keywords: comb copolymer, ionic liquid, solid-state supercapacitor, polymer electrolyte, copolymerization

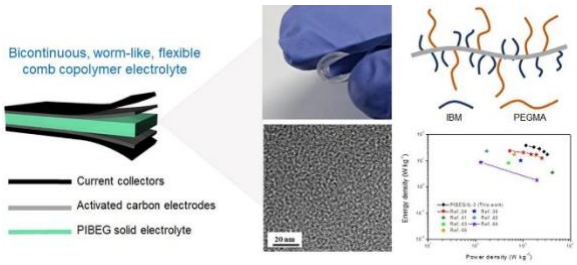

Figure 1: Figure illustrating the assembled PIBEG solid electrolyte-based supercapacitor and its flexibility, nanostructure, and electrochemical property.

References:

W.J. Mun, B. Kim, S.J. Moon, J.H. Kim, Multifunctional, bicontinuous, flexible comb copolymer electrolyte for solid-state supercapacitors. *Chem. Eng. J.*, 454 (2022), 140386.

Fabrication of solid flexible supercapacitors based on adhesively, mechanically strong partially fluorinated comb copolymer electrolyte films

Seung Jae Moon [1], Jong Hak Kim [1,*]
[1] Department of Chemical and Biomolecular Engineering, Yonsei University, Seoul, South Korea

Abstract:
Flexible, solid-state electrolytes exhibiting high electrochemical performance and robust mechanical properties, which can overcome a serious impediment of liquid electrolytes, play a pivital role in fabricating safe, flexible electronics. However, they are still suffering from their inherent, low ionic conductivity to restrict a practical use for energy devices. Herein, we report a flexible solid electrolyte with superior ionic conductivity based on a novel amphiphilic copolymer containing both hydrophobic fluorinated groups and hydrophilic ethylene oxide groups. The polymer electrolytes were prepared by incorporating the ionic liquid, [EMIM][TFSI]. A continuous, well-defined, and micro-phase separated structure was obtained when the IL penetrated into the polymer matrix, and this unique structure can function as ionic channels. The nanostructured ionic channels enhance the ion transport, leading to a high ionic conductivity. When the polymer electrolyte was employed to a supercapacitor with activated carbon-based electrodes, a wide potential window (2.2 V), high energy density (23.2 Wh kg^{-1}), and power density (530 W kg^{-1}) were obtained.

Keywords: polymer electrolyte, comb copolymer, ionic liquid, supercapacitor.

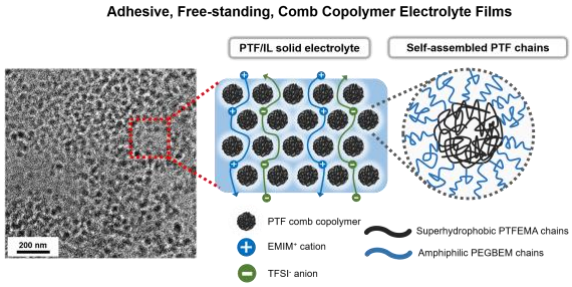

Figure 1: Figure illustrating the facilitated ion transport through PTF/IL comb copolymer electrolyte films in solid supercapacitor.

References:

1. S.J. Moon, H.J. Min, C.S. Lee, D.R. Kang, J.H. Kim, Adhesive, free-standing, partially fluorinated comb copolymer electrolyte films for solid flexible supercapacitors, *Chem. Eng. J.*, 429 (2022), 132240.
2. H. Dai, G. Zhang, D. Rawach, C. Fu, C. Wang, X. Liu, M. Dubois, C. Lai, S. Sun, Polymer gel electrolytes for flexible supercapacitors: recent progress, challenges, and perspectives, *Energy Storage Mater.*, 34 (2021), 320–355.

MoS_2 Nanowormes in-situ sputtered with Molybdenum Nitride Nanoflakes for high-performance Na-ion Supercapacitive Electrodes

B. Ranjan [1], D. Kaur [1,*]

[1] Functional Nanomaterials Research Laboratory, Department of Physics, Indian Institute of Technology Roorkee, Roorkee-247667, Uttarakhand, India

*Corresponding author: davinder.kaur@ph.iitr.ac.in

Abstract:

The present study reports the fabrication of binder-free, low-cost and efficient hybrid supercapacitive electrode based on the hexagonal phase of two-dimensional MoS_2 nanoworms reinforced with molybdenum nitride nanoflakes deposited on stainless steel (SS) substrate using reactive magnetron sputtering technique. The hybrid nanostructured MoS_2-Mo_2N/SS thin film working electrode delivers a high gravimetric capacitance (351.62 F/g at 0.25 mA/cm^2) investigated in 1M Na_2SO_4 aqueous solution. The physisorption/intercalation of sodium (Na^+) ions in electroactive sites of MoS_2-Mo_2N composite ensures remarkable electrochemical performance. The hybrid exhibits superior electrochemically rich performance compared to the pristine MoS_2 and Mo_2N, owing to the synergistic integration of EDLCs and pseudocapacitive characteristics of the constituent layers. Besides increasing the electrical conductivity of the hybrid, the presence of electrochemically active nitrogen and sulfur edges provides remarkable physio-chemical characteristics. The deposited porous nanostructure with good electrical conductivity and better adhesion with the current collector demonstrates a high energy density of 82.53 Wh/kg in addition to a high-power density of 24.98 kW/kg. Further, excellent capacitance retention of 93.62% after 4000 Galvanostatic Charge-Discharge (GCD) cycles elucidated it as a promising candidate for realizing high-performance supercapacitor applications.

Keywords: Pseudocapacitors, Na-ion Storage, Charge-Storage Mechanism, Flexible supercapacitors, High Power Density, High Energy Density, 2D Materials, Sputtering.

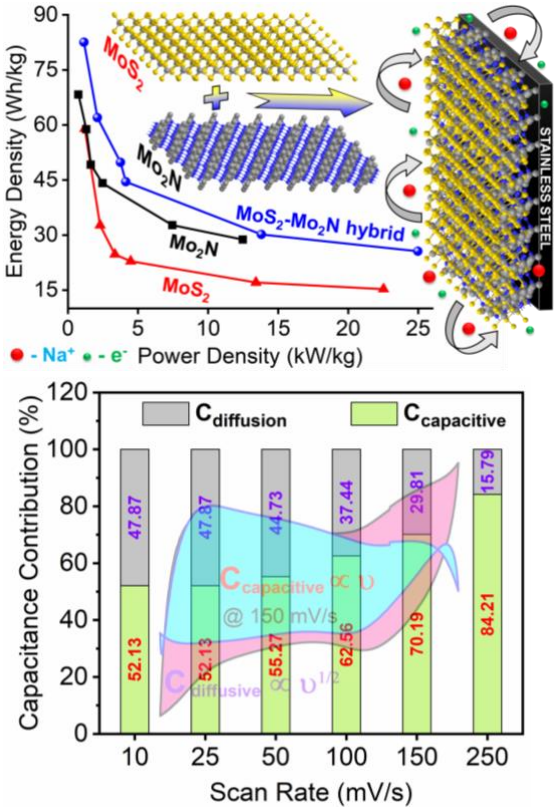

Figure 1: Revealing pseudocapacitive charge storage mechanism in binder-free, low-cost, and efficient supercapacitive electrode based on the hexagonal phase of two-dimensional MoS_2 nanoworms reinforced with molybdenum nitride nanoflakes deposited on stainless steel (SS) substrate using reactive magnetron sputtering technique.

References:

1. Ranjan, B., Sharma, G. K., Malik, G., Kumar, A., & Kaur, D. (2021). In-situ sputtered 2D-MoS2 nanoworms reinforced with molybdenum nitride towards enhanced Na-ion based supercapacitive electrodes. *Nanotechnology*, *32*(45), 455402.

Nanotech / NanoMetrolgy joint session I.B: Nanomaterials Modelling and Characterisation / Nanosafety

Evidence of the release of metals into the environment by the alteration of microplastics and focus on the potential contamination by Cr(VI)

Delphine Vantelon [1], Imane Khatib [1,2,3], Camille Rivard [1,4], Charlotte Catrouillet [2], Julien Gigault [5], Mélanie Davranche [2]

[1] Synchrotron SOLEIL, F-91192 Gif Sur Yvette, France
[2] Lab Geosci Rennes, UMR6118, 263 Ave Gen Leclerc, F-35042 Rennes, France
3 Univ Rennes, IPR Inst Phys Rennes, CNRS, UMR 6251, F-35000 Rennes, France
[4] INRAE, TRANSFORM, F-44316 Nantes, France
[5] Univ Laval, CNRS, UMI3376, TAKUVIK Lab, Quebec City, PQ, Canada

Abstract

The pollution of the environment by an increasing amount of plastic waste is now well established. All environments, water, soil, atmosphere, are contaminated. Biodiversity is therefore potentially at risk, and it is now recognized that the environmental risk is not only due to the presence of plastics but also to their ability to transport and release contaminants, such as metals (1). Metals, both inorganic and organic, are widely used in the formulation of plastic as colorants, anti-oxidants, etc (2). Once released into the environment, plastics are degraded under natural conditions, resulting in the concomitant production of oxidized micro to nano-size plastics particles and the release of metallic additives (3). The speciation of metals and how they are trapped in the plastic matrix determine the species and amounts released into the environment.

Thanks to a µXRF and µXAS study of polyethylene microplastics collected in the North Pacific gyre and altered by long-term photo-oxidation, we were able to observe the large variety of metals present in plastics, linked to their formulation. We were able to demonstrate that these metals are present in different sizes, from nano- to micro-particles, indifferently distributed or concentrated in pockets inside the polymer matrix, which gives them variable release properties during plastic weathering. Similarly, using chromium as an example, we were able to demonstrate that the wide variability of Cr(III) and Cr(VI) species resulting from the plastic formulation were not modified by plastic weathering but released as such into the environment.

Therefore, during oceanic photo-oxidation, nano- to micro-particles of metals are released upon fragmentation of plastic debris, and can further be released as toxic species.

References:

1. Catrouillet C. et al. (2021) Metals in Microplastics: Determining Which Are Additive, Adsorbed, and Bioavailable. *Environ. Sci. Process. Impacts*, *23* (4), 553–558.
2. Hahladakis J. et al. (2018) An overview of chemical additives present in plastics: Migration, release, fate and environmental impact during their use, disposal and recycling. J. Hazard. Mat., 344, 179–199
3. Fotopoulou K.N., & Karapanagioti H.K. (2019) Degradation of Various Plastics in the Environment, in: The Handbook of Environmental Chemistry. Springer International Publishing, Cham, pp. 71–92

A Verified and Validated Finite Element Solution of a Nano-Calibration Problem in Near-Field Scanning Microwave Microscopy[#]

J. T. Fong [1*], P. V. Marcal [2], N. A. Heckert [3], S. Berweger [4], T. M. Wallis [4], K. Genter [4], and P. Kabos [4]

[1] Applied & Computational Math., National Inst. of Standards & Tech., Gaithersburg, MD, U.S.A.
[2] MPACT, CORP., Oak Park, CA, U.S.A.
[3] Statistical Engineering, National Institute of Standards & Technology, Gaithersburg, MD, U.S.A.
[4] Applied Physics Division, National Institute of Standards & Technology, Boulder, CO, U.S.A.
[*] Corresponding author.

Abstract:
To detect nano-thin defects in computer chips, we use a near-field scanning microwave microscope (NSMM), as shown in Fig. 1 and described by Wallis and Kabos [1], with an 84 μm-square by 500 nm-thick calibration specimen containing 24 inclusions each 75 nm thick, as shown in Fig. 2. Using the classical finite element method (FEM) of analysis (see, e.g., Jin [2]) and having it implemented in the AC/DC and RF modules of a FEM software named COMSOL, we developed a FEM model for the NSMM nano-calibration geometry with a probe tip diameter equal to 200 nm. Using an uncertainty-based method to verify the mathematical accuracy of a FEM solution as first proposed by Fong, et al. [3], and the experimental measurements made on the calibration specimen by Kabos and his colleagues [in preparation], we present a verified and validated FEM solution of the NSMM nano-calibration problem. Significance and limitations of the modeling architecture, the analysis technique, and the solution verification/validation process, are discussed.

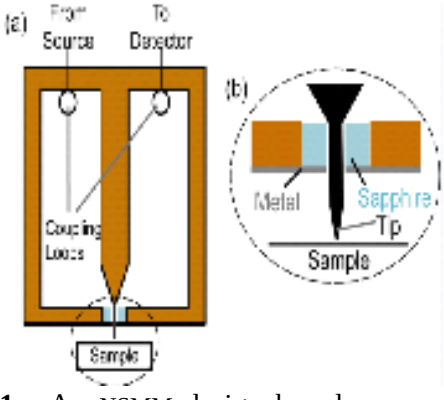

Fig. 1. An NSMM design based on a coaxial resonator. (a) A schematic of the coaxial resonator, operated in transmission mode. (b) A closer view of the prober tip, connected to the center conductor of the resonator and reaching sample through an opening at the bottom of the resonator.

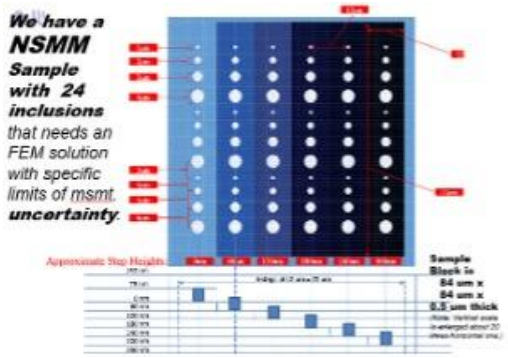

Fig. 2: The NSMM calibration specimen.

Keywords: AC/DC analysis module, applied mathematics, calibration; computer chip defects, COMSOL, finite element analysis, finite element method, finite element model, nano-calibration, nano-metrology, near-field scanning microwave microscope, NSMM, RF analysis module, statistical analysis, solution-validation, solution verification, uncertainty analysis.

References:

1. Wallis, T. M., and Kabos, P., Measurement Techniques for Radio Frequency Nanoelectronics. Cambridge University Press (2017).
2. Jin, J., The Finite Element Method in Electro-magnetics, 2nd ed. Wiley (2002).
3. Fong, J. T., Heckert, N. A., Filliben, J. J., Marcal, P. V., and Rainsberger, R., "Uncertainty of FEM Solutions Using a Nonlinear Least Squares Fit Method and a Design of Experiments Approach," Proc COMSOL Users' Conf, Oct. 7-9, 2015, Boston, MA, www.comsol.com/ed/direct/conf/conference2015papers/papers/ (2015).

Acknoledgment:
Contribution of the National Institute of Standards and Technology.

Towards time- and energy-resolved tabletop XUV photoelectron spectroscopy of solvated nanoparticle systems

Joel Trester [1,*], Pengju Zhang [1], Hans Jakob Wörner[1]
[1] Department of Chemistry and Applied Biosciences, Laboratory of Physical Chemistry, ETH Zürich, Switzerland

Abstract:
XUV photoelectron spectroscopy (PES) is a powerful tool for investigating the electronic properties of materials, but its application to nanoparticle systems in aqueous environments has been limited due to technical challenges. Indeed, due to the large cross-section of water in the XUV energy range, the study of solvated systems was only made possible at high concentrations of the studied substance.[1] As a consequence, the study of solvated nanoparticle systems was so far only possible in low concentrations and using x-ray radiation in the so called "water window".[2] With recent advancements in liquid sample delivery, we report the successful sample delivery of aqueous TiO_2 anatase nanoparticles (spherical, ~40 nm diameter) and subsequent time- and energy-resolved photoelectron spectroscopic measurements. Combining a liquid micro-jet and a magnetic-bottle time-of-flight spectrometer with a monochromatized table-top high-harmonic source, femtosecond time-resolved photoelectron spectroscopy has been performed.

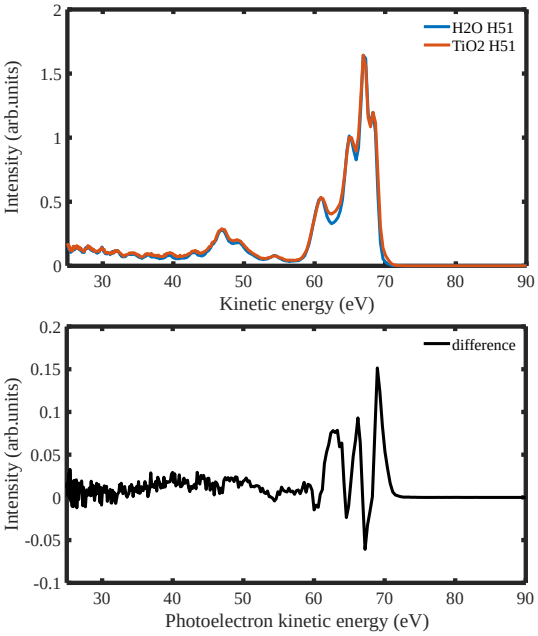

Figure 1: The photoelectron spectrum of TiO_2 in aqueous solution recorded at ~79 eV. The lower plot shows the difference where the water spectrum was subtracted from the TiO_2 spectrum.

Furthermore, using an XUV-NIR (800 nm) pump-probe scheme, time-resolved photoelectron spectroscopy was performed by utilizing the laser-assisted photoelectron technique (LAPE)[3].

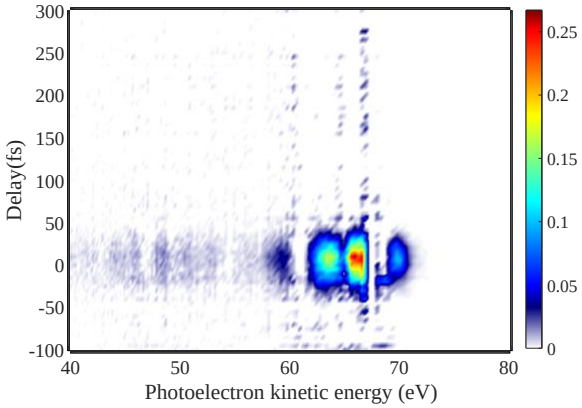

Figure 2: Time-resolved measurement of TiO_2 nanoparticle solution at 79 eV. The features show are sidebands of the main peaks created by one IR absorption or one IR stimulated emission according to the LAPE scheme.

These measurements pave the way for benchmarking measurements of charge carrier as well as early stage photocatalytic dynamics on ultrafast timescales.

Keywords: nanoparticles, photoelectron spectroscopy, ultrashort XUV pulses, solvated nanoparticles systems, time-resolved dynamics

References:

1. Winter, B., Faubel, M. (2006) Photoemission from Liquid Aqueous Solutions, *Chem. Rev.*, 106, 4, 1176–1211
2. Jordan, I. *et al.* (2014), Non-uniform spatial distribution of tin oxide (SnO_2) nanoparticles at the air–water interface, *Chem. Commun.*, 50, 4242-4244
3. Arrell, C. A. *et al.* (2016), Laser-Assisted Photoelectric Effect from Liquids, *Phys. Rev. Lett.*, 117, 143001

Contact Force in Current-Detecting Atomic Force Microscopy – Moving Towards C-AFM Tomography in Photovoltaic Research

M. Hývl [1], M. Ledinský [1], A. Fejfar [1]
[1] Institute of Physics, Academy of Sciences of the Czech Republic, Cukrovarnická 10, 162 00 Prague 6, Czech Republic

Abstract:
With the rise of nanostructured solar cells came the need for nano-characterisation of photovoltaic properties and the best candidate to fulfil this need is, in many cases, scanning probe microscopy (SPM). For electrical characterization, conductive AFM (C-AFM) is the natural candidate of choice. During any current-detecting AFM measurement, we detect current flowing through a circuit that consists of the microscope, the probe tip, cantilever and chip, sample and all the interfaces between them. Aside from spreading resistance of the sample (R_{sample}) we can see that the measurement is dependent on the resistance of the tip (R_{tip}) that changes with the tip material and shape. Most problematic part of the measurement circuit is, however, the electrical contact between the tip and the sample, characterized by R_{cont}.

While there is relatively large number of studies of the environmental effects on the current detection [1], [2] (with unsurprising conclusion that the optimal results can be achieved in protective atmosphere such as nitrogen one or, even better, in vacuum), we would like to focus on closer understanding of the sample geometry, tip-sample electrical contact and its evolution with changing normal contact force between the probe and the sample. A simple demonstration of the evolution of the contact resistance with changing force is demonstrated in Figure 1 that represents the stepping stone for our contact force research.

In my talk, I would like to share findings and thoughts regarding the tip-sample contact resistance and its changes caused by sample topography as well as practical demonstration on how to out-smart these and other inherently present shortcomings of current-detecting AFM in regard to characterization of solar cell electronic properties. Application of two new techniques, Scalpel C-AFM and C-AFM Tomography [3] will be demonstrated, on the silicon solar cell samples.

Keywords: SPM, current-detecting AFM, C-AFM Tomography, Photovoltaics, Solar Cells

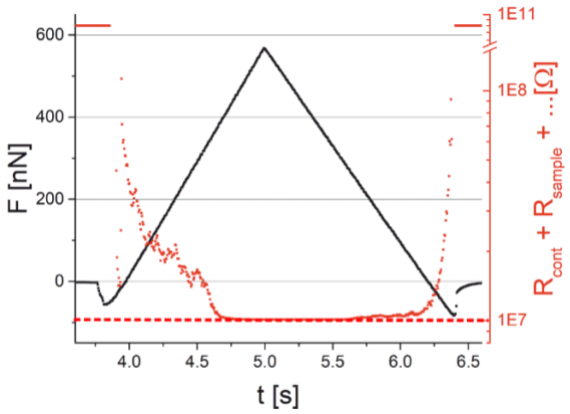

Figure 1: Resistance calculated from the current signal detected during the force ramp with constant negative bias

References:

1. S. A. Sumaiya et al. (2020) 'Improving the reliability of conductive atomic force microscopy-based electrical contact resistance measurements', *Nano Ex.*, vol. 1, no. 3, p. 030023
2. M. Lanza et al. (2010) 'Note: Electrical resolution during conductive atomic force microscopy measurements under different environmental conditions and contact forces', *Review of Scientific Instruments*, vol. 81, no. 10, p. 106110,
3. U. Celano *et al.*, (2013) 'Conductive-AFM tomography for 3D filament observation in resistive switching devices', in *2013 IEEE International Electron Devices Meeting*, p. 21.6.1-21.6.4.

Effect of Gaussian and Bessel laser beams on linear and nonlinear optical properties of vertically coupled cylindrical quantum dots

D.B. Hayrapetyan[1,2]
[1]Russian-Armenian University, 123 Hovsep Emin Str., Yerevan 0051, Armenia
[2]Institute of Chemical Physics National Academy of Science, Republic of Armenia, 5/2, Sevak Street, 0014 Yerevan, Armenia

Abstract:
Vertically coupled quantum dots are one of the most interesting and promising structures, which find their application in a wide range of fields. Particularly, they are noteworthy candidates as a source of single photon and entangled photon pair sources, as qubits and quantum gates in quantum computation, etc. Various external perturbations can act as an instrument for manipulation of properties of these structures and intense laser field is great example of it. In this work, vertically coupled cylindrical quantum dots made of InAs in a GaAs matrix with modified Pöschl-Teller potential have been considered under intense laser field with two laser beam profiles: Gaussian and Bessel. Energy levels and wave functions have been obtained for this structure. Linear and third-order nonlinear absorption coefficients and refractive index changes, second and third harmonic generation susceptibilities have been investigated at different temperatures and for different values of laser parameters.

Keywords: coupled quantum dots, Gaussian beam, Bessel beam, laser radiation, nonlinear absorption, second and third harmonic generation.

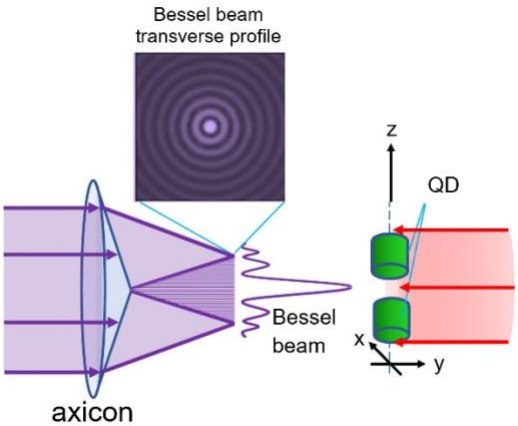

Figure 1: A feasible scheme of the irradiation of vertically coupled QDs by Bessel and Gaussian beams.

In this case, the Hamiltonian of an electron in cylindrical coordinates in the axial direction can be written as:

$$\left[-\frac{\hbar^2}{2m^*}\frac{\partial^2}{\partial z^2}+V\left(z+\alpha(t)\right)\right]\varphi(z,t)=i\hbar\frac{\partial}{\partial t}\varphi(z,t),$$

in which m^* is the effective mass of the electron and $V\left(z+\alpha(t)\right)$ is the confinement potential, where:

$$\alpha(t)=\alpha_0\sin(\Omega t)\hat{z},$$

represents the motion of an electron in a linearly polarized monochromatic laser field, with $\alpha_0=\frac{eA_0}{m^*\Omega}$ being the quiver amplitude or laser-dressing parameter that defines the amplitude of the electron oscillation in the laser field, e is the charge magnitude of the electron, A_0 is the amplitude of the vector potential, Ω is the angular frequency of the non-resonant laser field oriented along z-axis.

References:

1. Biolatti, E., Iotti, R.C., Zanardi, P. and Rossi, F. (2000) Quantum information processing with semiconductor macroatoms. *Physical review letters*, 85 (26), p.5647.
2. Al-Ahmadi, A. (2012) Quantum Dots - A Variety of New Applications. London: IntechOpen.
3. Kouwenhoven, L., (1995). Coupled quantum dots as artificial molecules. *Science*, 268 (5216), p.1440.

Talbot effect in InAs/GaAs coupled cylindrical quantum dots ensemble

P. Mantashyan [1,2,*], G. Mantashian [1,2], D. Hayrapetyan [1,2]
[1] Institute of Chemical Physics after A.B. Nalbandyan of NAS RA, Yerevan, Armenia
[2] Department of General Physics and Quantum Nanostructures, Russian-Armenian University, Yerevan, Armenia

Abstract:
Talbot effect is a self-imaging or lensless imaging phenomenon of a periodic grating illuminated by a collimated light beam at regular distances from the grating [1]. Research on the Talbot effect has recently made significant strides thanks to the quick development of optical superlattices. The emergence of various applications of this effect in fields such as optics, acoustics, X-ray, plasmonics, and information processing has led to the increasing importance of obtaining a Talbot carpet with the use of different structures. In this paper, we investigate the Talbot effect that originates from the tunneling effect between an ensemble of vertically coupled cylindrical InAs/GaAs quantum dots (QDs) [2]. The Talbot carpet can be manipulated by changing the parameters of the QD system.
In the current paper, two modified P¨oschl-Teller potentials were used to model the QDs ensemble (Figure 1). The exciton's lifetime and tunneling time's dependence on the first QD's potential half-width is found for a fixed value of the external electric field. The nonlinear changes in the refractive index and absorption spectrum dependent on the tunneling effect are obtained. Afterward, the Talbot carpet formation is investigated (Figure 2), particularly the dependences of the formed periodic wavefront's visibility on medium length, coupling field's strength,and tunneling parameter. Finally, we have observed the intensity distribution of the diffraction field at Talbot half-distance.

Keywords: coupled quantum dots, InAs/GaAs, tunneling effect, exciton, biexciton, Talbot effect, optical lattice

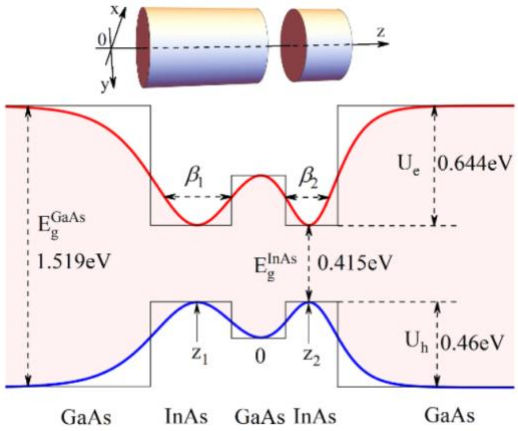

Figure 1: Energy band diagram of InAs/GaAs coupled cylindrical QDs system.

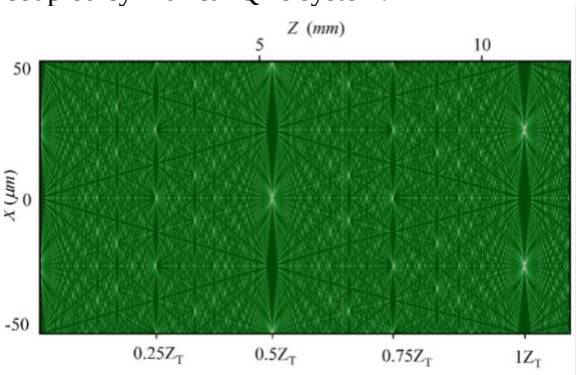

Figure 2: The formation of Talbot carpet from vertically coupled cylindrical QDs ensemble for the maximum value of tunneling parameter

References:

1. Talbot, H. F. (1836) Facts relating to optical science. *Philosophical Magazine*, 9, 401–407.
2. Azizi, B.; Amini Sabegh, Z.; Mahmoudi, M.; Rasouli, S. (2021) Tunneling-induced Talbot effect. *Scientific Reports*, 11(1), 1-14.

Wrinkling and crumpling in twisted few and multilayer CVD graphene: High density of edge modes influencing Raman spectra

D. Nikolaievskyi[1,3], M. Torregrosa[1], A. Merlen[2], S. Clair[2], O. Chuzel[3], J.-L. Parrain[3], T. Neisus[4], A. Campos[4], M. Cabie[4], C. Martin[1], C. Pardanaud[*1]

[1]Aix Marseille Univ, CNRS, PIIM, AMUTech, Marseille, France
[2]Aix Marseille Univ, Université de Toulon, CNRS, IM2NP, Marseille, France
[3]Aix Marseille Univ, CNRS, Centrale Marseille, iSm2, AMUTech, Marseille, France
[4]Aix Marseille Univ, CNRS, Centrale Marseille, FSCM, Marseille, France

Abstract:
Richness and complexity of Raman spectra related to graphene materials is established from years to decades, with, among others: the well-known G, D, 2D,... bands plus a plethora of weaker bands related to disorder behavior, doping, stress, crystal orientation or stacking information [1]. Herein, we report on how to detect crumpling effects in Raman spectra, using a large variety of few and multilayer graphene [2]. The main finding is that these crumples enhance the G band intensity like it does with twisted bi layer graphene. We updated the D over G band intens
ity ratio versus G band width plot, which is generally used to disentangle point and linear defects origin, by reporting surface defects created by crumples, introducing '2D defects'. Moreover, we report for the first time on the existence 23 resonant additional bands. These bands are only observed at 633 nm, with a resonance mechanism to identify and complete attribution still to be made. Twelve of these twenty-three bands are observed in the range 600-1600 cm^{-1}. The eleven other bands are observed at higher wavenumber, and are interpreted as second harmonic or a combination of the twelve wavenumbers cited previously. We attribute these bands to edge modes formed by high density of crumples and thanks to a literature survey. We use Raman plots (2D bands versus G band positions and widths) to gain qualitative information about the way layers are stacked [3]. For some samples, we also report on the Raman behavior of low frequency shear and layer breathing modes.

Keywords: modified graphene, multilayer graphene, Raman microscopy, wrinkles, 2D defects

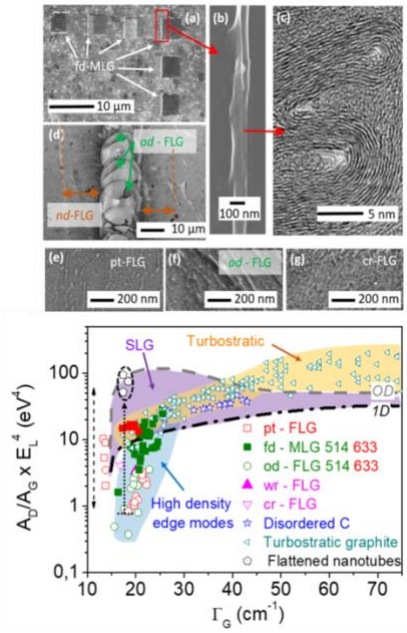

Figure 1: D band over G Raman band intensity ratio in function of G band width to identify new 2D defective carbons for many multilayers.

References:

1. A. Merlen, J. G. Buijnsters and C. Pardanaud A Guide to and Review of the Use of Multiwavelength Raman Spectroscopy for Characterizing Defective Aromatic Carbon Solids: from Graphene to Amorphous Carbons. **Coatings** *7* (2017), 153
2. D. Nikolaievskyi, et al. Wrinkling and crumpling in twisted few and multilayer CVD graphene: High density of edge modes influencing Raman spectra. **Carbon** 203 (2023) 650
3. C. Pardanaud, et al. Forming weakly interacting multi layers of graphene by using AFM tip scanning and evidence of competition between inner and outer Raman scattering processes piloted by structural defects. **The Journal of Physical Chemistry Letters** 10 (2019) 3571

*Corresponding author. Tel: +334 13 94 64 59. E-mail: cedric.pardanaud@univ-amu.fr

Degradation processes in two-dimensional lead iodide perovskites studied by Photoemission

Marie Krecmarova,[1] Jesús Rodríguez-Romero,[2] Iván Mora-Seró,[2] Juan P. Martínez-Pastor,[1] Maria C. Asensio,[3] Juan F. Sánchez-Royo[1]*
[1]Juan.F.Sanchez@uv.es, Materials Science Institute, University of Valencia, 46100 Paterna, Valencia, Spain
[2] Institute of Advanced Materials (INAM), Universitat Jaume I, 12006 Castellón, Spain.
[3] ICMM-CSIC Materials Science Institute of Madrid, 28049 Cantoblanco, Madrid, Spain.
*lead presenter

Abstract:
2D halide perovskites hold a great promise for electronics and optoelectronics applications due to the structural diversity, high absorption and photoluminescence, and tunable bandgap. Especially, they are one of the most promising studied material for photovoltaics. However critical issue is their low stability to ambient environment conditions. In this work, we have investigated degradation processes of 2D halide perovskites upon external factors such as oxygen, humidity, light, heat and photo-induced exposition. We have applied X-ray photoemission spectroscopy techniques, as well as optical techniques (micro-photoluminescence, micro-Raman spectroscopy), to demonstrate that 2D perovskites easy degrade upon heat and laser illumination in atmospheric conditions. Surprisingly, we have found a different aging chemical processes after crystal exposition to long periods (up to 1 year) in atmospheric conditions with and without the presence of external light. Crystals exposed to light aged into morphology with micro-holes and they are not photoluminescent active. On the other hand, crystals under dark conditions show wire-like morphology maintaining photoluminescence. The degradation processes finally results in removal of organic part from the crystal and formation of lead and iodine vacancies, which are probably related to side non-radiative recombination mechanisms responsible for the photoluminescence degradation. These vacancies are associated with crystal decomposition into PbI_2, metallic Pb, and Pb oxides. This work is benefical for development of long-term stable perovskite devices with an enhanced optical performance.

Is the Surface of Hofmann-like Spin-Crossover {Fe(pz)[Pt(CN)$_4$]} Same as its Bulk?

A. Martínez Serra [1*], A. Dhingra [1], M. C. Asensio [2,3], J. A. Real [4], and J. F. Sánchez Royo [1,3]
[1] Institut de Ciència dels Materials de la Universitat de València (ICMUV), University of Valencia, Carrer del Catedrátic José Beltrán Martinez, 2, 46980 Paterna, Valencia, Spain
[2] Materials Science Institute of Madrid (ICMM/CSIC), Cantoblanco, E-28049 Madrid, Spain
[3] MATINÉE, the CSIC Associated Unit between the Materials Science Institute (ICMUV) and the ICMM, Cantoblanco, E-28049 Madrid, Spain
[4] Institut de Ciència Molecular (ICMol), University of Valencia, Carrer del Catedrátic José Beltrán Martinez, 2, 46980 Paterna, Valencia, Spain

Abstract:
Temperature dependent X-ray photoemission spectroscopy (XPS) has been employed to examine the Fe 2p and N 1s core levels of the Fe(II) spin crossover (SCO) complex {Fe(pz)[Pt(CN)$_4$]}. The temperature-dependent variations in the Fe 2p core-level spectrum provide clear evidence of the spin-state transition in this SCO complex, which is consistent with one's expectations and the existing literature. A lack of discernible temperature-driven shifts in the binding energies of both the N 1s core-level components indicates that the HS electronic configuration of this molecule is somewhat immune to thermal fluctuations. The high-spin fraction versus temperature plot, extrapolated from the XPS measurements, reveals that the surface of {Fe(pz)[Pt(CN)$_4$]} is in the high-spin state at room temperature, rendering it promising for room-temperature spintronics and quantum information science applications.

Keywords: spin-crossover complexes, spin-state transition, X-ray photoemission spectroscopy; magnetic susceptibility, surface effects, room-temperature spintronics.

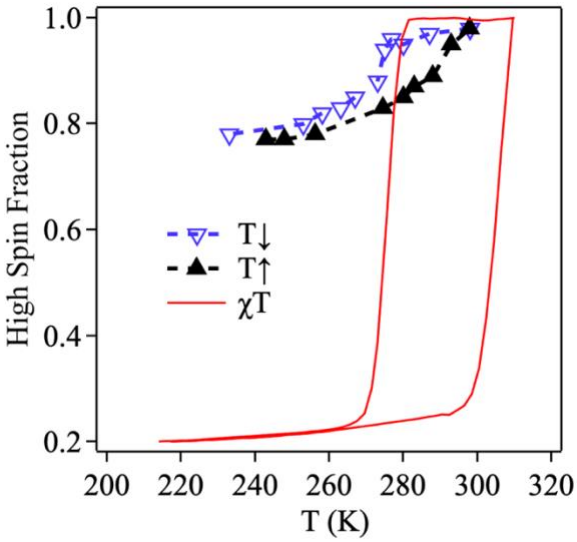

Figure 1: Normalized high-spin fraction of {Fe(pz)[Pt(CN)$_4$]}, extrapolated from XPS (solid black and hollow blue triangles) and magnetic susceptibility measurements (red curve), as a function of temperature.

References:

1. Levchenko, G., Gaspar, A. B., Bukin, G.; Berezhnaya, L., Real, J. A. (2018), Pressure Effect Studies on the Spin Transition of Microporous 3D Polymer [Fe(Pz)Pt(CN)$_4$], *Inorg Chem*., 57, 8458–8464.
2. Ohba, M., Yoneda, K., Agustí, G., Muñoz, M. C., Gaspar, A. B., Real, J. A., Yamasaki, M., Ando, H., Nakao, Y., Sakaki, S., Kitagawa, S. (2009), Bidirectional Chemo-Switching of Spin State in a Microporous Framework. *Angew. Chem. Int. Ed.*, 48, 4767–4771.

Surface Stabilisation of the High-Spin State of Fe(II) Spin-Crossover Complexes

A. Dhingra [1*], A. Martínez Serra [1], M. C. Asensio [2,3], J. A. Real [4], and J. F. Sánchez Royo [1,3]
[1] Institut de Ciència dels Materials de la Universitat de València (ICMUV), University of Valencia, Carrer del Catedrátic José Beltrán Martinez, 2, 46980 Paterna, Valencia, Spain
[2] Materials Science Institute of Madrid (ICMM/CSIC), Cantoblanco, E-28049 Madrid, Spain
[3] MATINÉE, the CSIC Associated Unit between the Materials Science Institute (ICMUV) and the ICMM, Cantoblanco, E-28049 Madrid, Spain
[4] Institut de Ciència Molecular (ICMol), University of Valencia, Carrer del Catedrátic José Beltrán Martinez, 2, 46980 Paterna, Valencia, Spain

Abstract:
Temperature dependent X-ray photoemission spectroscopy (XPS) has been employed to examine the Fe 2p and N 1s core levels of the studied Fe(II) spin crossover (SCO) complexes of interest, namely: $Fe(phen)_2(NCS)_2$, $[Fe(3\text{-}Fpy)_2\{Ni(CN)_4\}]$, and $[Fe(3\text{-}Fpy)_2\{Pt(CN)_4\}]$. The changes in the Fe 2p core-level spectra with temperature indicate spin state transitions in these SCO complexes, which are consistent with one's expectations and the existing literature. Additionally, the temperature dependence of the binding energy of the N 1s core-level provides further physical insights into the ligand-to-metal charge transfer phenomenon in these molecules. The high-spin fraction versus temperature plots reveal that the surface of each of the molecules studied herein is found to be in the high-spin state at temperatures both in the vicinity of room temperature and below their respective transition temperature alike, with the stability of the high-spin state of these molecules varying with the choice of ligand.

Keywords: spin-crossover complexes, spin-state transition, X-ray photoemission spectroscopy; magnetic susceptibility, surface effects.

References:

1. Gallois, B., Real, J. A., Hauw, C., and Zarembowitch, J. (1990), Structural changes associated with the spin transition in bis(isothiocyanato)bis(1,10-phenanthroline)iron: a single-crystal x-ray investigation, *Inorg. Chem.*, 29, 1152–1158.
2. Martínez, V., Gaspar, A. B., Muñoz, M. C., Bukin, G. V., Levchenko, G., and Real, J. A. (2009), Synthesis and Characterisation of a New Series of Bistable Iron(II) Spin-Crossover 2D Metal–Organic Frameworks, *Chemistry - A European Journal*, 15, 10960–10971.

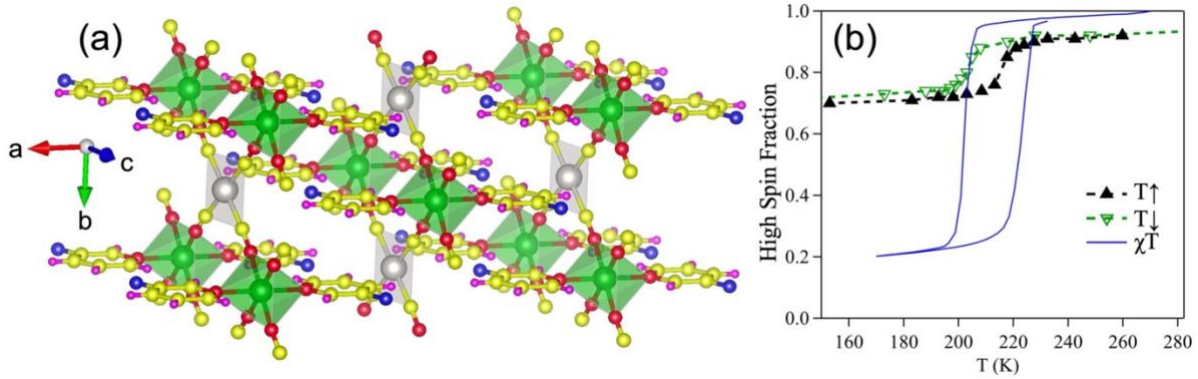

Figure 1: (a) Ball-and-stick model of the 2D Hofmann-like $[Fe(3\text{-}Fpy)_2\{Ni(CN)\}_4]$ with the Fe (green), Ni/Pt (silver), N (red), C (yellow), F (blue), and H (purple) atoms. (b) Normalized high-spin fraction of $[Fe(3\text{-}Fpy)_2\{Ni(CN)\}_4]$, extrapolated from XPS (black and green triangles) and magnetic susceptibility measurements (blue curve), as a function of temperature providing clear evidence of the spin-state transition.

Machine Learning-based Prediction and Inverse Design of 2D Metamaterial Structures with Tunable Deformation-Dependent Poisson's Ratio

Xianqiao Wang [1*], Jie Tian [2], Keke Tang [2]
[1] School of ECAM, University of Georgia, Athens, GA, 30602, USA
[2] School of Aerospace Engineering and Applied Mechanics, Tongji University, Shanghai 200092, China

Abstract:
With the aid of recent efficient and prior knowledge-free machine learning (ML) algorithms, extraordinary mechanical properties such as negative Poisson's ratio have extensively promoted the diverse designs of metamaterials with distinctive cellular structures. However, most existing ML approaches applied to the design of metamaterials are primarily based on a single property value with the assumption that the Poisson's ratio of a material is stationary, neglecting the dynamic variability of Poisson's ratio, termed deformation-dependent Poisson's ratio, during the loading process a metamaterial other than conventional materials may experience. This paper first proposes a crystallographic symmetry-based methodology to build 2D metamaterials with complex but patterned topological structures, and then convert them into computational models suitable for molecular dynamics simulations. Then we employ an integrated approach, consisting of molecular dynamics simulations competent to generate and collect a large dataset for training/validation, and ML algorithms (CNN and cycle-GAN) able to predict the dynamic characteristics of Poisson's ratio, as well as to offer the inverse design of a metamaterial structure based on a target quasi-continuous Poisson's ratio-strain curve, to eventually unravel the underlying mechanism and design principles of 2D metamaterial structures with tunable Poisson's ratio. The close match between the predefined Poisson's ratio response and that from the generated structure validates the feasibility of the proposed ML model. Thanks to high efficiency and complete independence from prior knowledge, our proposed approach offers a novel and robust technique for the prediction and inverse design of metamaterial structures with tailored deformation-dependent Poisson's ratio, an unprecedented property attractive in flexible electronics, soft robotics, nanodevices, etc.

Keywords: negative Poisson's ratio, 2D metamaterials, CNN, Cycle-GAN, inverse design

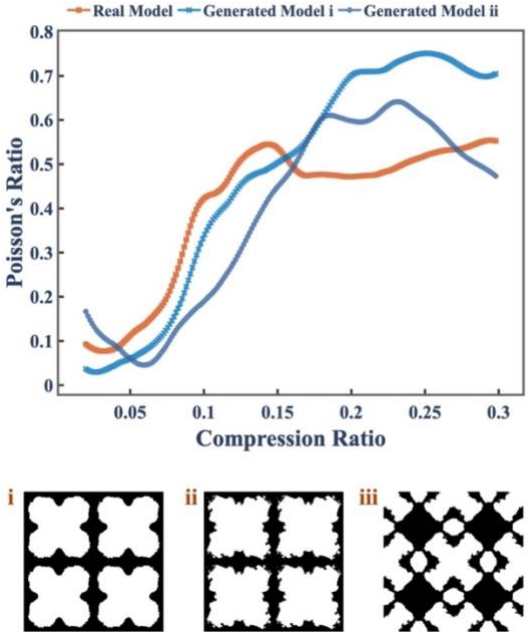

Figure 1: Figure illustrating the fundamental question that we are tempting to solve computationally: how to use the machine learning algorithm to help design 2D metamaterials with targarted Poisson's ratio.

References:

1. H. Wang, Y. X. Zhang, W. Q. Lin, and Q. H. Qin, "A novel two-dimensional mechanical metamaterial with negative Poisson's ratio," , Computational Materials Science, vol. 171, Jan 2020, doi: ARTN 109232.
2. W. Jin, W. Sun, X. Kuang, C. Lu, and L. Kou, "Negative Poisson Ratio in Two-Dimensional Tungsten Nitride: Synergistic Effect from Electronic and Structural Properties," J Phys Chem Lett, vol. 11, no. 22, pp. 9643-9648, Nov 19 2020, doi: 10.1021/acs.jpclett.0c02703.

Determination of Diazonium Compounds For Modification Silver Nanoparticles in Estrogen Detection using DFT calculation

S. Srisung[1]*, S. Nilrattanakoon[1], N. Wasukan[2]
[1]Department of Chemistry, Faculty of science, Srinakharinwirot University
[2]Toxicology and Bio Evaluation Service Center (TBES), National Science and Technology Development Agency

Abstract:
In humans, synthetic estrogens are used for medical purposes, such as hormone therapy for treatment of menopausal symptoms and the use of the combined oral contraceptive pill (COCP). However, long-term estrogen use may lead to serious health risks, such as ovarian cancer and breast cancer. Furthermore, contamination of estrogens are dangerous for fish because estrogens affect male fish. This study focused on the development of diazonium ligand as a colorimetric sensor in estradiol detections. In addition, computational chemistry was used to calculate the structures and energy of molecules and complexes. Silver nanoparticles (AgNPs) were synthesized by reducing silver(I) nitrate solution with sodium borohydride. Diazonium salts of sulfanilamide (Azo1) and sulfanilic acid (Azo2) were synthesized by dissolved sulfanilamide or sulfanilic acid in nitric acid before adding sodium nitrite to the solutions. After that, Diazonium salt and AgNPs solutions were applied for estradiol detection. The structural optimization and binding energies were determined using the density functional (DFT) calculation with B3LYP/6-311G(d,p) method. The results show binding behavior and indicated the chemical interaction of complexes. Therefore, this studies can determine the detection of estrogen and be applying to environment and health risks.

Keywords: estrogen, density functional, Diazonium salt, Silver nanoparticles

References:

1. C. Wang, et al. (2018), Adverse Effects of Triclosan and Binary Mixtures with 17β-Estradiol on Testicular Development and Reproduction in Japanese Medaka (Oryzias latipes) at Environmentally Relevant Concentrations, Environmental Science & Technology Letters, 5, 136-141.
2. F. Vaiano, et al. (2014) Enhancing the sensitivity of the LC-MS/MS detection of propofol in urine and blood by azo-coupling derivatization Anal Bioanal Chem, 406, 3579-3587.
3. Wasukan, N. , et al. (2015), Interaction evaluation of silver and dithizone complexes using DFT calculations and NMR analysis, Spectrochimica Acta Part A: Molecular and Biomolecular Spectroscopy, 149, 830-838.

MetamaterialFinder: A Software Framework for Discovering and Analyzing Mechanical Metamaterials Based on Simple Closed Curves

M. Fleisch [1*], A. Thalhamer [1], G. Pinter [2], S. Schlögl [1], M. Berer [1]
[1] Polymer Competence Center Leoben GmbH, Leoben, Austria
[2] Department of Polymer Engineering and Science, Montanuniversitaet Leoben, Leoben, Austria

Abstract:
Mechanical metamaterials have gained a lot of research interest over the last years due to their unusual mechanical properties and potential for structural applications. However, the design and analysis of mechanical metamaterials remains challenging and time consuming. Herein, we present a software framework for automated creation, finite element modeling and analysis of 2.5D mechanical metamaterials based on simple closed curves. By generalizing 2.5D unit cells with pores defined by simple closed curves, a wide variety of existing and novel metamaterials can be created and analyzed. Each pore can either be empty or filled with one or more materials, resulting in single- or multi-material metamaterials. Since part of the mechanical response of a metamaterial is defined by the geometric parameters of a unit cell, parameter studies are directly integrated into the framework. Examples of well-established mechanical metamaterials were used as benchmark structures and compared to their analytical solutions. We also demonstrate how generalized curves can further improve the mechanical properties of these structures. For example, the load bearing capabilities and range of Poisson's Ratios. Furthermore, novel single- and multi-material designs of mechanical metamaterials with tunable Poisson's Ratio are presented and analyzed with the proposed framework (see Figure 1). The framework is implemented in Python, executed via ABAQUS and allows for unit-cell based homogenization and full-scale 2D and 3D simulations. The scripts are made open source and publicly available.

Keywords: metamaterials, design, automation, numerical simulations, optimization, mechanical properties, Poisson's ratio, Young' modulus

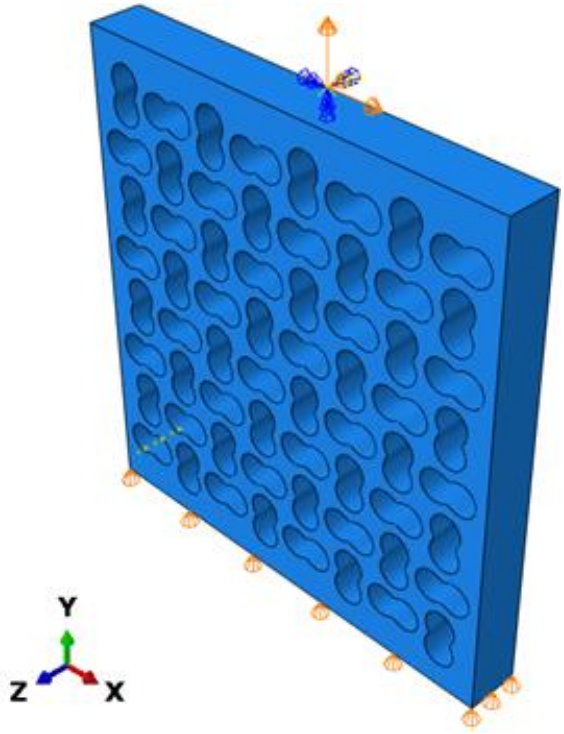

Figure 1: Example structure with hippopede shaped pores created with the software toolbox MetamaterialFinder with tunable Poisson's Ratio.

References:

1. Fleisch, M., Thalhamer, A., Meier, G., Raguž, I., Fuchs, P.F., Pinter, G., Schlögl, S., Berer, M. (2021) Functional mechanical metamaterial with independently tunable stiffness in the three spatial directions, *Mater. Today Adv.*, 11
2. Fleisch, M., Thalhamer, A., Meier, G., Fuchs, P.F., Pinter, G., Schlögl, S., Berer, M. (2022) Asymmetric chiral and antichiral mechanical metamaterial with tunable Poisson's ratio, *APL Mater.*, 10
3. Fleisch, M., Thalhamer, A., Meier, P.A.F., Huber., Fuchs, P.F., Pinter, G., Schlögl, S., Berer, M. (2023) Chiral-based mechanical metamaterial with tunable normal-strain shear coupling effect, *Eng. Struct..*, 284

In Operando Spectroscopic Ellipsometry Investigation of MOF Thin Films for the Selective Capture of Acetic Acid

S.Dasgupta [1], S.Biswas [1], K.Dedecker[1], E. Dumas[1], N. Menguy[2], B. Berini[3], B. Lavedrine[4], C. Serre [5,], C. Boissière[6,*], and N. Steunou[1,*]

[1] Institut Lavoisier de Versailles, UMR CNRS 8180, Université de Versailles St Quentin en Yvelines, Université Paris Saclay, 78035 Versailles, France

[2] UMR CNRS 7590, MNHN, IRD, Institut de Minéralogie, de Physique des Matériaux et de Cosmochimie (IMPMC), Sorbonne Université, 75005 Paris,France

[3] Groupe d'Etudes de la Matière Condensée, UMR CNRS 8635, Université de Versailles St Quentin en Yvelines, Université Paris Saclay, 78035 Versailles, France

[4] Centre de Recherche sur la Conservation, UAR CNRS 3224, Muséum National d'Histoire Naturelle, 75005 Paris, France

[5] Institut des Matériaux Poreux de Paris (IMAP), Ecole Normale Supérieure de Paris, ESPCI Paris, CNRS, PSL University, 75005 Paris, France

[6] CNRS, Collège de France, UMR Chimie de la Matière Condensée de Paris, Sorbonne Université,75005 Paris, France

Abstract:

The emission of polar volatile organic compounds (VOCs) is a major worldwide concern of air quality and equally impacts the preservation of cultural heritage (CH). The challenge is to design highly efficient adsorbents able to selectively capture traces of VOCs such as acetic acid (AA) in the presence of relative humidity (RH) normally found at storage in museums (40−80%). Although the selective capture of VOCs over water is still challenging, metal-organic frameworks (MOFs) possess some significant tunable features such as Lewis, Bronsted, or redox metal sites, functional groups, hydrophobicity, etc which are suitable for selective capture of a large variety of VOCs. In this context, we have explored the adsorption efficiency of a series of MOFs thin films (ZIF-8(Zn), MIL-101(Cr), and UiO-66(Zr)-2CF_3) for the selective capture of AA close to realistic environmental storage conditions of cultural artifacts (2−6% of relative pressure of AA under 40% of RH) using UV/vis and FT-IR spectroscopic ellipsometry in operando study. For that purpose, optical quality thin films of MOFs were prepared by dip-coating method, and their AA adsorption capacity and selectivity were evaluated under humid conditions by measuring the variation of the refractive index as a function of the vapor pressures while the chemical nature of the coadsorbed analytes (water and AA) was identified by FT-IR ellipsometry. While thin films of ZIF-8(Zn) strongly degraded upon exposure to AA/water vapors, films of MIL-101(Cr) and UiO-66(Zr)-2CF_3 present a high chemical stability under those conditions. It was shown that MIL-101(Cr) presents a high AA adsorption capacity due to its high pore volume but exhibits a poor AA adsorption selectivity under humid conditions. In contrast, UiO-66(Zr)-2CF_3 was shown to overpass MIL-101(Cr) in terms of AA/ H_2O adsorption selectivity and AA adsorption/desorption cycling stability because of its high hydrophobic character, suitable pore size for adequate confinement, and specific interactions.

Keywords: MOFs, volatile organic compounds, adsorption, thin films, ellipsometry

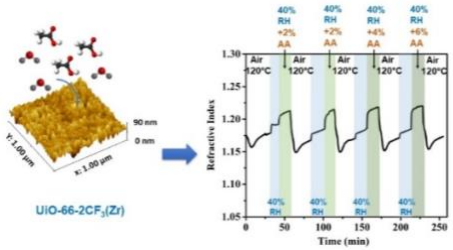

Figure 1: Ellipsometric experiment performed with MOF thin films.

References:

1. Dasgupta, S; Biswas, S.; Dedecker, K.; Dumas, E.; Menguy, N.; Berini, B; Lavedrine, B; Serre, C.; Boissière, C ; Steunou, N. In Operando Spectroscopic Ellipsometry Investigation of MOF Thin Films for the Selective Capture of Acetic Acid. *ACS Appl. Mater. Interfaces* 2023, *15*, 6069-6078.
2. Dedecker, K.; Pillai, R. S.; Nouar, F.; Pires, J.; Steunou, N.; Dumas, E.; Maurin, G.; Serre, C.; Pinto, M. L. Metal-Organic Frameworks for Cultural Heritage Preservation: The Case of Acetic Acid Removal. *ACS Appl. Mater. Interfaces* 2018, *10*, 13886-13894.
3. Biswas, S.; Haouas, M.; Freitas, C.; Soares, C. V.; Al Mohtar, A.; Saad, A.; Zhao, H.; Mouchaham, G.; Livage, C.; Carn, F.; Menguy, N.; Maurin, G.; Pinto, M. L.; Steunou, N. Engineering of Metal- Organic Frameworks/Gelatin Hydrogel Composites Mediated by the Coacervation Process for the Capture of Acetic Acid. Chem. Mater. 2022, 34, 9760-9774.

Nanotech / GAMS 2023 - Joint Session II.A - Nanocoatings/ Thin films and nanostructured surfaces

Liquid crystals, topological defects and nanoparticles

Emmanuelle Lacaze[1]
[1] Institut des Nano-Sciences de Paris (INSP), CNRS, Sorbonne University, Paris, France

Abstract:
The synthesis of colloidal nanoparticles in solution now makes it possible to cover a wide range of specific properties for nanoparticles depending on their nature, size and shape, such as magnetic, catalytic or optical properties. Optical properties in particular consist in light absorption for metallic nanoparticles in relation to the so-called plasmonic resonance, or in light emission at well-defined wavelengths for semi-conducting nanoparticles. Controlling these optical properties involves controlling the organisation and orientation of these nanoparticles on a substrate after they have been deposited from solution, on a macroscopic scale. I will show how a unique nanoparticle organization of controlled orientation can be achieved everywhere on a given sample using a liquid crystal matrix made of arrays of topological defects. The defects confine nanoparticles leading to the formation of original nanoparticle assemblies templated by the defect geometry [1]. I will show how X-ray scattering measurements performed at synchrotron facilities combined with optical microscopies and spectroscopies reveal both the liquid crystal defect structure and the nanoparticle assembly structure, ultimately allowing to understand the intimate interaction between liquid crystal defects and nanoparticles [2, 3, 4]. We are now able to form nanoparticle assemblies of various nature depending on the liquid crystal defect which is chosen for the confinement, on the nanoparticle size and shape. Confinement of nanoparticles by oriented defects finally lead to the emergence of new kinds of optical properties, that become activated by external parameters like incident light polarization or temperature.

Keywords: nanoparticle optical properties, fluorescence, plasmonic resonance, x-ray scattering, synchrotron, liquid crystals, topological defects.

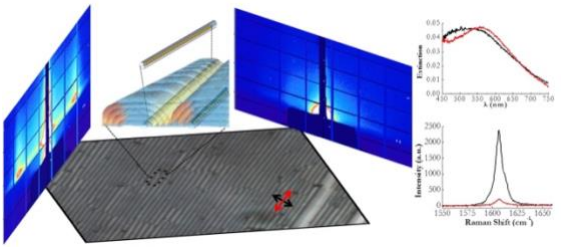

Figure 1: Scheme of chains of gold nanospheres confined in smectic toplogical defects and measured combining Optical Microscopy (below), ellipsometry (above), GISAXS (on the left and right), spectrophotometry (right top) and Raman spectroscopy (right bottom).

References:

1. Zappone, B. and Lacaze E. (2022), One-dimensional patterns and topological defects in smectic liquid crystal films films, *Liq. Cryst. Rev*. https://doi.org/10.1080/21680396.2022.2076748
2. Coursault, D., Zappone, B., Coati, A., Boulaoued A., Pelliser L., Limagne D., Boudet N., Haj Ibrahim B., de Martino A., Alba M., Goldmann M., Garreau Y., Gallas B. and Lacaze E. (2016), Self-organized arrays of dislocations in thin smectic A films, *Soft Matter*,. **12**, p.678-688.
3. Do S.-P., Missaoui A., Coati A., Resta A., Goubet N., Wojcik M. M., Choux A., Royer S, Briand E., Donnio B., Gallani J-L., Pansu B., Lhuillier E., Garreau Y., Babonneau D., Goldmann M., Constantin D., Croset B., Gallas B. and Lacaze E. (2020), From Chains to Monolayers: Nanoparticle Assembly Driven by Smectic Topological Defects, *Nano Letters*, **20**, 1598-1606.
4. Jeridi, H. Niyonzima, J. D., Sakr, C., Missaoui, A., Shahini, S., Vlad, A., Coati, A., Goubet, N., Royer, S., Vickridge, I., Goldmann, M., Constantin, D., Garreau, Y., Babonneau, D., Croset, B., Gallas, B., Lhuillier E. and Lacaze, E. (2022), Unique orientation of 1D and 2D nanoparticle assemblies confined in smectic topological defects, *Soft Matter* **18** 4792-4802.

Ultrathin NiFe nanoalloyed films as low-cost and stable oxygen evolution reaction catalysts

Luca Ciambriello [1,2], Luca Gavioli [1,2]
[1] i-LAMP center, Dept. of Mathematics and Physics
Università Cattolica del Sacro Cuore, via della Garzetta 46, 25133 Brescia, Italy

Abstract:
Hydrogen can be produced electrochemically through the water splitting process, where H_2 and O_2 are obtained from the Hydrogen- and Oxygen-evolution half reactions, respectively. The high energy cost of the Oxygen evolution reaction (OER) is the bottleneck of the entire process, hampering the large scale development of Hydrogen fuels. The solution is the identification of efficient catalysts to be employed as anodes in the electrochemical cell.
In this framework, Ni/Fe nanoalloyed films have a great potential as OER catalysts, thanks to a) synthesis costs lower than noble metals, b) an improved reactivity typical of the first transition metal alloys, c) an enhanced metal/electrolyte interaction determined by the nanoscale morphology. However, the link between the electrode chemical/physical properties with the OER efficiency, in particular the nanoscale morphology evolution during the duty cycles, is still largely unknown. This hinders the possibility to improve the electrode stability, necessary for a large scale production.
In this work, we present a novel type of electrodes obtained by a gas phase deposition synthesis method. By Supersonic Cluster Beam Deposition (SCBD) we synthesize nanogranular films composed of NiFe (90%/10%) alloyed nanoparticles over a large thickness range (15 – 88 nm). The films are characterized by a porous matrix due to 0.4-3 nm size nanoparticles and a surface roughness between 4 and 6 nm. A high reactivity with the alkaline electrolyte solution results in the metal phase being converted into OER active oxides/hydroxides, and provide an excellent catalytic efficiency, with 380 mV overpotential at 10 mA/cm^2.
We show that such excellent efficiency is independent of the film thickness, identifying the ultrathin electrodes (15 nm thick) as the most promising catalysts and suggesting an excess mass loading for the thicker ones. This demonstrates that lowering NiFe mass is an effective way of decreasing significantly the synthesis cost without affecting the electrode activity.
Moreover, we assess the NiFe film stability under prolonged cyclic voltammetry conditions. In the first hours of the activity, an initial process of oxy/hydroxidation of the metal species, resulting in a film thickness growth, is then followed by an exfoliation of the NiFe film from the electrode to the electrolyte. Afterwards, a steady morphology is achieved, in which a minor fraction of the nanoparticles left over the electrode generate a considerable OER current with excellent stability.
This work puts a crucial step towards the identification and optimization of highly stable and low-cost OER electrocatalysts, towards their large-scale development as an alternative to fossil fuels.

Keywords: catalysis, OER, water splitting, efficiency, optimization, mass loading, TOF, transition metals, noble metal-free, low-cost, hydrogen, NiFe, nanomaterial, nanoalloy, thin, thickness, stability

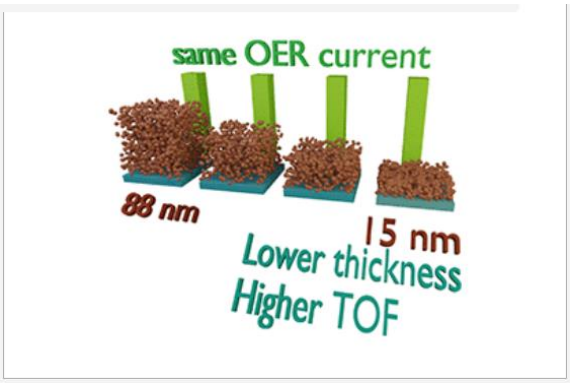

Figure 1: The NiFe electrode OER efficiency is independent of the film thickness. Therefore, decreasing the electrode mass loading is an effective strategy to reduce the synthesis costs without affecting the electrochemical activity.

References:

1. Ciambriello, L., Cavaliere, E., Vassalini, I., Alessandri, I., Ferroni, M., Leoncino, L., Brescia, R., and Gavioli, L., Role of electrode thickness in NiFe nanogranular films for oxygen evolution reaction. *J. Phys. Chem. C, 2022, 126, 5, 21759-21770*

Fabrication of a nanoporous filter for disposable facemasks out of biodegradable Polyesteramide through electrospinning: PublicMask

S. Hengsberger, R. Marti, J. Charmet
University of Applied Sciences and Arts Western Switzerland, HES-SO

Abstract:
Facemasks have gained unexpected attention during the Covid-19 pandemic. The high and sudden demand of facemasks has caused a serious shortage during several weeks on the European market. This experience underlines the importance that Europe must become more independent from Asian products. Beside that, the use of Polypropylene based facemasks on public places that are thrown away in nature raises an important concern. Biodegradable disposable facemasks are therefore a first step to avoid an increasing pollution of the environment (Aziz et al., Pandit et al.). The target group of our PublicMask project are people who are less exposed to viruses and who make a less responsible evacuation of the facemask after utilization.

In the context of this project, stakeholders in the field of biomedical engineering, industrial chemistry, plasturgy and nanotechnology have collaborated. The goal was to develop a biodegradable filter for a use in disposable facemasks. This filter material has been fabricated by electro-spinning. This method allows for a fabrication of thin continuous polymer fibers by accelerating a polar polymer/solvent mixture through an electric field. Dense networks with fibers of less than 1 micrometer in diameter have been obtained and these membranes have shown a high absorption efficiency of particles of the typical size of viruses (1 um for streptococcus).

The innovative part of this project was the development of biodegradable filters using three polyester-amide (PEA) grades that have been developed "in-house" by our Institute of Chemical Technology. We could successfully tune the melting temperature and viscosity of these PEA grades for an adaptation to the electro-spinning process. In a first step, we have set up and optimized the electro-spinning process with a solvent-based (solvent HFIP) PEA polymer solution. Filters of different thickness and fiber dimensions have been fabricated using different spinning parameters and PEA grades. For benchmarking the performance of the filter membranes, a test stage has been developed. The filters, that must fulfill two main requirements, high virus absorption and a high air transmission, have successfully been tested and their performance compared to the efficiency of validated commercial facemasks. Biodegradation tests have been successfully conducted and the kinetic of the degradation process has been evaluated for three grades of PEA polymers.

Furthermore, the potential fabrication of the PEA filter applying the alternative melt-spinning process has been demonstrated for one of the PEA polymer grades. The latter method is a solvent-free and economically and ecologically interesting process that is close to the industrially applied melt-blowing method. We have therefore demonstrated the in-house synthesis of Polyester-amide and their potential application for the fabrication of biodegradable disposable facemasks.

Keywords: Electrospinning; biodegradable polymers; disposable facemask; nanofiber; nanoparticles; Polyester-amide, meltspinning

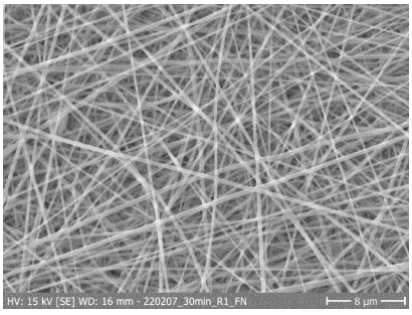

Figure 1: Electron microscope image of a submicron sized fiber network obtained by electro-spinning of PEA with HFIP as solvent. This nanoporous filter has shown efficient particle absorption comparable to non-degradable disposable mask filters. Furthermore, the biodegradation of this PEA grade has been demonstrated.

References:

1. Aziz et al. 2019 Preparation of electrospun nanofibers based on wheat gluten containing azathioprine for biomedical application. Int. J. Polym. Mater. Polym. Biomater. 68, 639–646.
2. Pandit et al. Potential biodegradable face mask to counter environmental impact of Covid-Cleaner Engineering and Technology 4 (2021) 10021

Highly TCO-$Zn_{0.99}B_{0.01}O$ nanostructured thin films achieved by coupling rf magnetron sputtering and sol gel process

K. Medjnoun [1,2,*], A-R. Moussa Tankari [1,2] , K. Djessas [1,2] , M. Nouiri [3]
[1]Laboratoire Procédés, Matériaux et Energie Solaire (PROMES)-CNRS, Tecnosud, Rambla de la thermodynamique, 66100 Perpignan, France
[2] Université de Perpignan Via Domitia, 52 avenue Paul Alduy, 68860, Perpignan Cedex 9, France
[3] Laboratoire de Physique des Matériaux et des Nanomatériaux appliquée à l'Environnement, Université de Gabès, Faculté des Sciences de Gabès, Cité Erriadh Manara Zrig, 6072 Gabès, Tunisie.

Abstract:
Nanostructured $Zn_{0.99}B_{0.01}O$ films with thicknesses varying from 300 to 700 nm were grown at room temperature on glass substrates using the rf-magnetron sputtering technique from a single target of $Zn_{0.99}B_{0.01}O$ nanoparticles previously prepared via the sol–gel process. The nanoparticles crystallize in the hexagonal wurtzite structure without secondary phases. Their size is ~ 40 nm. EDS analysis confirms the presence of the boron element in the ZnO matrix. The films exhibit a polycrystalline wurtzite structure. They have a dense columnar nanostructure. The effect of thickness on the physico-chemical properties of thin films has been investigated. The best optoelectronic properties were achieved for the $Zn_{0.99}B_{0.01}O$ thin films with 500 nm thickness: Tr ~ 90 % in the visible region, $\rho = 8x10^{-4}$ Ω.cm, $\mu_H = 35$ cm^2/Vs and $n_e = 2x10^{20}$ cm^{-3}. Considering their optoelectronic properties, $Zn_{0.99}B_{0.01}O$ films of 500 nm thickness may be promising candidates for application as TCO in solar cells.

Keywords: $Zn_{0.99}B_{0.01}O$, nanoparticles, Sol-gel, thin films, nanostructure, rf-magnetron sputtering, TCO, carrier mobility, resistivity, carrier concentration, transmission, band gap.

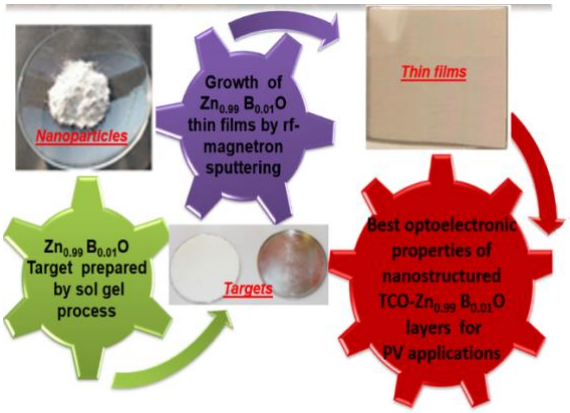

Figure 1: Original approach for preparing nanostructured TCO-$Zn_{0.99}B_{0.01}O$ thin films.

Influence of ion bombardment on nanostructured DLC:N films deposited by RF magnetron sputtering.

A. Lousa [1*], M. Punset[2,3], J. Caro[4], C. Díaz[5], G. García-Fuentes[5], R. Bonet[4], E. Rupérez [2,3], J. Esteve[1]
[1] Department of Applied Physics, University of Barcelona, E08023 Barcelona, Spain
[2] Engineering, Technical University of Catalonia (UPC), Barcelona East School of Engineering (EEBE), Barcelona, Spain
[3] Barcelona Research Center in Multiscale Science and Engineering, UPC, EEBE, Barcelona, Spain
[4] Eurecat,Centre Tecnològic de Catalunya, Unit of Metallic and Ceramic Materials,Manresa, Spain.
[5] Asociación de la Industria Navarra, Edificio AIN, 31191 Cordovilla, Pamplona, Spain.

Abstract:
The incorporation of Nitrogen into Amorphous Carbon hard coatings has been a research subject since the early times of the Diamond-Like Carbon (DLC) and tetrahedral amorphous carbon development [1-2]. Nitrogen has been added to Amorphous Carbon trying to enhance diverse coating properties: increase the mechanical hardness, reduce friction, increase wear resistance, reduce internal stress as to improve adhesion to substrates, introduce some electrical conductivity and finally, modifying its microstructure.
DLC:N films were deposited by RF magnetron sputtering with N concentration of around 10%, using different negative bias voltage. Films were characterized by, SEM, XPS, Raman spectroscopy, FTIR and HRTEM.
Well adhered films, 0.5 microns thick, were deposited with low compressive stress. The XPS N1s spectra shows two well defined C–N contributions. The XPS C1s difference spectra makes clear the presence of at least two extra contributions attributed to C–N bonds. Raman bands at 400, 700 and 1100 cm^{-1} much more intense for N doped DLC, reflecting and increasing formation of fullerene-like structures. TEM images show a fullerene-like amorphous matrix containing nanocrystalline clusters with a diameter size of 0.23 nm.
Varying the **negative bias voltage** does not change the composition of the films, but the macroscopic effect of a minimum of compressive stress at a negative bias voltage of 80 V, is clearly related to the microscopic changes in the density of nanoclusters observed by TEM, and the strong changes in the contributions of the different N-C bonds observed by XPS.

Keywords: N doped DLC film, XPS, Raman, Microstructure, HRTEM.

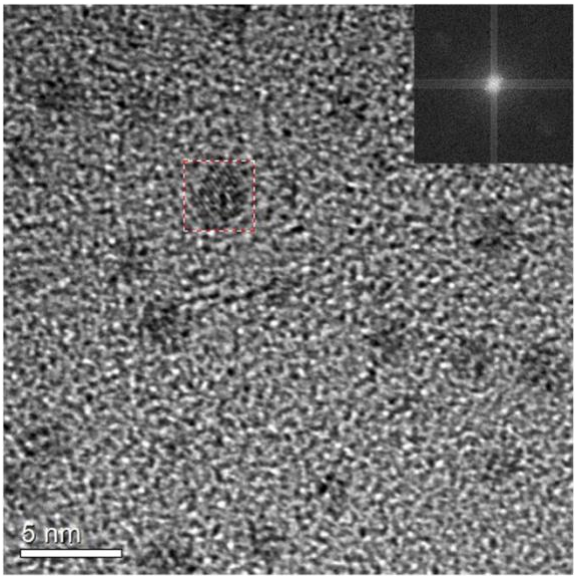

Figure 1: HRTEM image of the film showing crystalline nanoparticles uniformly dispersed and embedded in the amorphous matrix film.

References:

1. Erdemir, A., Donnet, C. (2006) Tribology of diamond-like carbon films: recent progress and future prospects, *Journal of Physics D-Applied Physics*, 39(8) R311-R327.
2. Vetter, J., (2014) 60 years of DLC coatings: Historical highlights and technical review of cathodic arc processes to synthesize various DLC types, and their evolution for industrial applications, Surface & Coatings Technology, 257, 213-240.

Growth of luminescent rare-earth doped LaNbO compounds thin films by magnetron sputtering for the improvement of solar cells

E. Salas-Colera [1,*], M. Tardío [1], E. García-Tabarés [1], B. Perea [1], M.L. Crespillo [2], J.E. Muñoz-Santiuste [1], B. Galiana [1]

[1] Departamento de Física, Universidad Carlos III de Madrid, Avda. Universidad 30, 28911 Leganés, Madrid, Spain

[2] Centro de Microánalisis de Materiales, CMAM-UAM, C) Faraday 3, 28049, Cantoblanco, Madrid, Spain.

Abstract:

Research on device architecture improvement is a hot topic that aims to increase the efficiency of solar cells devices. In this work we focus on the use of rare-earths doped oxides to tune the resulting spectrum, which the solar cell will transform into photocurrent. Mainly, the proposal is based on the photon recycling mechanisms presented by phosphors materials.

Current efforts to increase the quantum efficiency of Up/Down conversion (UC/DC) processes are focused upon the selection of a suitable host for this activator ion. Among the lanthanum niobates, the weberite-type La_3NbO_7 compound has attracted great attention because it exhibits interesting properties and great mechanical and chemical stability. In adittion, it has relatively low phonon frequencies that inhibit nonradiative pathways, thus allowing the electronic levels of the rare earth ions to have long lifetimes.

Nd^{3+} and $Er^{3+}Yb^{3+}$ doped La_3NbO_7 phosphor thin films were prepared by radio-frequency magnetron sputtering on Si substrates to achieve DC and UC processes respectively.

On one side, the effects of 1% Nd doped concentration, after annealing at 1200°C for 12h, on the light-emitting properties of the sputtered thin films are discussed as a function of the sputtering condition. Photoluminescence characterization (Figure 1) shows strong emission peaks typical of Nd^{3+} centres at 880 nm and 1060 nm when a 325 nm wavelength laser source is applied. Similar responses were detected in Nd^{3+} doped La_3NbO_7 powder samples fabricated by solid state reaction method. According to the structural analysis carried out, it appears that two lanthanum niobate phases ($LaNbO_4$ and La_3NbO_7) coexist in high thickness continuous layer (800 nm), whereas low thickness samples (200 nm) show a discontinuous layer mainly composed by La_3NbO_7 structure.

On the other side, 1% Er and 10% Yb doped La_3NbO_7 phosphors show strong green (centred at 532 and 555 nm) and red (centred at 670 nm) emissions when 980 nm wavelength laser source is applied. That emission lines are associated to UC processes related to Er ions. The effects of Yb ions and sputtering growth conditions are also discussed.

These results opens the possibility of developing phosphor substrates as a preliminary step for the improvement of solar cells based on photon recycling mechanisms.

Keywords: oxides doped with rare earths, photon recycling, magnetron sputtering

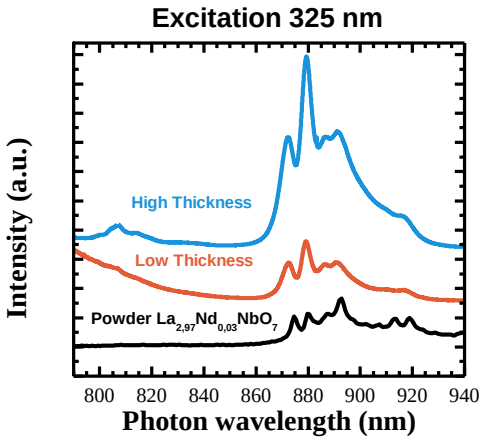

Figure 1: Comparison between the near-IR photoluminiscence spectra (excited at 325 nm) of two Nd doped lanthanum niobate thin films, with different thickness, with the spectra of La_3NbO_7:Nd(1%) powder reference.

References:

1. Chen, K., Yin, S., Xue, D. (2019) Active La–Nb–O compounds for fast lithium-ion energy storage, *Tungsten*, 1, 287-296.
2. Francis, L.T., Rao, P.P., Thomas, M., Mahesh, S.K., Reshmi, V.R., Thampi, V.D.S. (2012), New orange-red emitting phosphor $La_3NbO_7:Eu^{3+}$ under blue excitation, *Mater. Lett.*, 81, 142-144.
3. Egaña A., Cantelar E., Tardío M., Muñoz-Santiuste J.E. (2019) *Opt. Mater.*, 97, 109393.

Modular UV Curing Sol-Gel Coating for Levelling and Easy to Clean Multi-layer Systems.

L. Florentino [1,2,*]
[1] Surface Deparment. Idonial Foundation, C/ Calafates, 33417 Avilés, Spain
[2] Research funded by the Ministry of Science and Innovation through the Center for Industrial Technological Development (CDTI), contract number CER-20191003, within the framework of the «Cervera Technology Centers of Excellence» program.

Abstract:
The research of sol gel coatings cured under UV light without requiring high thermal hardening processes in plastic surfaces have been the center of attention nowadays. Apart from the low temperature curing process, the UV-cured films have various advantages such as high chemical and thermal stability, less harm for the environment, lower processing costs, and higher rates of hardening if the adequate medium pressure lamps are employed. Employing this methodology it is possible to reach very interesting properties in the surface of materials, simply by choosing and combining the correct precursors of the formulation and the suitable application and curing conditions.
A photopolymerisable coating formulation essentially consists of a polymerisable molecule (oligomer, in the present work DPHA) and a light sensitive compound or photoinitiator that is able to convert the absorbed light energy into a more useful form capable of causing the binder to polymerise into a hard solid film. In addition, the light absorption properties of the selected photoinitiator need to match the emission wavelength of the light source. In these systems, photoinitiators affect mainly cure speed.
We report here a simple and low cost methodology for the functionalization of different surfaces, which is modular, depending of the functionality pursued: a levelling layer for smooth the surface of the material, an "easy to clean" property, or both of them. It is possible to coat multilayer systems to reach interesting features on the selected materials, and the results are fully characterized. This formulation is well defined also for scaling up the process, so it is possible to perform a continuous coating in large areas by employing an specific pilot plant installed at our organization. In addition, the sol gel solution was studied in order to guarantee a long service life before deposition, focused on industrial applications involved in the automotive, domestic and machine-tool sectors.

Keywords: surface modification, sol-gel, UV curing, levelling coating, hydrophobic coating, easy to clean surface, multilayer system, photopolymerization, industrial application.

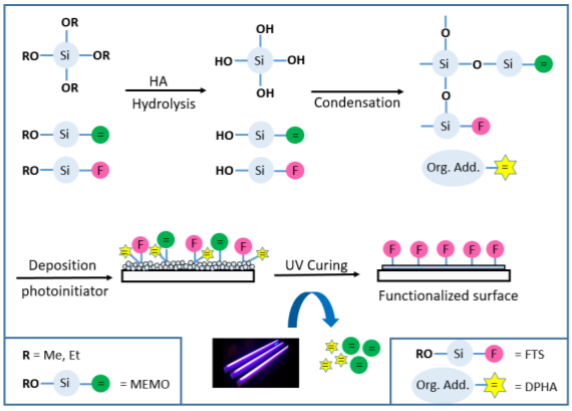

Figure 1: General procedure for the materials surface modification through UV curing sol gel coating technique.

References:

1. Shukla, V., Bajpai, M., Singh, D.K., Singh, M. and Shukla, R. Review of basic chemistry of UV-curing technology. *Pigment & Resin Technology* **2004**, Vol. 33, pp. 272-279.
2. Yusuf Y., Steffen J., and Nicholas J. T. Photoinitiated Polymerization: Advances, Challenges, and Opportunities. *Macromolecules* **2010**, Vol. 43, 6245–6260.
3. K. Vidal, E. Gómez, A. M. Goitandia, A. Angulo-Ibáñez and E. Aranzabe. The Synthesis of a Superhydrophobic and Thermal Stable Silica Coating via Sol-Gel Process. *Coatings* **2019**, 9, 627.
4. C. Carrera-Figueiras, Y. Pérez-Padilla, M. A. Estrella-Gutiérrez, E. G. Uc-Cayetano, J. A. Juárez-Moreno and A. Avila-Ortega. Surface Science Engineering through Sol-Gel Process. Chapter of Applied Surface Science
Edited by Gurrappa Injeti, **2018**.

NanoMatEn / GAMS Joint Session II.B: Materials and Nanomaterials for Energy / Nanoelectronics/ Nanophotonics

Nanogenerator: A Horizon of Green Power

R. Martins [1*], E. Fortunato [1*], S. Nandy [1]
[1] Department of Materials Science, CENIMAT-i3N Research Center
NOVA School of Science and Technology, Portugal

Abstract:
2020, world is taken aback by a pandemic. It is turning into an unprecedented crisis in people's lives and economy. But it warns us too, to be careful and prepare for the future. We can live better now, but we must think best for tomorrow. Today, another threatening part is increasing global emissions significantly, the majority caused by energy production that consumed in industry, services, households, and transport.[1] The worldwide concern over energy security and environmental issues due to fossil fuel consumption has generated the urgent need of sustainable and renewable energy sources. Therefore, alternative energy actions can support the goals of green world with economic stimulus programs. The majority of renewable energy sources are based on solar, wind, hydroelectric, geothermal or biomass.[2] But most of them needs a huge plant. Though, in this faster digitalization era, most of the technologies are portable that connected with IoTs which requires a flexible energy resource that will provide power uninterrupted. Still today, the battery is a prime option. But super flexibility and biocompatibility is still a limitation for it. Moreover, the native drawbacks of conventional systems are recharging, periodical maintenance and replacement that causes environmental pollution. Therefore, the biggest challenge in smart technology is sustainable power sources, that can back up the electronics unconditionally. This situation nanogenerator considers a new platform of green power technology, where everyone who will using it in daily life, realize that they can really make an impact on society through producing electrical power from any of their physical interaction which they have wasted as a mechanical movement (motion, vibration, or any touch interaction). [3,4]

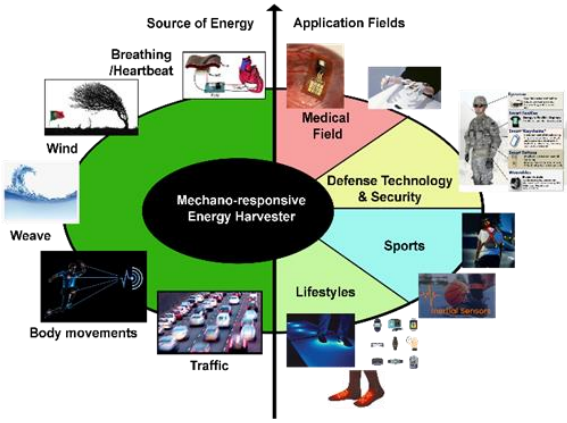

Figure 1: Source of mechanical energy ang probable application area of nanogenerator

References:

1. IEA (2019), Global Energy & CO2 Status Report 2019, IEA, Paris, https://www.iea.org/reports/global-energy-co2-status-report-2019
2. Chapter 24 - Renewable Energy Sources, P.S.R. Murty, in Electrical Power Systems, 2017, Pages 783-800, Imprint: Butterworth-Heinemann, Published Date: 14th June 2017, https://doi.org/10.1016/B978-0-08-101124-9.00024-3
3. "Touch-Interactive Flexible Sustainable Energy Harvester and Self-Powered Smart Card", G. Ferreira, S. Goswami, S. Nandy, L. Pereira, R. Martins, E. Fortunato, *Advanced Functional Materials 30 (2019) 1908994.*
4. "Smart IoT enabled interactive self-powered security tag designed with functionalized paper", G. Ferreira, A. Opinião, S. Das, S. Goswami, L. Pereira, S. Nandy, R. Martins, E. Fortunato, *Nano Energy 95 (2022) 10702*

Exploring Memristive Squaraine Microtubes: Programmable Multi-Level Memory Behaviour for Neuromorphic Applications

Prof. Gareth Redmond
School of Chemistry, University College Dublin, Dublin, Ireland

Abstract:
Typically, the demand for faster, cheaper, more efficient computing has been answered by device miniaturisation. However, device down-scaling (particularly that of transistors) is fast approaching the atomic scale, resulting in a gulf between the computational efficiency required by data scientists and hardware capacity available from conventional computing based on the von Neumann architecture and binary operations.[1] Artificial electronic synapse (e-synapse) devices are necessary in order for the effective implementation of artificial neural networks (ANNs) in hardware / machine learning operations to occur.[2] Organic memristors can provide the functionality required to meet these computational demands by providing multi-level memory coupled with high-density integration, as well as possessing all of the advantages inherent to organic materials such as flexibility and biocompatibility.[3] Memristors are two-terminal resistive switches which can encode information in the form of programmable internal resistance, the evolution of which can be modulated by the history of its external stimuli.[4] Memristors offers much greater memory density than typical devices by enabling 'multi-bit' memory, as well as facilitating the co-location of memory and logic operations, overcoming the energy- and time-expensive separation between memory and computation execution.[5]

Herein we demonstrate self-assembled microtubes (MTs) with analog resistive switching / programmable multi-level memory based on 2,4-bis[4-(N,N-diisobutylamino)-2-6-dihydroxyphenyl]squaraine ($SQ(OH)_2$), a small-molecule organic semiconductor. The device shows the typical pinched hysteretic *I-V* loop of a memristor with gradual changes in conductance upon successive sweeps, akin to the synaptic weight update processes in the human brain. The memory retention is shown to decay to its original state within a relatively short time in the absence of external voltage application, which is satisfactory for neuromorphic computing applications such as online learning where the synaptic weight values can be stored elsewhere following the training process.[2] This time-dependence enables short-term plasticity functionality to be demonstrated (paired-pulse facilitation and post-tetanic potentiation). Potentiation and depression cycles are shown to exhibit linear and symmetric conductance tuning, a key requirement for implementation of neuromorphic computing. Furthermore, short-term memory to long-term memory conversion is demonstrated through repeated sequences of voltage pulses. Overall, $SQ(OH)_2$ MTs appear to present attractive properties that could enable the successful embedding of organic MT-based ANNs directly in hardware circuits.

Keywords: squaraine, microtube, memristor, analog, neuromorphic

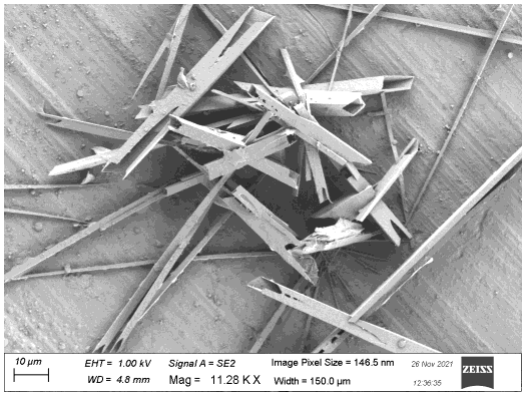

Figure 1: SEM image of $SQ(OH)_2$ MTs.

References:

1. Xu, X.; Ding, Y.; Hu, S. X.; Niemier, M.; Cong, J.; Hu, Y.; Shi, Y., Scaling for edge inference of deep neural networks. *Nature Electronics* **2018,** *1* (4), 216-222.
2. van de Burgt, Y.; Melianas, A.; Keene, S. T.; Malliaras, G.; Salleo, A., Organic electronics for neuromorphic computing. *Nature Electronics* **2018,** *1* (7), 386-397.
3. Someya, T.; Bao, Z.; Malliaras, G. G., The rise of plastic bioelectronics. *Nature* **2016,** *540* (7633), 379-385.
4. Chua, L., Memristor: The missing circuit element. *IEEE Transactions on Circuit Theory* **1971,** *18*, 507-519.
5. Zidan, M. A.; Strachan, J. P.; Lu, W. D., The future of electronics based on memristive systems. *Nature Electronics* **2018,** *1* (1), 22-29.

Fractional-Order Fast Integral Terminal Sliding Mode Control for A Piezoelectric Feeding Tool Holder System

Kuo-Ming Chang[1], Jian-Ming Chen[1], Wang-Long Li[2] and Yung-Tien Liu[3,*]
[1] Department of Mechatronics Engineering, National Kaohsiung University of Science and Technology (NKUST), Kaohsiung 807, Taiwan
[2] Department of Materials Science and Engineering, National Cheng Kung University Tainan 701, Taiwan
[3] Department of Mechatronics Engineering, NKUST, 1, University Rd., Yanchao, Kaohsiung 824, Taiwan
* Corresponding author

Abstract:
In this paper, an adaptive fractional-order fast integral terminal sliding mode control (AFOFITSMC) and a fractional-order fast integral terminal sliding mode control based on disturbance observer (FOFITSMC-DO) are proposed for a piezoelectric (PZT) feeding tool holder with nano-positioning ability and with bellows-typed hydraulic displacement amplification mechanism system in the presence of system uncertainties. The hysteresis effect of the PZT actuator is considered and modeled by the Bouc-Wen hysteresis model. In order to enhance the tracking control performance, the hysteresis quantity obtained from the Bouc-Wen hysteresis model and system uncertainties estimated by an adaptive law or a disturbance observer are taken into the control laws in the AFOFITSMC and the FOFITSMC-DO control methods, respectively. Furthermore, the Lyapunov method is used to prove the system stability and the tracking control performance of the PZT feeding tool holder control system subjected to the hysteresis effect and system uncertainties. Finally, numerical simulations and experimental results are presented to show the efficacy of the AFOFITSMC and the FOFITSMC-DO control methods proposed in this paper.

Keywords: fractional-order, terminal sliding mode control, hysteresis, piezoelectric feeding tool holder, system uncertainty.

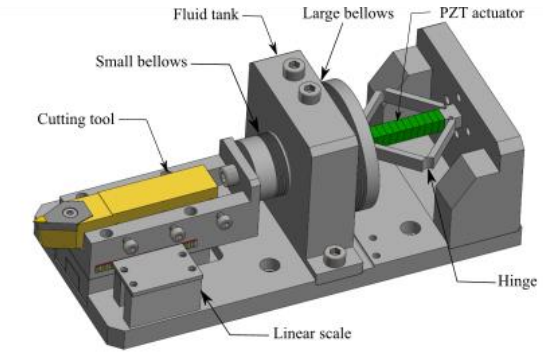

Figure 1: Schematic of the PZT feeding tool holder with with nano-positioning ability and with bellows-typed hydraulic displacement amplification mechanism system.

References:

1. Liu,Y. T., Chang, W. C., Yamagata, Y. (2013) A study on optimal comensationcutting for an aspheric surface using the Taguchi method, *CIPR J Manuf Sci Technol.*, 3, 40-48.
2. Chang, K. M., Cheng, W. T., Liu, Y. T. (2019) Developmint of non-axisymmetric aspheric ultraprecision machining using FPGA-based piezoelectric FPS, *Sensor Actuator Phys.*, 291, 99-106.
3. Labbadi, M. Moussaoui,H. (2021) An improved adaptive fractional-order fast integral terminal sliding mode control for distributed quadrotor, *Mathematics and Computers in Simulation*, 188, 120-134.

Spatially-assisted electron-hole pair separation in core/shell quantum dots for energy conversion

David Barba[1], Chao Wang[1], Gurpreet Singh Selopal[1,2], Haiguang Zhao[3], Federico Rosei[1]
[1] INRS, Centre : Énergie Matériaux et Télécommunications, Varennes (Québec), Canada
[2] Département of Engineering, Dalhousie University, Truro (Nova Scotia), Canada
[3] College of Physics, Qingdao University, Qingdao, P.R. China

Abstract:
Core-shell semiconducting quantum dots (QDs) have stable physical properties that make them interesting candidates for numerous applications in optical sensing, photocatalysis and solar photovoltaics. When exposed to light, the delocalization of their photoelectrons into the outer shell improves their catalytic capabilities, as well as the conversion of optical energy into electrical current. This presentation will focus on colloidal heterostructured group II/VI CdSe/(CdS)x core/shell QDs with tunable shell and core thicknesses. Their morphology, bandgap structures, photoluminescence, photo-electrical and photo-chemical properties are investigated by advanced characterizations based on transmission electron microscopy, x-ray photoelectron spectroscopy and time-resolved photoluminescence measurements, for solar energy conversion in photoelectrochemical (PEC) and photovoltaic (PV) cells. Using specific ion-beam treatments to control the concentration of structural defects generated inside the different regions of the QDs, it is shown that the presence of non-radiative centers in their outer part promotes the generation of photocurrent, through enhanced current linkages exacerbating the release of photoelectrons. This feature is attributed to the occurrence of a spacially-assisted charge carrier separation, resulting from the delocalization of the photo-electrons over the whole conduction band of the core-shell system. In addition to provide physical insight regarding the charge carrier exchanges, bandgap alignment and electron dynamics (Figure 1), the exciton dissociation based on wavefunction engineering and the implementation of post-growth processes aiming to enhance charge transfers are found to increase the solar energy conversion, which makes such an approach relevant for the development of new nanomaterials of advanced properties.

Keywords: colloidal quantum dots, core-shell nanoparticles, optical spectroscopy, transmission electron microscopy, structural defects, ion implantation, exciton separation, solar PV and PEC cells.

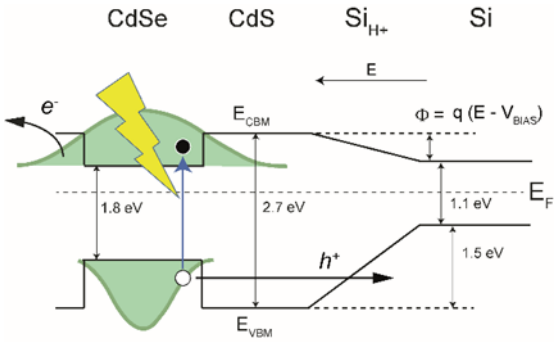

Figure 1: Figure illustrating both the bandgap arrangement and the spatially-assited electron-hole separation of proton-irradiated CdSe/(CdS) core/shell QDs incorporated into illuminated solar cells.

References:

1. G. S. Selopal, H. Zhao, X. Tong, D. Benetti, F. Navarro Pardo, D. Barba, F. Vidal, Z., M. Wang, F. Rosei, *Advanced Functional Materials*, 1701768 (2017).
2. C. Wang, D. Barba, G. S. Selopal, H. Zhao, J. Liu, H. Zhang, F. Rosei, *Advanced Functional Materials*, 1904501 (2019).
3. H. Zhang, L. V. Besteiro, J. Liu, C. Wang, G. S. Selopal, Z. Chen, D. Barba, Z. M. Wang, H. Zhao, G. P. Lopinski, S. Sun, F. Rosei, *Nano Energy* 79, 105416 (2021).

Spectrally Selective Multilayer Coating System to Improve the Thermo-Optical Properties of New-Designed Particle Receiver for Concentrated Solar Power Plant.

E. Salas-Colera [1,*], E. García-Tabarés [1], M.R. Rodríguez-Sánchez [2], A. Acosta-Iborra [2], F. Hernández-Jiménez [2]

[1] Physics Department, Universidad Carlos III de Madrid, Avda. Universidad 30, 28911 Leganés, Madrid, Spain.

[2] Thermal and Fluids Engineering Department, Universidad Carlos III de Madrid, Avda. Universidad 30, 28911 Leganés, Madrid, Spain.

Abstract:

The development of clean energies is mandatory to reduce environmental contamination. Among renewable energies, solar energy is one of the most promising fields. In recent years, the installation of power generation technology based on solar energy has been a leader among renewable sources. One of the most significant research challenges is to increase the efficiency of thermo-solar devices in concentrated solar power (CSP) plants.

In a CSP plant, the receiver is the most critical element, since it is responsible fro capturing the solar irradiation reflected by the heliostats field and transferring it to the working fluid. The main challenge associated with this process is the high thermal gradient and variability of the solar irradiation. In this regard, research and development of novel designs of central receivers is one of the main priorities.

We have proposed a new-designed receiver based on fluidized bed technology, whose properties will be optimized and enhanced using spectrally selective multilayer coatings (SSMC) deposited by magnetron sputtering techniques. It is a receiver formed by several panels, each of them being a bed fluidized with air. Particle receivers are becoming of great interest to achieve higher temperatures, beyond 700°C, to allow the operation of high efficiency power cycles. The main difference with the conventional receivers is that particles can be directly irradiated, eliminating the tubes where the working fluid flows. It allows the possibility of reach higher concentrations and temperatures. The prototype proposed allows the operation under direct and indirect radiation. Heat will be transferred to the air directly from the solar radiation and subsequently from the heat absorbed by the particles. The latter will be the most important heat transfer mechanism because the contact area between the particles and the air will be huge.

A SSMC system has been used as a complement to enhance the absorption capabilities at the UV-visible range and to reduce the thermal emittance of new-desgined particle receiver. For that purpose, a combination of ceramic and metallic materials (cermet) have been used. SSMC were grown by means of magnetron sputtering techniques.

MoSi2-Si3N4 cermet hybrid material was deposited spectrally selective multilayer coating to enhance the thermo-optical properties of new-designed receiver based on fluidized bed technologhy. The samples have been grown on glass and Inconel 625 stainless steel substrates. In addition, Al2O3 layer has been grown to provide both protection against the oxidation and high reflectance at the IR region.

The hybrid cermet compound has demonstrated to increase the thermal stability of the devices, maintaining the thermal absorption capabilities at higher working temperatures.

Keywords: solar energy, fluidized bed, spectrally selective coating, sputtering

References:

1. Alonso E., Romero, M. (2015) Review of experimental investigation on directly irradiated particles solar reactors, *Renew Sustain Energy Rev*, 41, 53-67.
2. Cao F., McEnaney K., Chen G., Ren Z. (2014), A review of cermet-based spectrally selective solar absorbers, *Energy Environ. Sci.*, 7, 1615-1627.
3. Céspedes E., Rodríguez-Palomo A., Salas-Colera E., Fonda E., Jiménez-Villacorta F., Vila M., de Andrés A., Prieto C. (2018) *ACS Appl. Energy Mater.*, 1, 6252-6160.

Up-Converting NaY(Gd)F_4:Yb^{3+},Er^{3+} β-phase Nanorods with Enhanced Red Emission for Perovskite Solar Cells

A. Gonzalo[1*], E. García-Tabarés[1], B. Serrano[2], J. E. Muñoz Santiuste[1], B. Galiana[1]
[1]Department of Physics, Universidad Carlos III de Madrid, Leganés (Madrid), Spain.
[2] Department of Materials Science, Universidad Carlos III de Madrid, Leganés (Madrid), Spain.

Abstract:
Solar cells have the inherent major drawback of their mismatch to the full solar spectrum, which unfolds in two ways: thermalization of photons with above-bandgap energies, and non-absorption of photons with sub-bandgap energies. A relevant strategy to reduce non-absorption losses consists of the inclusion into the solar cells of spectral converting layers made of up-conversion (UC) luminescent materials, which are able to transform two or more sub-bandgap photons into one useful photon with energy above the solar cell bandgap.[1] In particular, perovskite-based solar cells are able to absorb incident light within the spectral range 300-800/850 nm, the range where many UC systems emit.

In this work, we have successfully developed UC nanorods made of the fluoride host NaY(Gd)F_4, synthesized in a hexagonal β-phase (inset Figure 1), which provides enhanced UC efficiency as compared to its cubic phase,[2] doped with a combination of UC Yb^{3+}-Er^{3+} ions. The nanorods have been fabricated by hydrothermal synthesis using an autoclave reactor. This is a rapid, low-cost, simple, and energetically efficient process, requiring significantly shorter reaction times and lower temperatures than other techniques usually employed to obtain this kind of nanoparticles, while yielding high crystalline quality. Several different series of samples have been fabricated consistently varying several parameters such as Yb^{3+}-Er^{3+} concentration (to analyze changes in the UC spectra), Y-Gd concentration (which plays a main role in the size of the obtained nanorods), and synthesis parameters (reaction time and temperature), maintaining the same amount of oleic acid, which has been used as ligand.

When illuminated with a 980 nm laser, the nanorods provide UC emission within the wavelengths response of solar cells, particularly in the green region (with two emission bands around 530 and 550 nm), and in the red region (one band around 660 nm). The red band has a particularly intense emission as compared to the green ones, which is the opposite result to the usually observed in particles with similar compositions also fabricated by hydrothermal processes[3] (Figure 1). This enhanced UC red emission is particularly interesting for increasing solar cell efficiency as the solar spectral irradiance is more intense in the red area vs. the green area. The reason behind the high red emission intensity is currently under investigation, but we suspect that it is related to the hydrophobic environment of the nanorod's surfaces induced by the oleate ligands. Furthermore, the influence of the Y-Gd relative concentration on nanorods' size (which in turn affects nanorods' emission properties) is also analyzed.

Keywords: upconverting nanoparticles, photon recycling, enhancing solar cell efficiency, $NaYF_4$ nanocrystals, lanthanide ions, hydrothermal synthesis, perovskite solar cell.

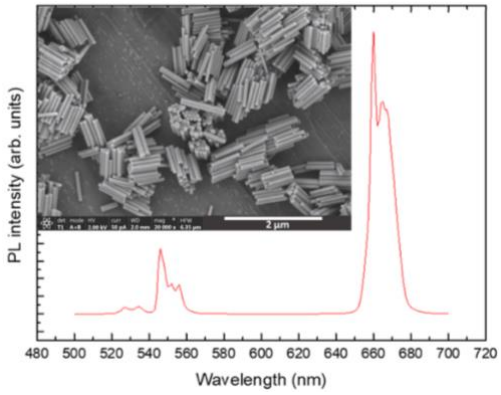

Figure 1: PL spectra of NaY(Gd)F_4:Yb^{3+},Er^{3+} nanorods. Inset: SEM image with 2 a µm scale bar showing the hexagonal phase nanorods.

References:

1. Huang, X., Han, S., Huang, W., Liu, X. (2013) Enhancing solar cell efficiency: the search for luminescent materials as spectral converters, *Chem. Soc. Rev.*, 42, 173-201.
2. Yi, G.S., Chow, G.M. (2006) Synthesis of Hexagonal-Phase NaYF4:Yb,Er and NaYF4:Yb,Tm Nanocrystals with Efficient Up-Conversion Fluorescence, *Adv. Funct. Mater.*, 16, 2324-2329.
3. Wu, Y. et al. (2016) Enhanced up-conversion luminescence from $NaYF_4$:Yb,Er nanocrystals by Gd^{3+} ions induced phase transformation and plasmonic Au nanosphere arrays, *RSC Adv.*, 6, 102869-102874.

The influence of material synthesis parameters on the electrocatalytic activity of NiMo-oxide nanostructures as anode electrocatalysts in alkaline water splitting towards green hydrogen production

M.Rammal, S.Omanovic
Department of Chemical Engineering, McGill University, Montreal, QC, Canada

Abstract:
Green hydrogen is a viable, sustainable option to counter the fossil fuel dilemma[1]. Currently, most industrial applications, employing water electrolysis to produce green H_2, utilize classical well-established alkaline electrolysers; however their power efficiency is relatively low, and they are not suitable for applications with variable power loads (*e.g.* for energy storage with surplus electricity produced by solar/wind systems). On the other hand, the new type of water alkaline electrolysers based on the use of an anion-exchange membranes (AEM) can partially address the two above-mentioned drawbacks of the classical water electrolysers[2]. Still, development of better electrodes for AEM water electrolysers is needed, especially the anodes where the oxygen evolution reaction (OER) occurs. Namely, the OER is a key reaction in water splitting and has been long considered the bottleneck of the process due to its sluggish kinetics and high energy consumption, compared to the hydrogen evolution reaction (HER). Transition metal oxides have been demonstrated to be interesting electrocatalytic materials for the OER due to their low cost, high activity, thermodynamic stability, and ease of synthesis and scaleup. In particular, NiMo-oxide-based materials exhibit favorable electrochemical and structural properties that motivate their use as an OER electrocatalyst. Herein, NiMo-oxide nanostructures of different physicochemical properties and microstructures were prepared through a green solution combustion synthesis method by altering the initial experimental parameters, and those products were investigated as electrocatalytic materials in the OER. The results showed that β-$NiMoO_4$ yielded a higher OER activity than the α-phase. In comparison to the OER benchmark electrocatalysts (Figure 1a), the in-house-developed $NiMoO_4$ electrocatalyst performed significantly better, yielding an OER overpotential of 290 mV at 10 mA cm^{-2}, and also good stability (Figure 1b). The performance enhancement observed is likely due to the formation of NiOOH and the increase in specific surface area of the electrocatalytic layer.

Keywords: hydrogen economy, water electrolysis, nanostructured electrodes, mixed-metal oxides, oxygen evolution reaction

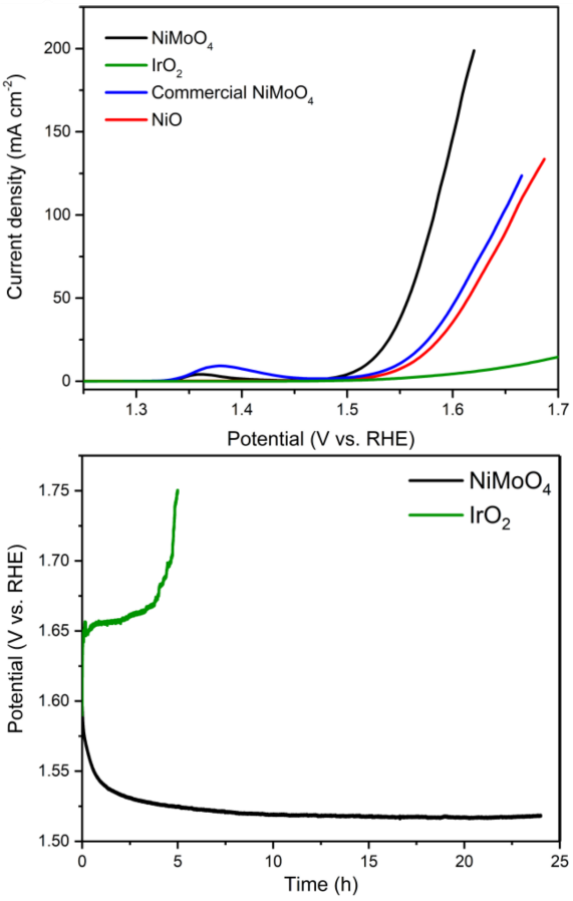

Figure 1: (a) Linear polarization curves of the in-house synthesized $NiMoO_4$ and other benchmarks, recorded in 1 M KOH at a scan rate of 5 mVs^{-1}. (*b*) stability of $NiMoO_4$ and IrO_2 conducted galvanostatically at 10 mA cm^{-2}.

References:

1. Abdin, Z., et al. (2020) Hydrogen as an energy vector, *Renewable and Sustainable Energy Reviews*, 120, 109620.
2. Kumar, S.S., et al., (2022) An overview of water electrolysis technologies for green hydrogen production, *Energy Reports*, 8, 13793.

Anomaly in potential-composition-temperature isotherms during electrochemical hydrogenation of Pd thin films in an alkaline medium

M. T. Pise [1], Arnomitra Chatterjee [2], Bhagwati P. Kashyap [3], Ram N. Singh [2], Sankara Sarma V. Tatiparti [1,*]

[1] Department of Energy Science and Engineering, Indian Institute of Technology Bombay, Mumbai, India

[2] Mechanical Metallurgy Division, Bhabha Atomic Research Centre, Mumbai, India

[3] Department of Metallurgical and Materials Engineering, Indian Institute of Technology, Jodhpur, India

Abstract:

Electrodeposited palladium (Pd) thin films were potentiostatically hydrogenated in the range of –0.700 to –1.300 V vs SCE at 30-60 °C in 0.6 M KOH. The potential-concentration-temperature isotherms (*E*-*C*-*T*s) were constructed, in a similar way as the pressure-concentration-temperature (*P*-*C*-*T*s) isotherms, during potentiostatic hydrogenation of Pd. The *E*-*C*-*T*s exhibit three regions viz. Regions I, II and III. Region I spans between –0.70 and –0.950 V and corresponds to Pd-H solid solution (α). Region III appears at potentials >–1.000 V vs SCE and corresponds to hydride (β) formation. Region III is also characterized by a steep rise in the potential with an insignificant change in concentration (H/Pd atom-ratio). Region II appears between –0.950 and –1.000 V vs SCE and is a plateau explaining the coexistence of α and β phases. Interestingly, Region II exhibits an anomaly with plateaus at lower temperatures possessing higher potentials (magnitude-wise) in these isotherms. This is unlike in the *P*-*C*-*T*s, where the plateaus at lower temperatures possess lower pressures. This anomaly is supported by the estimated fugacities (equivalent to pressure) and positive hydrogenation enthalpies during hydrogenation. The reason for such an anomaly was investigated through cyclic voltammograms (CV). From CVs, the *E*s corresponding to Regions II-III result in simultaneous water reduction and hydrogen absorption. Hence, the *E*s within the *E*-*C*-*T* plateaus do not always result in sole hydrogen absorption, unlike Ps within the *P*-*C*-*T* plateaus. Further, water reduction dominates with an increase in *E* and *T* within Regions II-III of *E*-*C*-*T*s, leading to the *E*-*T* anomaly. Such an inability of *E* to correspond to hydrogen absorption leads to a lower *C* (~0.7) in Region III than expected. This work enables choosing appropriate *E*-*T*s for electrochemical hydrogenation.

Keywords: Palladium, potentiostatic, electrochemical hydrogenation, isotherm, plateau, anomaly

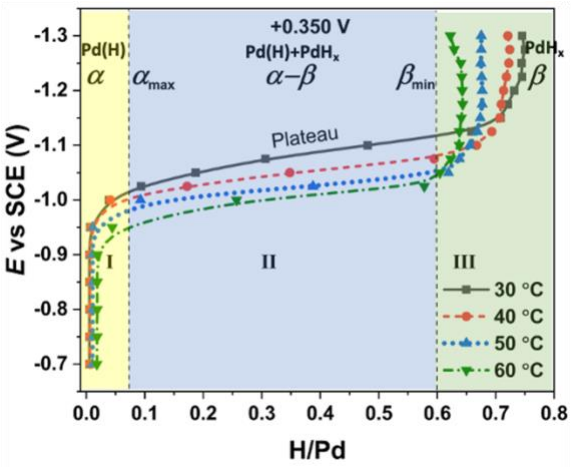

Figure 1: Potential-Concentration-Temperature isotherms (*E*-*C*-*T*s) showing anomaly in terms of temperature.

Hydrogen storage capacity of titanium, zirconium and Ti_xZr_{1-x} thin films

I. Zukerman[1], M. Buzaglo[1], S. Hayun[2]
[1]Divison of Chemistry, NRC-Negev, P.O.Box 9001, Beer-Sheva 84190, Israel
[2]Department of Materials Engineering, Ben Gurion University of the Negev, Beer-Sheva, Israel

Abstract:
Metal hydrides (MH_x) provide a promising solution for a future hydrogen-based energy system due to their high hydrogen storage density and safety advantages compared to compressed or liquefied hydrogen. Thin films were proposed to ease the absorption/desorption cycles by maximizing the surface-to-volume ratio. In this study, we suggest controlling the macro- and micro- structure of thin films, in order to reduce the absorption/desorption temperature and to increase the rate and absorbed hydrogen volume. To achieve this goal, a series of titanium, zirconium and Ti_xZr_{1-x} thin films were deposited using pulsed-DC magnetron co-sputtering technique. Low sputtering power, high working pressure, or floating bias conditions resulted in an open columnar structure (i.e., zone 1 microstructure). High negative bias (< -150 V), however, promoted a dense columnar structure (i.e., zone T microstructure). The thin film's hydrogenation was conducted at 623 K and 1.0±0.05 atm of pure hydrogen (99.999%) for up to 6 hour. Temperature-Programmed Desorption (TPD), Glow Discharge Spectroscopy (GDS), electron microscopy and X-Ray diffraction were used to study the microstructure of the films, hydrogen storage capacity, desorption temperature, and the durability for multiple absorption/desorption cycles.

Concrete modules for energy harvesting

R. Campos[1]*, Rúben Pedroso[1], David Esteves[1], José Gonçalves[1],
João Serafim[2], Diana Correia[2], Daniela Gaspar[2], Ângela Nunes[2]
1 CeNTI – Centre of Nanotechnology and Smart Materials
2 Secil, Companhia Geral de Cal e Cimento, S. A., Setúbal, Portugal

Abstract:
Concrete is one of the materials most used in civil construction, and the expansion of urban areas has led to an escalating interest in enabling concrete structures to harvest energy. Roads and sidewalks are examples of concrete structures exposed to different energy sources being solar irradiation the most relevant. This fact justifies the interest in integrating thermoelectric generators (TEGs) in concrete structures to ensure the harvesting of this energy source.
In the reported work, the main theme was the integration of commercial thermoelectric generators in concrete modules. The principle behind this study is to generate electric power by harnessing the energy present in a temperature gradient established inside a concrete block through the thermoelectric effect. This gradient is defined by (i) an underground isothermal level (of 18°C), (ii) the solar irradiation incident on the concrete block surface and (iii) atmospheric convection that dissipates thermal energy through the block surface. The three main factors contribute to establishing a dynamic thermal gradient inside the concrete module.
The concrete module optimization and engineering were studied mainly using finite elements' numerical analysis. We started identifying the most important geometrical parameters of the module that influence the thermal gradient inside it. These parameters included: (i) the TEG position, (ii) the presence or absence of a thermal isolator layer, (iii) the dimensions of the concrete layers, (iv) the type of concrete used and (v) the inclusion of structures for thermal energy transportation.
Using 2D and 3D Computational Fluid Dynamics (CFD) analysis, the optimal position for the TEG inside the module was achieved. The studies have shown that the thermal isolator significantly impacts thermal gradients. The inclusion of thermal exchangers like metallic heat sinks was important to facilitate the establishment of the temperature gradient between the TEG's faces. The simulation included a model for solar irradiation and another one for atmospheric thermal convection. These two models were adjusted using experimental values.
A concrete module was engineered with energy capabilities based on the best results. This module was tested in a real environment, buried in the soil. A good correlation between experimental and simulation data was found.

This work was developed within the scope of the Baterias2030 project (POCI-01-0247-FEDER-046109), which was co-financed by Portugal 2020, under the Operational Program for Competitiveness and Internationalization (COMPETE 2020) through the European Regional Development Fund (ERDF).

Keywords: Thermoelectric generators, concrete structures

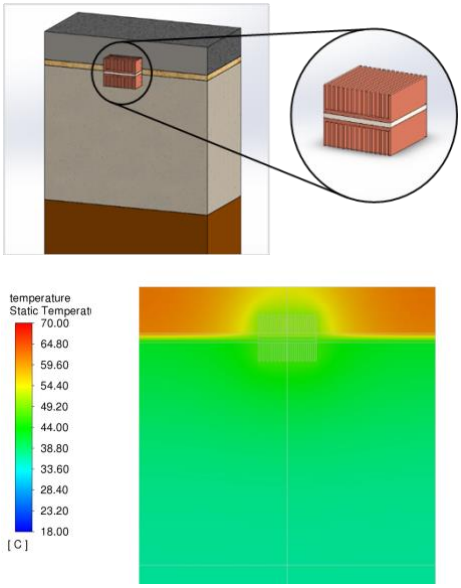

Figure 1: Thermoelectric concrete block and thermal gradients.

References:

1. Kanimba E, Tian Z. Modeling of a Thermoelectric Generator Device. Thermoelectrics for Power Generation - A Look at Trends in the Technology, 2016, 18, p. 461
2. Nesarajah M, Frey G. Thermoelectric power generation: Peltier element versus thermoelectric generator. IECON 2016 - 42nd Annual Conference of the IEEE Industrial Electronics Society, Florence, 2016, p. 4252-4257.

Sustainability of Expanded Polystyrene as a Preferred Thermal Insulation Material

C. Martins [1,*], J. Araújo [1], J. Coutinho [1], D. Rodrigues [1], A. Moreira [1], P.F. Teixeira [1], N.O. Ferreira [2], D. Queiroz [3] and N.B Pereira [4]

[1] CeNTI - Centre for Nanotechnology and Smart Materials, VN Famalicão, Portugal

[2] Houselab Technologies, São Mamede de Infesta, Portugal

[3] FEUP - Faculty of Engineering of the University of Porto, Porto, Portugal

[4] CICon - Center for Innovation in Construction, Vila Pouca de Aguiar, Portugal

Abstract:

Construction is one of the largest sectors of the world economy, however, it appears to be conservative and slow to adopt changes and innovations. If the construction paradigm does not change, it will be difficult to meet the global demand for infrastructure and housing. Moreover, with the construction industry accounting for a high percentage of global energy-related carbon-dioxide emissions, it is imperative to work toward making the industry more sustainable. The project STEPS aims at the development of a new advanced building system that reduces the environmental impact of the production chain, improving substantially and productivity of the construction sector. Insulation materials are an important component in construction as they contribute to energy efficiency and, therefore, to the achievement of climate goals. Expandable polystyrene (EPS) is one of the most used materials for thermal insulation in buildings. Despite the technical properties of EPS, which make it a material with remarkable performance, it presents a high ecological footprint, since its production requires significant energy consumption and is difficult to dispose of. The present work discusses the development of a numerical model for the maximization of thermal performance in terms of predicting the best combination of materials and geometry, as well as development in thermal-insulation systems, including EPS, with an improved ecological footprint, will be presented.
This work was developed in the scope of project STEPS, which was co-financed by Portugal 2020, under the Norte 2020, through the European Regional Development Fund (ERDF) (NORTE-01-0247-FEDER-047054).

Keywords: Sustainability, thermal insulation, EPS, civil construction, modular construction.

.

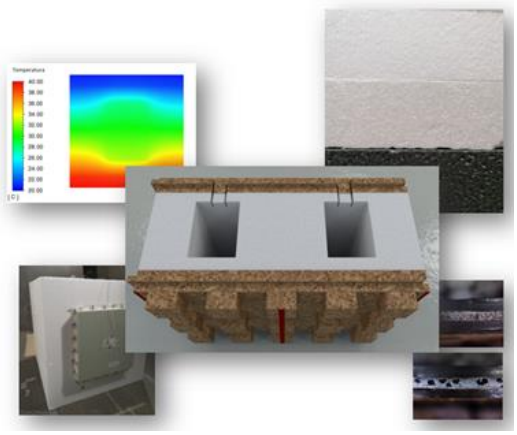

Figure 1: Graphical abstract.

Investigation of the Physical Properties of New Binary Mixed Oxide Nanocomposites for Environmental Applications

Meshal Alzaid [1,*]
[1] Department of Physics, College of Science, Jouf University, Al-Jouf, Sakaka, P.O. Box: 2014, Saudi Arabia.

Abstract:
In the current study, novel (Y2O3) x (CdO) 1-x mixed oxides nanocomposites (NCs) with different Y2O3 loadings ($0.0 \leq x \leq 0.2$) have been synthesized via a facile precipitation approach. The structural analysis by x-ray diffraction reveals that both pure CdO nanoparticles (NPs) and (Y2O3) x (CdO) 1-x NCs possess crystalline and cubic-phase purity. Based on the concentration of Y2O3 in the mixing nanocomposition (NCs), it was found that the crystallite size in the NCs ranged from 45 to 52 nm. Field emission scanning electron microscopy was used to examine the morphologies of CdO NPs and (Y2O3) x (CdO) 1-x NCs. This confirmed that the collected NCs had an irregular semi-spherical morphology. Based on the Tauc figure, it was determined that the optical band gap of the produced NCs had decreased from 3.35 to 2.96. According to Brunauer-Emmett-Teller (BET) testing, the increase in surface area and pore volume after Y2O3 addition indicates enhanced porosity. UV-vis spectroscopy's optical study reveals that Y2O3 loading significantly improves the photocatalytic activities of (Y2O3) x (CdO) 1-x NCs. The photodegradation efficiency of methylene blue (MB) was higher (94.6%) for the (Y2O3) 0.2 (CdO) 0.8 NCs under solar irradiation compared to (45.6%) for pure CdO NPs. The (Y2O3) 0.2 (CdO) 0.8 NCs photocatalyst was stable in six cycles of MB degradation, according to a study on reusability. The high BET-surface area, small particle size, and narrow energy gap of the photocatalytic system with the optimal Y2O3 loading are responsible for the improvement in photocatalytic activity.

Keywords:.Mixed Oxides Nanocomposites X-ray diffraction, BET-surface area, Pore volume photocatalytic activity

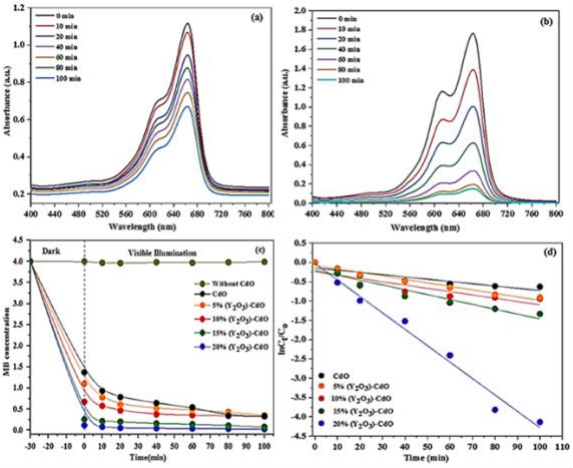

Figure 1: Time-dependent variations in absorption spectrum of MB during visible illumination in the presence of (a) CdO, (b) 20%Y2O3eCdO (c) photodegradation performance, (D) First-order photodegradation kinetics of MB in presence of pure CdO and Y2O3eCdO catalysts.

References:

1. Abu-Dief Ahmed M, Essawy Amr A, Diab AK, Mohamed WS. Facile synthesis and characterization of novel Gd2O3eCdO binary mixed oxide nanocomposites of highly photocatalytic activity for wastewater remediation under solar illumination. J Phys Chem Solid 2021;148:109666.
2. Mohamed WS, Hadia NMA, Al bakheet B, Alzaid M, Abu- Dief AM. Impact of Cu2þ cations substitution on structural, morphological, optical and magnetic properties of Co1- xCuxFe2O4 nanoparticles synthesized by a facile hydrothermal approach. Solid State Sci 2022;125:106841.

Nanotech France / GAMS
Joint Session II.C:
Nano for life science and Medicine

Carbon nano-onions for biomedical applications

S. Giordani [1,*]
[1] School of Chemical Sciences, Dublin City University, Dublin, Ireland

Abstract:
In this presentation, carbon nano-onions (CNOs) will be discussed as a potential vesicle for nanocarrier-type drug delivery systems.1 CNOs, or multi-layer fullerenes, consist of multiple concentric layers of sp2 hybridized carbon and are emerging as platforms for biomedical applications because of their ability to be internalized by cells and low toxicity.2
In my research group we have developed methodology for the synthesis of pure, monodispersed CNOs and various chemical functionalization strategies for the introduction of different functionalities (receptor targeting unit and imaging unit) onto the surface of the CNOs. The modified CNOs display high brightness and photostability in aqueous solutions and are selectively taken up by different cancer cell lines without significant cytotoxicity. Supramolecular functionalization with biocompatible polymers is an effective strategy to develop engineered drug carriers for targeted delivery applications. We reported the use of a hyaluronic acid-phospholipid (HA-DMPE) conjugate to target CD44 overexpressing cancer cells, while enhancing solubility of the nanoconstruct. Non-covalently functionalized CNOs with HA-DMPE show excellent in vitro cell viability in human breast carcinoma cells overexpressing CD44 and are uptaken to a greater extent compared to human ovarian carcinoma cells with an undetectable amount of CD44. In addition, they possess high in vivo biocompatibility in zebrafish during the different stages of development suggesting a high degree of biosafety of this class of nanomaterials.3
We recently synthesized Boron/nitrogen co-doped carbon nano-onions (BN-CNOs) 4 and examined their interactions with biological systems. Our study on the toxicological profiles of BN-CNOs and oxidized BN-CNOs in vitro in both healthy and cancer cell lines, as well as in vivo on the embryonic stages of zebrafish (Danio rerio) demonstrate that these new class of carbon nanoparticles have high cyto-biocompatibility and a high biosafety. 5 Noncovalent functionalization of BN-CNOs with HA-DMPE gave dispersions with long term aqueous stability. 6
Our results encourage further development as targeted diagnostics or therapeutics nanocarriers.

Keywords: carbon, nanomaterials, imaging, targeted delivery, hyaluronic acid, nanosafety, biomedical applications.

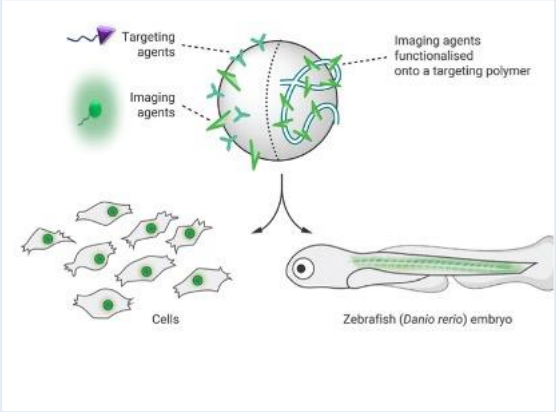

Figure 1: Figure illustrating the carbon nano-onion surface modification with imaging and targeting units and the *in vitro* and *in vivo* biocompatibility studies.

References:

1. M. Bartkowski and S. Giordani (2021), *Dalton Transactions* 50 (7), 23.
2. S. Giordani et al. (2019) *Current Medicinal Chemistry* 26 (38), 6915.
3. M d'Amora et al. (2020) *Colloids and Surfaces B: Biointerfaces* 110779.
4. A. Camisasca et al. (2018) *ACS Applied NanoMaterials* 1, 5763.
5. M d'Amora et al. (2021) *Nanomaterials* 11 (11), 3017.
6. H. Mohan et al. (2022) *Applied Sciences* 11 (22), 10565.

Motile micro- and nanorobotics: System integration, autonomy and biomedical applications

Oliver G. Schmidt
Research Center for Materials, Architectures and Integration of Nanomembranes (MAIN),
Chemnitz University of Technology, Germany
oliver.schmidt@main.tu-chemnitz.de

Abstract:
This talk addresses key challenges in the field of motile micro- and nanorobotics [1]. One of these include the concept of system-engineered propulsion units that integrate diverse functions into a single microrobot such as wireless energy transfer, controllable catalytic reactions, structural flexibility and steerability in the absence of magnetic fields [2,3]. On-board energy and power-supply for autonomous micro- and nansystems are further pressing challenges [4] and will be addressed by producing world's smallest self-assembled batteries and bionsupercapacitors [5,6]. Micro- and nanorobots can also be created in a hybrid form, for instance, as sperm-based cybernetic organisms [7,8] that are promising candidates for biomedical applications such as artificial reproduction technologies and active targeted drug delivery [9,10], even through the flowing streams of blood [11].

Keywords: nanorobotics, microrobotics, microsystems integration, biohybrid microrobots, biomedical applications, microbatteries, nanobiosupercapacitors, biomedical applications, targeted drug delivery

References:

1. M. Medina-Sánchez, O. G. Schmidt, *Nature* 545, 406 (2017)
2. Y. Mei, A.A. Solovev, S. Sanchez, O.G. Schmidt, *Chem. Soc. Rev.* 40, 2109 (2011)
3. V. K. Bandari, Y. Nan, D. Karnaushenko, Y. Hong, B. Sun, F. Striggow, D. D. Karnaushenko, C. Becker, M. Faghih, M. Medina-Sanchez, F. Zhu, O. G. Schmidt, Nature Electron. 3, 172 (2020)
4. M. Zhu, O. G. Schmidt, *Nature* 589, 195 (2021)
5. Y. Li, M. Zhu, V. K. Bandari, D. D. Karnaushenko, D. Karnaushenko, F. Zhu, O. G. Schmidt, *Adv. Energy Mater.* 12, 2103641 (2022)
6. Y. Lee, V. K. Bandari, Z. Li, M. Medina-Sanchez, M. F. Maitz, D. Karnaushenko, M. V. Tsurkan, D. D. Karnaushenko, O. G. Schmidt, *Nature Comm.* 12, 4967 (2021)
7. V. Magdanz, S. Sanchez, O. G. Schmidt, *Adv. Mater.* 25, 6581 (2013)
8. M. Medina-Sánchez, L. Schwarz, A. K. Meyer, F. Hebenstreit, O. G. Schmidt, *Nano Lett.* 16, 555 (2016)
9. H. Xu, M. Medina-Sanchez, V. Magdanz, L. Schwarz, F. Hebenstreit, O. G. Schmidt, *ACS Nano* 12, 327 (2018)
10. F. Rajabasadi, S. Moreno, K. Fichna, A. Aziz, D. Appelhans, O. G. Schmidt, M. Medina-Sanchez, *Adv. Mater.* 34, 2204257 (2022)
11. H. Xu, M. Medina-Sanchez, M. F. Maitz, C. Werner, O. G. Schmidt, *ACS Nano* 14, 2982 (2020)

Genetically Encoded Biosensor Development and Its Application in Regulating Microbial Biosynthesis

Tian Jiang, Chenyi Li, Yusong Zou, Jianli Zhang, Qi Gan, Yajun Yan*
School of Chemical, Materials, and Biomedical Engineering, College of Engineering, The University of Georgia, Athens, Georgia, USA

Abstract:
Endogenous metabolic pathways in microbial cells are usually precisely controlled by sophisticated regulation networks. However, the lack of such regulations when introducing heterologous pathways in microbial hosts often causes unbalanced enzyme expression and carbon flux distribution, hindering the construction of highly efficient microbial biosynthesis systems. To address this issue, genetically encoded biosensors have been developed as efficient tools for dynamically regulating metabolic pathways. In this study, we engineered the *p*-coumaric acid responsive regulator PadR from *Bacillus subtilis* and identified two previously uncharacterized components, yveF and yveG, that positively impact the regulation of the PadR-PpadC biosensor system (Figure 1). We also obtained two PadR mutants, K64A and H38A, that exhibit increased dynamic range and superior sensitivity. To increase the responsive strength and investigate whether PadR binding boxes can function in a "plug-and-play" manner, we constructed a series of hybrid biosensors, four of which showed increased strength compared to PpadC and could be regulated by PadR and *p*-coumaric acid. Using the developed biosensor, we developed an Autonomous Cascaded Artificial Dynamic (AutoCAD) regulation system that coordinates pathway expression and redirects carbon fluxes for enhanced naringenin production. The AutoCAD regulation system includes intermediate-based feedforward and product-based feedback control genetic circuits and resulted in a 16.5-fold increase in naringenin titer compared to the static control. Fed-batch fermentation using the strain with AutoCAD regulation further enhanced the naringenin titer to 277.2 mg/L. Our study demonstrates the potential of genetically encoded biosensors and the AutoCAD regulation system to engineer heterologous pathways with sophisticated cascade dynamic control, providing new avenues for developing highly efficient microbial biosynthesis systems.

Keywords: PadR, *p*-coumaric acid, biosensor, genetic circuit, cascaded dynamic regulation

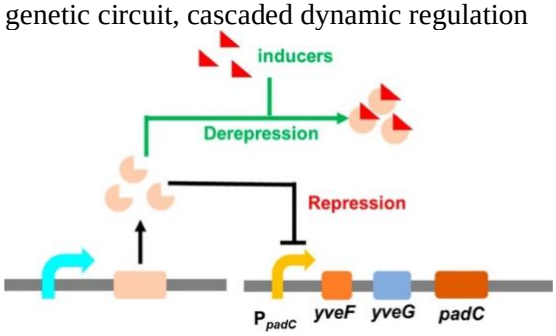

Figure 1: Figure illustrating the mechanism of PadR-PpadC biosensor system. Repression: PadR binds in the specific regions of PpadC, which represses the expression of *padC* gene. Derepression: with the presence of inducers, they can combine with PadR and release its repression on PpadC. *padC* gene can be expressed.

References:

1. Jiang, T., Li C., Zou, Y., Zhang, J., Gan, Q., Yan, Y., Establishing an Autonomous Cascaded Artificial Dynamic (AutoCAD) regulation system for improved pathway performance. *Metabolic Engineering* 2022; 74: 1-10.
2. Jiang, T., Li, C., Yan, Y. Optimization of a *p*-coumaric acid biosensor system for versatile dynamic performance. *ACS Synthetic Biology* 2021; 10: 132-144.

Macrophage-targeted nanotherapies for hard-to-treat malignancies in females

B. Godin
Department of Nanomedicine, Houston Methodist Research Institute, Houston, TX, USA; Department of Obstetrics and Gynecology, Weill Cornell Medicine College (WCMC), New York, NY, USA; Department of Obstetrics and Gynecology and Cancer Center, Houston Methodist Hospital, Houston, TX, USA; Department of Biomedical Engineering, Texas A&M, College Station, TX, USA.

Abstract:
Organ microenvironment represents the first frontier and an efficient barrier for delivery of nanotherapeutics to the cells where these should act. Thus, organ microenvironment should be considered when developing strategies for drug delivery to an ailment.

As an example, in the primary breast tumors, the lesions are angiogenic and are characterized by developed and permeable vasculature. However, in conditions such as liver metastasis the lesions from the same origin are less vascularized than the surrounding normal tissue, thus, the structure of the organ itself conjures with cancer-specific behavior to impair drug transport and uptake by cancer cells. Thus, strategies to enhance the accumulation of the medicines in the liver lesions, while preventing the wash out should be pursued.

Macrophages are abundant in the liver cell population. Studies by others and our group show that concentration of macrophages in the peritumoral regions of liver metastasis lesions is significantly increased. Since these cells are professional phagocytes, we hypothesized that the drug can be anchored by encapsulation in nanovectors that will preferentially be taken up by the peritumoral macrophages. This can shift the transport of therapeutics towards the tumor in the liver, thus potentially overcoming physiological resistance.

In vitro studies demonstrated that macrophages can take up and release albumin bound paclitaxel when encapsulated in solid porous particles. In vivo studies show that the proposed strategy was efficient in decreasing the tumor burden and increasing survival of the animals with liver metastasis. Interestingly, macrophage phenotype was also affected from pro-tumorigenic to antitumorigenic.

Another strategy we are pursuing in our research involves affecting the CD47-sIRP alpha axis between cancer cells and macrophages. CD47 is a “don’t eat me” signaling moiety that is overexpressed on cancer cells and is recognized by sIRP alpha receptor on macrophages. This recognition yields pro-tumorigenic signaling, encouraging tumor growth and enabling resistance to therapy.

We analyzed clinical samples of ovarian cancer patients, showing that the axis is upregulated in advanced disease stages. Our studies show that disrupting this axis with nanotherapeutics overcomes resistance to carboplatin in the models of advanced ovarian cancer.

Cells and elements in the organ microenvironment that play a key role in the process of delivery and retention of therapeutics by nanocarriers, as well as ways to personalize nanotherapy based on the organ’s features using cell culture models and computational modeling will be discussed.

Keywords: breast cancer, ovarian cancer, liver metastasis, nanomedicine.

Boosting translation in nano-enabled medical technologies: Lessons learned in the H2020 OITB Project Safe-N-Medtech

Angel del Pozo [1]
[1] Department of Programmes Strategy, Biokeralty Research Institute AIE, Miñano, Spain

Abstract:
Society and clinical practice pose a growing demand on novel biomaterials, ICT, micro and nanotechnologies for innovative medical devices (MDs) and *in vitro* diagnostics (**Medical Technologies-MTs**). In addition to the challenge of time to market, the new technologies are subjected to other pressing factors such as qualification,regulation, cost, biocompatibility and the need to be applicable worldwide.
In order to balance between the rapid development of innovative MTs and the safety and/or efficacy aspects, the newEU Medical Device and IVD Regulation was published in May of 2017, addressing, among other issues, patientsafety and the use of nanomaterials in MTs. This changing framework has opened a multiple challenge for the HealthTech Industry, R&D institutions, public administrations and healthcare providers, including introduction ofstandardized methodology, equipment and facilities for up-scaled production, characterization, testing, clinicalvalidation and certification, as well as business development of novel MTs. Safe-N-Medtech H2020 project has developed an Open Innovation Test Bed including last advances in all the related fileds, in order to offer the developers an integrated development pathway based on early regulatory guidance and early advice based on Health Technology Assessemnt. Four demo cases in the filed of nano cancer treatment (including a 1st in human clinical application), nano estructured implants, antimicrobial surfaces and patient biomonitoring will be also presented, together with the achievements in characterization, *in vitro*, *in vivo* and clinical research, prototyping, regulatory pathway and HTA, and how nano-medtech/nanomedicine developers can face translation in an easier and safer way.

Keywords: nanotechnology, medical devices, *in vitro* diagnostics, translation, biomaterials, clinical research, nanosafety, regulatory science, biomedical applications, cancer treatment, implants, biomonitoring

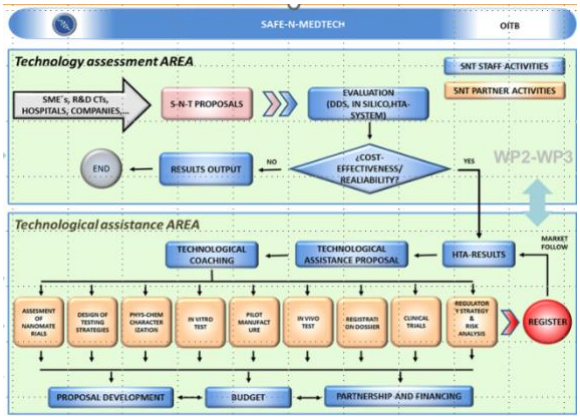

Figure 1: Figure illustrating the proposed workflow,activities, innovative tools, early technology assessment and development plan for the translation of nano-enabled medical technologies into the clinical settings and healthcare markets

References:

1. www.safenmt.com
2. Halamoda-Kenzaoui, B., Box, H., van Elk, M., Gaitan, S., Geertsma, R. E., Lafuente, E. Del Pozo, A., ... & Bremer-Hoffmann, S. (2019). Anticipation of regulatory needs.
3. Germain, M., Caputo, F., Metcalfe, S., Tosi, G., Spring, K., Åslund, A. K., ... & Schmid, R. (2020). Delivering the power of nanomedicine to patients today. *Journal of Controlled Release*, *326*, 164-171.

This project has received funding from the European Union's Horizon 2020 research and innovation program under grant agreement No 814607.

Nanotechnological Approaches against Leishmaniasis: Aerosol Therapy with Pentamidine-loaded Liposomes and Discovery of New β-sheet Intercalator Drugs

L. Román-Álamo [1,2,3]*, M. Allaw [4], Y. Avalos-Padilla [1,2,3], M.L. Manca [4], M. Manconi [4], J.A. Vázquez [5], J.E. Peris [6], X. Roca-Geronès [7], S. Poonlaphdecha [7], M.M. Alcover [7], R. Fisa [7], C. Riera [7], E.M. Arce [8,9], D. Muñoz-Torrero [8,9], X. Fernàndez-Busquets [1,2,3,]*

[1] Barcelona Institute for Global Health (ISGlobal), Barcelona, Spain
[2] Nanomalaria Group, Institute for Bioengineering of Catalonia (IBEC), Barcelona, Spain
[3] Nanoscience and Nanotechnology Institute (IN2UB), Barcelona, Spain
[4] Dept. of Life and Environmental Sciences, University of Cagliari, Cagliari, Italy
[5] Group of Recycling and Valorization of Waste Materials, Marine Research Institute, Vigo, Spain
[6] Department of Pharmacy and Pharmaceutical Technology, University of Valencia, Burjassot, Spain
[7] Departament de Biologia, Sanitat i Medi Ambient, Universitat de Barcelona, Spain
[8] Laboratory of Medicinal Chemistry (CSIC Associated Unit), University of Barcelona, Spain
[9] Institute of Biomedicine (IBUB), University of Barcelona, Spain

Abstract:
The treatment for leishmaniasis has relied for over 70 years on pentavalent antimonials as first therapeutic choice, although they have a well-known toxicity and may require long and painful dosing regimes. Pentamidine is administered intramuscularly or, preferably, by intravenous infusion, with its use limited by severe adverse effects including diabetes, severe hypoglycemia, myocarditis and renal toxicity. We sought to test the potential of phospholipid vesicles to improve patient compliance and efficacy of this drug for the treatment of leishmaniasis by means of aerosol therapy. The encapsulation of pentamidine in liposomes slightly ameliorated its activity on the amastigote form of *Leishmania infantum* and reduced unspecific cytotoxicity. The coating of pentamidine-loaded liposomes with chondroitin sulfate or heparin significantly improved their targeting to macrophages. The deposition of liposome dispersions after nebulization was evaluated with the Next Generation Impactor, which mimics the human airways. Nebulizing pentamidine in solution, its deposition in the deeper stages of the impactor was ~53% of the total initial drug and the median aerodynamic diameter was ~2.8 µm, indicating a partial deposition on the lung alveoli. Upon loading pentamidine in phospholipid vesicles, its deposition in the deeper stages increased up to ~68% and the median aerodynamic diameter decreased to a range between 1.4 and 1.8 µm, suggesting a better aptitude to reach in higher amounts the deeper lung airways.

In the search for new drugs, inhibiting protein aggregation with small β-sheet intercalators showed a significant antileishmanial effect. In particular, the styrylpyridinium salt YAT2150 had a better activity against *L. infantum* than some drugs currently used for the clinical treatment of leishmaniasis, such as miltefosine or pentamidine. The encapsulation of YAT2150 in the lipid bilayer (Figure 1) of immunoliposomes targeted to *Leishmania* through their functionalization with antibodies against lipophosphoglycan improved drug activity.

Keywords: *Leishmania infantum*, leishmaniasis, pentamidine, liposomes, drug encapsulation, aerosol therapy, YAT2150, β-sheet intercalators.

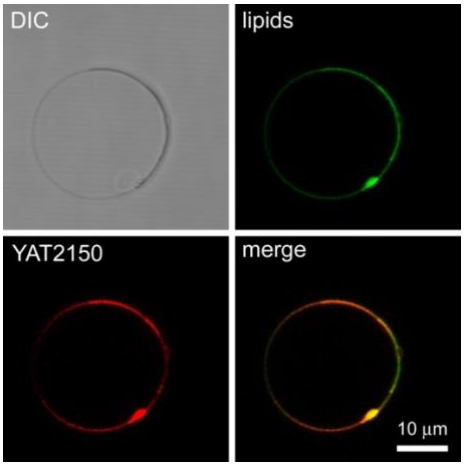

Figure 1: Encapsulation of 2.5 µM YAT2150 in the lipid bilayer of giant unilamellar vesicles (10 mM total lipid concentration). DIC: differential interference contrast image.

Funding: This project was funded by *Fundació La Marató de TV3* (Ref. 201811) and MCIN/AEI (Refs. PID2021-128325OB-I00 and PDC2022-133085-I00), Spain.

Fabricating Quantum Dots for Technological Applications

Kevin Critchley
School of Physics and Astronomy, University of Leeds, Leeds, LS2 9JT. UK, k.critchley@leeds.ac.uk

Abstract
Quantum dots (QDs) are a successful outcome of nanoscience research. They have unique properties which have been intensely studied for many promising technological applications. For example, unique properties of semiconductor nanoparticles are ideally suited for fluorescence imaging. Advanced fluorescence imaging will provide a high-resolution means of detecting diseased cells; tracking nano-encapsulated drugs; and studying intracellular mechanisms. These semiconductor nanoparticles are commonly known as quantum dots - derived from the fact that decreasing the size of the nanoparticles introduces quantum confinement of the charge carriers leading to an increased bandgap. By tuning the size of the semiconductor one can therefore tune the emission wavelength. To date, the most studied semiconductor nanoparticles are cadmium-based (CdTe, CdSe, and CdS). These cadmium-based quantum dots have excellent optical properties, stability, and monodisperisty. However, increasing global restrictions and lack of biocompatibility of cadmium has led to questions about the future of quantum dots for many applications. This has led to the investigation of other alternatives [1]. This report shows the characterisation of $CuInS_2$ and InP quantum dots and their physical and chemical properties – such as the broad defect state emission of $CuInS_2$ QDs and their origin (Fig. 1) [2, 3]. Using this example, recent research on QD- QD interactions under aqueous conditions to produce nanoclusters of QDs in a controlled manner will be described.

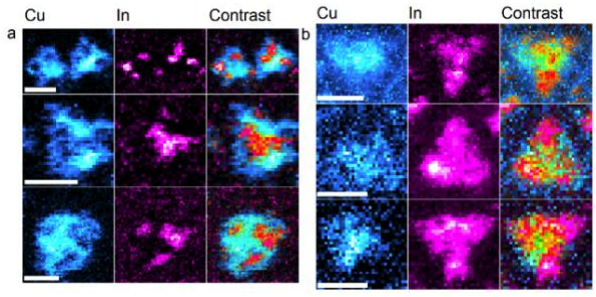

Fig 1. Elemental maps of Cu and In for CuInS2 core (a) and CuInS2/ZnS "core/shell" (b) QDs. The column labelled "Contrast" is a subtractive RGB difference overlay of the respective Cu and In maps. On each QD, areas of high In signal correspond with a low Cusignal and vice versa, showing segregation of Cu and In within particles. Scale bars 2 nm.

References

1. Morselli, G., et al., *Luminescent copper indium sulfide (CIS) quantum dots for bioimaging applications.* Nanoscale Horizons, 2021. **6**(9): p. 676-695.
2. Harvie, A.J., et al., *Observation of compositional domains within individual copper indium sulfide quantum dots.* Nanoscale, 2016. **8**(36): p. 16157-16161.
3. Kraatz, I.T., et al., *Sub-Bandgap Emission and Intraband Defect-Related Excited-State Dynamics in Colloidal CuInS2/ZnS Quantum Dots Revealed by Femtosecond Pump–Dump–Probe Spectroscopy.* The Journal of Physical Chemistry C, 2014. **118**(41): p. 24102-24109.

Combination Therapy at the Nanoscale for the Targeted Delivery of New β-sheet Intercalator Antimalarial Drugs

I. Bouzón-Arnáiz [1,2,3], Y. Avalos-Padilla[1,2,3], V. Iglesias [1,2,3,4], O. Cuspinera-Darnaculleta [1,2,3], L. Román-Álamo [1,2,3], C. Camarero-Hoyos [1,2,3], M. Ramírez [1], M. Rawat [5], R. Coyle [5], M. Lee [5], E.M. Arce [6,7], D. Muñoz-Torrero [6,7], X. Fernàndez-Busquets [1,2,3,*]

[1] Barcelona Institute for Global Health (ISGlobal), Barcelona, Spain

[2] Nanomalaria Group, Institute for Bioengineering of Catalonia (IBEC), Barcelona, Spain

[3] Nanoscience and Nanotechnology Institute (IN2UB), Barcelona, Spain

[4] Institut de Biotecnologia i Biomedicina and Departament de Bioquímica i Biologia Molecular, Universitat Autònoma de Barcelona, Bellaterra, Spain

[5] Wellcome Sanger Institute, Wellcome Genome Campus, Hinxton, United Kingdom

[6] Laboratory of Medicinal Chemistry (CSIC Associated Unit), University of Barcelona, Spain

[7] Institute of Biomedicine (IBUB), University of Barcelona, Spain

Abstract:

All *Plasmodium falciparum* stages have abundant intracellular protein aggregation, which is predicted to have a functional essential role for the pathogen. The inhibition of protein aggregation in malaria parasites has been recently proposed as a novel mode of action for new drugs. This mechanism presumably targets multiple proteins, which will likely prevent a rapid resistance evolution by the pathogen, as opposed to most other current antimalarial drugs which target products of one or a few genes. One such compound that targets protein aggregation, the bis(styrylpyridinium) salt YAT2150, a β-sheet intercalator, has a number of additional properties that make it a promising antiplasmodial agent, namely: (i) fast-acting drug without cross resistance to chloroquine and artemisinin; (ii) it fluoresces when interacting with its molecular targets in *Plasmodium* cells, which makes it a potential theragnostic agent; (iii) *in vitro* IC_{50} below 100 nM against *P. falciparum* asexual blood stages and similar potency on early and late stage gametocytes; (iv) it belongs to an unexplored chemical family where no other antimalarial has been described up to date, which will prevent the adaptation by the parasite of preexisting resistance mechanisms to currently used drugs; (v) inability to select resistant mutants *in vitro* after 60 days of incubation, which postulates this compound as an 'irresistible' antimalarial drug deserving attention in a likely future scenario of widespread resistance to artemisinin; (vi) its synthesis is easy and rapid (only two steps), resulting in an attractive activity/cost ratio; (vii) a long shelf life (months) at room temperature. We have characterized the PK/PD profile of YAT2150, and our current efforts are focused on widening its therapeutic window through the synthesis of chemical derivatives of lower toxicity and higher antiplasmodial activity, and their encapsulation in targeted nanocarriers. To conclude, we will present our latest proteomics results pointing at the functionality of protein aggregation in *P. falciparum* and our current hypothesis regarding why and how its inhibition can be lethal for the pathogen.

Keywords: *Plasmodium falciparum*, malaria, liposomes, drug encapsulation, YAT2150, β-sheet intercalators, giant unilamellar vesicles, targeted drug delivery.

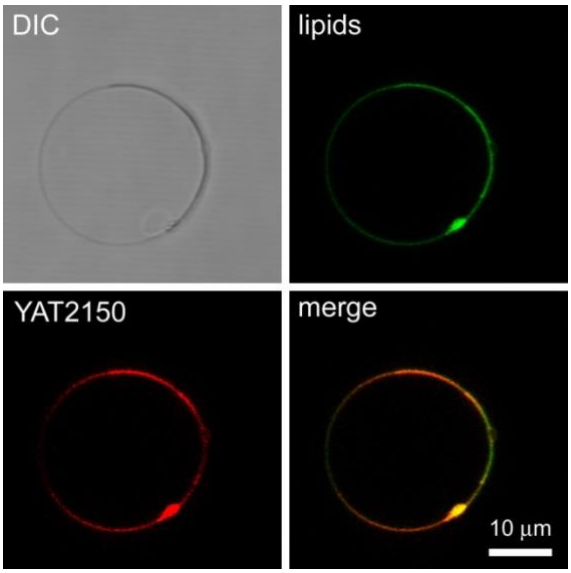

Figure 1: Encapsulation of 2.5 µM YAT2150 in the lipid bilayer of giant unilamellar vesicles (10 mM total lipid concentration). DIC: differential interference contrast image.

Funding: This work was supported by grants PID2021-128325OB-I00 and PDC2022-133085-I00, funded by *Ministerio de Ciencia e Innovación/Agencia Estatal de Investigación* (MCIN/AEI/ 10.13039/501100011033), which included FEDER funds.

Erythrocytes derived vesicles as platform for therapeutic nucleic acid delivery

G. Della Pelle [1*], T. Božič [2,] B. Markelc [2], J. Šribar [3], K. Žagar Soderžnik [1] M. Erdani-Kreft[4], S. Hudoklin[4], N. Kostevšek[1]

[1] Nanostructured materials, Jožef Stefan Institute, Ljubljana 1000 Slovenija

[2] Department of Experimental Oncology, Oncology Institute, Ljubljana 1000, Slovenija

[3] Department of Molecular and Biomedical Science, Jožef Stefan Institute, Ljubljana 1000 Slovenija

[4] Faculty of Medicine, Institute of Cell Biology, University of Ljubljana, Ljubljana 1000 Slovenija

Abstract:

Biomimetic approach is the next challenge for nanomedicine. With the discovery of extracellular vesicles, natural miRNAs carriers, research has attempted to take advantage and scale up EV/exosomes based formulations. On the other hand, erythrocytes have long been employed as enzyme carriers (Rossi et al., 2019), therefore solving the ancient allergy related problem and achieving perfect biocompatibility. Erythrocytes are the most abundant cells in human body and the unique properties of their membrane make them a good scaffold for liposomal-like formulations: they possess on their surface CD47, a marker for macrophages, escaping immune system recognition. Erythrocytes-membrane vesicles (EMVs) are obtained via extrusion of erythrocytes ghosts, i.e. depleted from hemoglobin: we demonstrated already their superiority as MRI T2 contrast agent and cyanine dyes for IR in vivo imaging (Della Pelle et al., 2021; Kostevšek et al., 2021), increasing, respectively, r2 relaxivity times of 5 nm SPIONs and reducing indocyanine green degradation upon infrared laser irradiation. Lastly, we aimed to ascertain whether or not EMVs would represent suitable therapeutic nucleic acid carriers. We chose Tdtomato gene as reporter gene for the proof-of-concept. We developed an efficient and time-cost effective method of small interference RNA loading, with extremely high encapsulation efficiency, and we thoroughly characterized siRNA-EMVs, proving both their efficacy, in terms of safe payload delivery to cytoplasm, developing an easy storage protocol, and their safety as carriers. Our platform is prone to surface modification and theranostic functionalization.

Keywords: nanomedicine, biomimetic carriers, erythrocytes, gene therapy, precision medicine

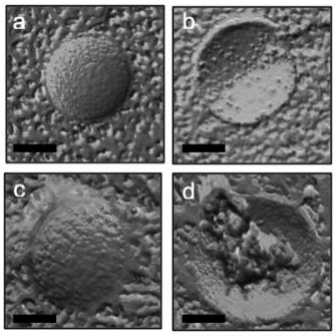

Figure 1: Freeze fracture TEM pictures of: a) empty EMVs, outside; b) empty EMVs, inner side; c) siRNA-EMVs, outer shell; d) siRNA EMVs, inner shell.

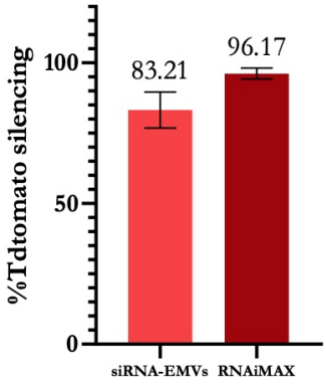

Figure 2: Silencing efficacy of siRNA-EMVs compared with RNAiMAX against TdTomato expression.

References:

1. Della Pelle, et al (2021). Cyanine Dyes for Photo-Thermal Therapy: A Comparison of Synthetic Liposomes and Natural Erythrocyte-Based Carriers. *Int. J. Mol. Sci*, *22*(13), 6914.
2. Kostevšek, N., et al. (2021). Magneto-erythrocyte membrane vesicles' superior t2 mri contrast agents to magneto-liposomes. *Magnetochemistry*, *7*(4), 51.
3. Rossi, L.,et al (2019). *Red Blood Cell Membrane Processing for Biomedical Applications*. *10*, 1070.

Use of nanostructured MOX sensors to detect colorectal cancer by measuring blood samples and post-surgical follow-up

M. Astolfi [1,2,*], G. Rispoli [3], G. Anania [4], G. Zonta [1,2], C. Malagù [1,2]
[1] Department of Physics and Earth Sciences, University of Ferrara, Via Saragat 1, Ferrara (FE), Italy
[2] SCENT S.r.l., Via Quadrifoglio 11, Ferrara (FE), Italy
[3] Department of Neurosciences and Rehabilitation, University of Ferrara, Via Fossato di Mortara 17-19, Ferrara (FE), Italy
[4] Department of Medical Sciences, University of Ferrara, Corso Giovecca 203, Ferrara (FE), Italy

Abstract:
Nowadays, cancer is a serious public health problem, and it is the cause of many and many deaths worldwide. Its incidence and mortality are progressively increasing due to the fast population growth and the increase of their average age [1]. Therefore, early cancer detection is a challenge for many researchers working in many different fields, and, in particular, it is crucial to develop innovative low-invasive and reliable cancer screening techniques and post-treatment (pharmacological and/or surgical) follow-up protocols [2].
On this basis, the research team of the "Laboratorio Sensori" (University of Ferrrara) enterely developed a sensor device (as a prototype), hosting four different concurrently-working nanostructured metal-oxide (MOX) sensors, in order to detect and study the volatile organic compounds (VOCs) related to a neoplastic formation, by analyzing blood samples collected from patients affected by colorectal cancer (CRC) [3]. The chosen sensors were based on proper combinations of different semiconductor metal-oxide materials, and in particular they were: ST25 (Tin, Titanium oxides), W11 (Tungstenum oxide), STN (Tin, Titanium, and Niobium oxides), and TiTaV (Titanium, Tantalum, and Vanadium oxides). The sensor sensing material consists in a porous thick-film (20-30 μm) made up of an interconnected network of semiconductor nano grains with size ranging between 50 and 200 nm. Therefore, these sensors are nanostructured and their working principle resides in the chemoresistivity: the sensor resistance variation is related to the chemical redox reactions occurring between the sensing film and the surrounding gas[3-5]. A first feseability study was carried out by comparing the sensor outcomes related to blood samples (CB) collected (in K3-EDTA vials) from twenty five CRC-affected patients, with the ones (the same number of samples) collected from healthy people (CH), used as controls; the latter were selected as people who has the least possible number of risk factors (young, non-smoking, not overweight, etc.) [3]. The obtained outcomes demonstrated that all the selected sensors, but W11, were undoubtedly able to discern between CB and CH as shown in Figure 1a. Moreover, these outcomes were furtherly processed through principal component analysis and the ROC curves in order to emphasize the reliability of the sensors in this application, by evaluating their sensitivity and specificity. Concerning this, ST-based sensors (ST25 and STN) demonstrated to be the most performing ones for this application [3].
Given these encouraging results, a new study was undertaken in 2020, foreseeing a follow-up protocol on CRC surgically treated patients, by measuring blood samples during their post-surgery path. By using an updated version of the aforementioned device, and after the W11 senosor replacement (that demonstrated to be the worst one in the previous study) with a $SmFeO_3$ one (sensor based on Iron and Samarium oxides), the follow-up protocol was applied to thirty patients, subjected to a surgical (laparoscopic or laparotomic) treatment, by performing four blood sample collections: T1, before surgery; T2, before the patient dehospitalization (about six days after surgery); T3 and T4 after one month and ten-twelve months from surgery, respectively. The preliminary statistical results are reported in Figure 1b, where it is shown that all the sensors provided lower responses for T4 samples with respect to T1 ones; this response difference could be attributed to the presence and the absence of the tumoral mass respectively, that, if present, it discharges tumoral products (deriving from the cancer cell alterations) in the blood stream [6]. The sensor responses to T2 and T3 samples were not included in this analysis because of their unreliability (i.e. the hospitalization period was not standardized, the results could be altered by drug deliveries, anesthesia, etc.) These results were furtherly processed by principal component analysis and

ROC curves in order to statistically quantize the sensor device performances; the device sensibility and specificity were 93% and 82%, respectively, showing a future huge suitability of this device to monitor the post-surgical patient's health status.

Keywords: metal-oxides, sensors, cancer, VOCs, chemoresistivity, blood, screening, gas detection, colorectal cancer.

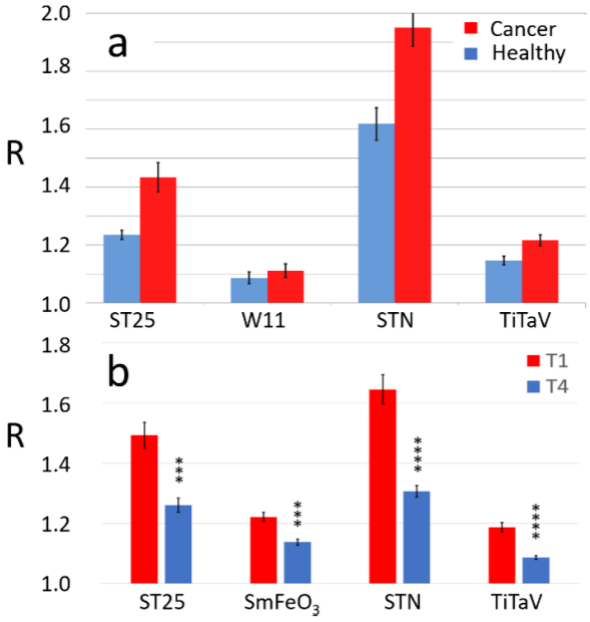

Figure 1: Sensor average responses: a) comparison between the average of the sensor responses to blood samples collected from CRC affected patients (n=25) and the ones collected from heathy-supposed people (n=25); b)comparison between the average sensor responses to T1 and T4 blood samples (n=30).

References:

1. Siegel, R. L., Miller, K. D., Fuchs, H. E., Jemal, A. (2022), Cancer statistics, *CA Cancer J Clin.*, 72(1), 7–33.
2. Strul, H., Arber, N. (2007), Screening techniques for prevention and early detection of colorectal cancer in the average-risk population, *Gastrointestinal cancer research: GCR*, 1(3), 98–106.
3. Astolfi, M., Rispoli, G., Anania, G., Artioli, E., Nevoso, V., Zonta, G., Malagù, C. (2021), Tin, Titanium, Tantalum, Vanadium and Niobium Oxide Based Sensors to Detect Colorectal Cancer Exhalations in Blood Samples, *Molecules*, 26, 466.
4. Astolfi, M., Rispoli, G., Anania, G., Nevoso, V., Artioli, E., Landini, N., Benedusi, M., Melloni, E., Secchiero, P., Tisato, V., Zonta, G., Malagù, C. (2020), Colorectal Cancer Study with Nanostructured Sensors: Tumor Marker Screening of Patient Biopsies, *Nanomaterials*, 10, 606.
5. Astolfi, M., Rispoli, G., Benedusi, M., Zonta, G., Landini, N., Valacchi, G., Malagù, C. (2022), Chemoresistive Sensors for Cellular Type Discrimination Based on Their Exhalations, *Nanomaterials*, 12(7), 1111.
6. Wang, C., Li, P., Lian, A., Sun, B., Wang, X., Guo, L., Chi, C., Liu, S., Zhao, W., Luo, S., et al. (2013), Blood volatile compounds as biomarkers for colorectal cancer, *Cancer Biol. Ther.*, 15, 200–206.

High-fidelity heart valve biomodel for aortic root and mitral valve surgery simulation training applications

David Varghese, Klaudiusz Stoklosa , Abhishek Joshi, Wael Awad, Philip Curry, Arash Shahidi, Richard Arm

Abstract:

The purpose of this study was to develop a realistic, cost-effective, high-fidelity heart valve model for cardiac surgeons and trainees to practice aortic root and mitral valve surgical procedures.

The heart valve model was created based on computed tomography coronary angiography images of a consenting patient. Image processing software was used to produce digital models from the computed tomography data for additive manufacturing. Novel post-print processing and synthetic, modified polydimethylsiloxane gels, additives, fibres and fabrics were used to recreate soft tissue tactility that was analogous to living human tissues. Tissue hardness's were matched to the data published in the literature and substitute materials were mechanically tested for comparison.

The model was assessed based on qualitative comparison to the real life, aortic root and mitral valve surgical procedures by surgeons. Several different procedures were trailed using the model, such as aortic valve replacement, the David, Ozaki, Bentall, and Yang aortic root procedures, as well as mitral valve replacement and repair. Manufacturing methodology ensured unit costs remained under fifty US dollars each.

The focus on affordability and reusability may encourage widespread use in 'dry-lab' training scenarios. The versatility of the model's included anatomy offers the potential to enhance surgical training while increasing trainees' aortic root and mitral valve procedural understanding and proficiency. Because anatomy is taken from scan data, the manufacturing methodologies are transferable to different pathologies based on real-life cases. Access to high-fidelity models also empowers consultant surgeons looking to add to their armamentarium of surgical procedures through preoperative practice.

Keywords: Surgical simulation; cardiac surgery; surgical skills; cardiac surgery residency; aortic root; mitral valve

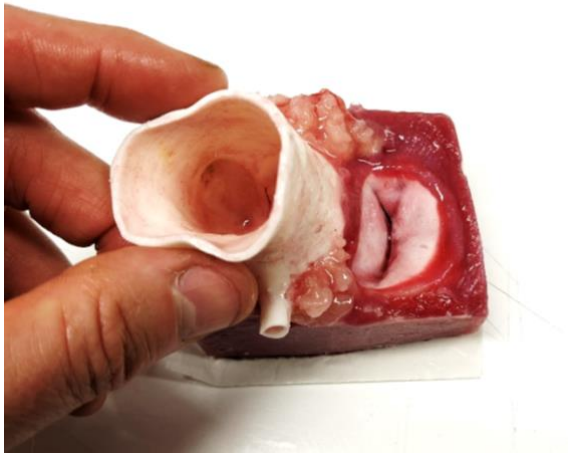

Figure 1: Heart Valve model showing Left coronary cusp. Right coronary cusp, Noncoronary cusp, Left coronary artery, Right coronary artery, Mitral valve and Aortic root.

References:

1. Clark RE. Stress-strain characteristics of fresh and frozen human aortic and mitral leaflets and chordae tendineae: implications for clinical use. J Thoracic Cardiovasc Surg 1973;66(2):202-8
2. Mohan D, Melvin JW. Failure properties of passive human aortic tissue. II—Biaxial tension tests. J Biomech 1983;16(1):31-44.
3. Arm R, Shahidi A, Clarke C, Alabraba E. Synthesis and characterisation of a cancerous liver for presurgical planning and training applications. BMJ Open Gastroenterology 2022;9(1):e000909.

NanoMatEn - Session III. Nanotechnology for Environmental Application / Water treatment

Laba and Organs on Chip for Health and Climate

Albert van den Berg
BIOS-Lab on a Chip group, MESA+ Institute, University of Twente, The Netherlands

Abstract:
The recent rapid developments in bionanotech and micro/nanofluidic technologies has enabled the realization of miniaturized laboratories. These Labs-on-a-Chip will play an important role in future medicine, both in point-of-care devices for drug or biomarker monitoring, as well as in early diagnostic devices. Microfluidics can also be exploited to manipulate and experiment with cells on chip. We have developed a microsystem for sperm analysis and selection for artificial insemination, where we can electrically detect and sort healthy sperm cells. Apart from diagnostic and cell manipulation devices, microfluidic devices are increasingly used to realise advanced disease and organ-models, as illustrated by the blood-brain barrier chip, a blood vessel on a chip to study atherosclerosis and cancer spheroids on chip for dynamic drug dosing. These Organs on Chip may lead to more rapid and cheaper drug development, personalised medicine and improved disease models, while minimizing or even eliminating animal testing (3R principle). We have developed a Translational Organ on Chip Platform (TOP) that enables simple plug and play connection of different Organ on Chip modules to a fluidic base plate. Finally, a microfluidic impedance spectroscopy system will be presented that can monitor the calcification of coccolithophores (algae), which plays an important role in the oceanic carbon cycle, and some preliminary results on the study of accelerated weathering of olivine using micoreactors will be presented.

Keywords: microfluidics, Lab on Chip, Organs on Chip, micro/nanofabrication, biomedical applications, medical diagnostics.

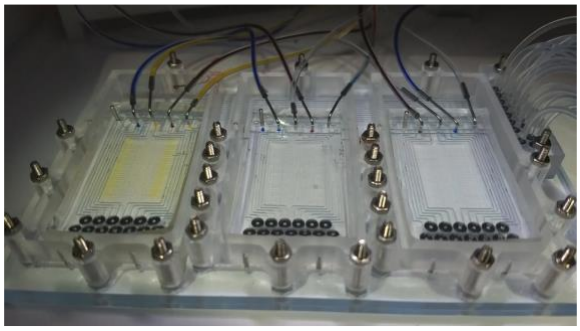

Figure 1: Illustration of 3 Organ on Chip baseplates, each containing 64 micro culture chambers

From the Atomic Structure to the Optoelectronic Properties Studies of Low Dimensional Inorganic NanoMaterials via TEM

R. Arenal[1,2,3,*]
[1] Instituto de Nanociencia y Materiales de Aragon (INMA), CSIC-U. Zaragoza, 50009 Zaragoza – Spain
[2] Fundacion ARAID, 50018 Zaragoza – Spain
[3] Laboratorio Microscopias Avanzadas, U. Zaragoza, 50018 Zaragoza – Spain

Abstract:
Detailed structural and chemical composition analyses, at the atomic scale, of nanomaterials are required in order to determine their impact on the properties of such objects. Transmission electron microscopy (TEM) and in particular, spatially-resolved electron energy loss spectroscopy (SR-EELS) developed in an aberration-corrected TEM, is the most powerful technique to get this information. Indeed, having access to a close to 1 angstrom electron probe, the atomic configuration of these nanomaterials can be obtained [1-10].
In this communication, I will present a selection of recent works involving all these matters. These works will concern the study of the atomic structure & configuration of 1D and 2D atomically thin nanostructures (including nanotubes & graphene/graphene-like material in pristine and hybrid forms) as well as the opto-electronic properties studies carried out via EELS measurements [1-10]. These works will illustrate the excellent capabilities offered by the use of a Cs probe-corrected (S)TEM, combined with the use of a monochromator, to study these properties within a very good spatial resolution. Furthermore, I will also present some recent in-situ TEM-EELS studies showing how powerful this approach can be for allowing the simultaneous measurement of various physical and chemical features of high interest for the study of different phenomena as the reduction of graphene oxide (GO) thin films [7,8].

Keywords: low dimensional materials, 2D materials, nanotubes, nanowires, TEM studies, electron spectroscopy investigations.

References:

1. K.S. Roy, S. Hettler, R. Arenal, L.S. Panchakarla, Mat. Horizons 9, 2115-2127 (2022).
2. A. Cohen, P. K. Mohapatra, S. Hettler, A. Patsha, K.V.L.V. Narayanachari, P. Shekhter, J. Cavin, J.M. Rondinelli, M. Bedzyk, O. Dieguez, R. Arenal, A Ismach, ACS Nano 17, 5399–5411 (2023).
3. M. Pelaez-Fernandez, B. Majerus, D. Funes-Hernando, R. Dufour, J.-L. Duvail, L. Henrard, R. Arenal, Nanophotonics 11, 3719–3728 (2022).
4. S. Hettler, M.B. Sreedhara, M. Serra, S.S. Sinha, R. Popovitz-Biro, I. Pinkas, A.N. Enyashin, R. Tenne, R. Arenal, ACS Nano 14, 5445 (2020).
5. M. B. Sreedharaa, S. Hettler, I. Kaplan-Ashiri, K. Rechav, Y. Feldman, A. Enyashin, L. Houben, R. Arenal, R. Tenne, PNAS 118, e2109945118 (2021).
6. M. Pelaez-Fernandez, Y.C. Lin, K. Suenaga, R. Arenal, Nanomaterials 11, 3218 (2021).
7. M. Pelaez-Fernandez, A. Bermejo Solis, A.M. Benito, W.K. Maser, R. Arenal, Carbon 178, 477 (2021).
8. S. Hettler, D. Sebastian, M. Pelaez, A.M. Benito, W.K. Maser, R. Arenal, 2D Materials 8, 031001 (2021).
9. A. Kagkoura, R. Arenal, N. Tagmatarchis, Advanced Functional Materials 31, 2105287 (2021).
10. S. Hettler, M. Sreedhara, M. Serra, S. Sinha, R. Popovitz, I. Pinkas, A. Enyashin, R. Tenne, R. Arenal, ACS Nano 14, 5445 (2020).

2D Nanostructures at Atomic Scale: From Energy and Environmental Applications to Quantum Devices

J. Arbiol [1,2,*]
[1] Catalan Institute of Nanoscience and Nanotechnology (ICN2), CSIC and BIST, Campus UAB, Bellaterra, 08193 Barcelona, Catalonia, Spain
[2] ICREA, Pg. Lluís Companys 23, 08010 Barcelona, Catalonia, Spain

Abstract:
Technology at the nanoscale has become one of the main challenges in science as new physical effects appear and can be modulated at will. As developments in materials science are pushing to the size limits of physics and chemistry, there is a critical need for understanding the origin of these unique properties and relate them to the changes originated at the atomic scale, e.g.: linked to structural changes of the material, many times related to the presence of crystal defects or crystal surface terminations. Especially on 2D materials designed for electrocatalysis in energy and environmental applications, crystallography and distribution of the atomic species are of outmost importance in order to determine the active sites that will improve the reaction performance, including efficiency and selectivity towards certain reactions. In 2D nanomaterials the distribution and coordination of metal species at the surface are determining their final electrocatalytic behavior as the reactions of interest mainly occur at the surface. The presentation will show how pristine and perfect crystalline surfaces may tend to be inert versus particular reactions, while creation of certain types of defects or even a predetermined surface amorphization may highly improve the catalytic activity of these 2D nanomaterials [1-2].
In the present work, a combination of advanced electron microscopy imaging with electron spectroscopy, in an aberration corrected STEM will allow us to probe the elemental composition and structure in a high spatial detail, while determining the growth mechanisms and correlating the structural properties to their electrocatalytic performance.
The first electrocatalyst system to study is based on 2D MoS2 nanoflakes. MoS2 basal plane is not pretty catalytically active, in this sense, we need to find other ways to improve the activity of this material for example for the electrocatalytic hydrogen evolution reaction (HER). The hypothesis of the work considers that the grain boundaries (GBs) created at the interface between nanoflake domains, can be considered as a highly defective perimeter which can certainly improve the density of active sites. Taking this idea in mind, we engineered MoS2 connected nanoflakes at 5nm diameter range, which create a, ultra-high density of GBs (up to ~1012 cm−2). The obtained GBs present a complex bonding coordination that could be studied by atomic resolution aberration corrected (AC) high angle annular dark field (HAADF) scanning transmission electron microscopy (STEM). Using the 2D atomic models obtained from our AC HAADF STEM observations we could study the different hydrogen adsorption preferential sites on the different atomic arrangements in MoS2 (including different GBs and Edges). Theoretical DFT calculations of the H2 absorption free energy in these preferential sites in comparison to the MoS2 Basal Plane (BP) were performed, showing that some GB structures show better electrocatalytic activity than edges, and much better than the MoS2 BP [1].
In a second part, we study the way to obtain the maximum utilization of noble metal atoms in our 2D catalysts. We demonstrate the fabrication of a wafer-size amorphous PtSex films on a SiO2 substate via a low-temperature amorphization strategy, which offers single-atom-layer Pt catalysts with high atom-utilization efficiency (~26 wt%). This amorphous PtSex behaves as a fully activated surface, accessible to catalytic reactions, and features a nearly 100% current density relative to a pure Pt surface and reliable production of sustained high-flux hydrogen. Such an amorphization strategy is potentially extendable to other noble metals, including the Pd, Ir, Os, Rh and Ru elements, demonstrating the universality of single-atom-layer catalysts. The study is performed by combining AC HAADF STEM with DFT calculations and precise electrochemical tests [2].

Keywords: 2D materials, hydrogen evolution, energy, MoS2, PtSe2, ZnTe, ZnSe, bandgap energy mapping, electrocatalysis, direct to indirect bangap transitions, quantum materials, nanowires.

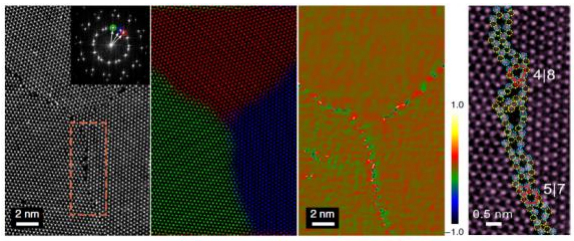

Figure 1: AC HAADF STEM magnified example of a triple grain boundary in MoS2 nanosheets and a detail of the complex bonding coordination [1].

References:

1. He, Y., et al. (2020) Engineering grain boundaries at the 2D limit for the hydrogen evolution reaction, *Nature Commun.*, 11, 57.
2. He, Y., et al. (2022) Amorphizing noble metal chalcogenide catalysts at the single-layer limit towards hydrogen production, *Nature Catal.*, 5, 212-221.
3. Martí-Sánchez, S., et al. (2022) Sub-nanometer mapping of strain-induced band structure variations in planar nanowire core-shell heterostructures, *Nature Commun.*, 13, 4089.

Metalorganic Copolymers From Iron(II) Clathrochelates: Versatile Materials and Conspicuous Adsorbents of Lithium Ions, Iodine, and Organic Dyes

S. Shetty [1,2], N. Baig [1,2], Bassam Alameddine [1,2,*]
[1] Department of Mathematics and Natural Sciences, Gulf University for Science and Technology, West Mishref, Kuwait
[2] Functional Materials Group, Gulf University for Science and Technology, West Mishref, Kuwait
* alameddine.b@gust.edu.kw

Abstract:
The organometallic copolymers with butyl, cyclohexyl and phenyl lateral groups were made from a one-pot complexation of iron(II) clathrochelate units that are interconnected by various thioether-containing contorted groups and tetraphenylbenzene units. The resultant copolymers were converted into their poly(vinyl sulfone) derivatives OTCP1-3 , OICP1-3 and CTP4-6 quantitatively via the selective oxidation of the thioether moieties into their respective sulfones using mild oxidation reaction conditions. The target copolymers were characterized by various instrumental analysis techniques. The copolymers were tested as potent lithium ions adsorbents revealing a maximum adsorption (q_m) value of 2.31 mg g^{-1} for OTCP2. Furthermore, this same copolymer was found to be a promising adsorbent of methylene blue (MEB); an isothermal adsorption study divulged that OTCP2's uptake of MEB from an aqueous solution (following the Langmuir model) was, at maximum adsorption capacity, (q_m) of 480.77 mg g^{-1}-; whereas the kinetic study divulged that the adsorption follows pseudo second-order kinetics with an equilibrium adsorption capacity ($q_{e,cal}$) of 45.40 mg g^{-1}. The iodine uptake studies of copolymers disclosed excellent iodine properties, reaching a maximum of 360 wt.% (q_e = 3600 mg g^{-1}). The adsorption mechanisms of the copolymers were explored using pseudo-first-order and pseudo-second-order kinetic models. Furthermore, regeneration tests confirmed the efficiency of the target copolymers for their iodine adsorption even after several adsorption-desorption cycles.

Keywords: Porous Polymers, Adsorbent Materials, Lithium Adsorption, Iodine Uptake, Dyes Adsorption.

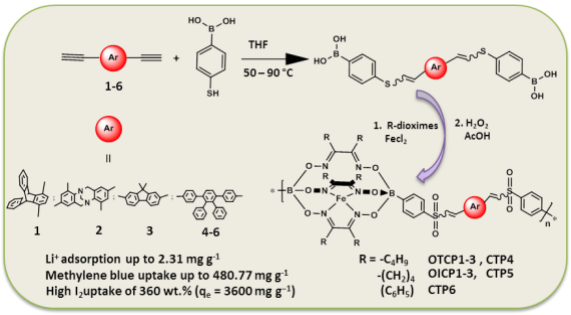

Figure 1: Synthesis of iron(II) clathrochelate adsorbents.

References:

1. Shetty, S.; Noorullah, B.; S., M. M.; Saleh, A.-M.; Bassam, A. Synthesis of Metalorganic Copolymers Containing Various Con-torted Units and Iron(II) Clathrochelates with Lateral Butyl Chains: Conspicuous Adsorbents of Lithium Ions and Methylene Blue Polymers 2022, p. 3394.
2. Shetty, S.; Noorullah, B.; Bassam, A. Synthesis and Iodine Adsorption Properties of Organometallic Copolymers with Propeller-Shaped Fe(II) Clathrochelates Bridged by Different Diaryl Thioether and Their Oxidized Sulfone Derivatives Polymers 2022, p. 4818
3. Baig, N.; Suchetha, S.; S., H. S.; A., H. A.; Saleh, A.-M.; Bassam, A. Synthesis of Iron Clathrochelate-Based Poly with Tetra-phenylbenzene Bridging Units Their Selective Oxidation into Their Corresponding Poly Copolymers: Promising Materials for Iodine, Capture Polymers 2022, p. 3727

Naphthyridine-based Luminophores for Highly Efficient ThermallyActivated Delayed Fluorescence Organic Light-Emitting Diodes

R. Keruckiene[1], E. Vijaikis[1], C.-H. Chen[2], B.-Y. Lin[3], J.-X. Huang[2], C.-C.Chu[2], Y.-C. Dzeng[4], C. Chen[4], .J.-H. Lee[2], T.-L. Chiu[5], S. Macionis[1], J. Keruckas[1], R. Butkute[1], J. V. Grazulevicius[1], E. Skuodis[1]

[1]Department of Polymer Chemistry and Technology, Kaunas University of Technology, K. Barsausko St. 59, LT-50254, Kaunas, Lithuania

[2]Graduate Institute of Photonics and Optoelectronics and Department of Electrical Engineering, Material Science and Engineering, and Physics, National Taiwan University, Taipei 10617, Taiwan

[3]Department of Opto-Electronic Engineering, National Dong Hwa University, Shoufeng, Hualien 974301, Taiwan

[4]Research Center for Applied Sciences, Academia Sinica, Taipei 11529, Taiwan

[5]Department of Electrical Engineering, Yuan Ze University, Taiwan

Abstract:

Organic light-emitting diodes (OLEDs) have made great progress in display technologies due to the advantages of low weight, low power consumption, and high colour saturation[1]. Organic compounds exhibiting phosphorescence and thermally activated delayed fluorescence (TADF) are versatile candidates for the improvement of device efficiency by extracting non-radiative triplet excitons, due to their ability to strong spin orbital coupling (SOC) and small singlet-triplet splitting (ΔE_{ST})[2]. Easily obtainable and efficient materials are preferred for the advancement of OLED technologies. The naphthyridine moiety has recently attracted attention as the acceptor moiety for the design of donor-acceptor (D-A) electroactive compounds[3]. The cyclization of amino-substituted phenylaldehyde can be performed using green chemistry methods that allow a mild and greener synthesis of substituted naphthyridines[4]. They have attracted interest due to their electron-deficient characteristic, tuneable luminescence, ease of structural modification and processing[5]

Four new emitters based on naphthyridine acceptor moiety and various donor units exhibiting TADF will be presented. The emitters exhibit excellent TADF properties with small ΔEST and high photoluminescence quantum yield. Green TADF-OLED based on 10-(4-(1,8-naphthyridin-2-yl)phenyl)-10H-phenothiazine exhibit maximum external quantum efficiency of 16.4 % with a Commission Internationale de L'éclairage coordinates of (0.368, 0.569) as well as high current and power efficiency of 58.6 cd/ A and 57.1 lm/ W. The supreme power efficiency is of record high value among the reported values for devices with naphthyridine-based emitters. This results from its high photoluminescence quantum yield, efficient TADF, and horizontal molecular orientation that was explored by angle-dependent photoluminescence and grazing-incidence small-angle X-ray scattering.

Acknowledgment. This project has received funding from European Regional Development Fund (project No 01.2.2-LMT-K-718-03-0019) under grant agreement with the Research Council of Lithuania (LMTLT).

References:

1. Kim, H.-B. & Kim, J.-J. Recent progress on exciplex-emitting OLEDs. (2019) *Journal of Information Display* **20**, 105–121.
2. Braveenth, R. *et al.* (2021) Achieving Narrow FWHM and High EQE Over 38% in Blue OLEDs Using Rigid Heteroatom-Based Deep Blue TADF Sensitized Host.
3. Lee, Y. & Hong, J.-I. (2020) High-efficiency thermally activated delayed fluorescence emitters via a high horizontal dipole ratio and controlled dual emission. *Journal of Materials Chemistry C* **8**, 8012–8017.
4. Anderson, E. C., Sneddon, H. F. & Hayes, C. J. (2019) A mild synthesis of substituted 1,8-naphthyridines. *Green Chemistry* **21**, 3050–3058.
5. Wang, K., Bao, Y., Zhu, S., Liu, R. & Zhu, H. (2020) Novel 1,5-naphthyridine-chromophores with D-A-D architecture: Synthesis, synthesis, luminescence and electrochemical properties. *Dyes and Pigments* **181**, 108596.

Nanostructured thin films of manganese oxide coupled with electrochemistry: an innovative eco-friendly water depollution process

C. Boillereau [1,*], S. Peulon [1*]
[1] University Paris-Saclay, CEA, CNRS, NIMBE, 91191, Gif-sur-Yvette, FRANCE

Abstract:
The consequences of human activities on the environment and human health are multiple due to air and soil pollution, the scarcity of water resources, and the abundance of wastes, recoverable or not. Although there are different kind of treatments to deal with this pollution, they become ill suited to the multitude of chemical molecules that is why it is constantly essential to improve them.
The innovative processes we are developing to treat water pollution are based on the use of nanostructured thin films of material, non-toxic and eco-friendly, with natural properties of redox and/or sorption reaction. These perfectly controlled materials, synthesized under the form of thin films by electrochemical methods (**Figure 1**), offer many advantages in terms of simplicity and adaptability, with very good robustness compared to powder due to their high-self regeneration capacity [1-5]. Moreover, these films can also be used as electrode materials to significantly increase their degradation power and to reduce interaction times, with extremely low energy inputs [4].
For example, birnessite thin films can spontaneously eliminate, degrade, and mineralize many organic and inorganic pollutants [1-6], with results comparable to other processes, while being much less energy-intensive. Moreover, such solids, used as electrodes materials, are particularly efficient to degrade until mineralization at room temperature the most persistent pollutants such as AMPA, organic dye or drug (phenothiazines molecules), which are particularly difficult to be eliminated by classical treatments in wastewater treatment plant (WWTP) [4,7,8].
Some pertinent results will be detailed in this presentation concerning phenothiazines molecules degradation, with solution analysis (ion chromatography) and solid characterization (SEM, XRD, Raman spectroscopy) [8]. Interfacial mechanisms, essential steps for process optimization, were elucidated thanks to complementary *in situ* and real-time monitoring (e.g. electrochemistry with UV-visible spectroscopy measurements).
This global strategy offers particularly interesting and promising prospects for potential applications with many pollutants, due to possible industrial development, at low energy costs and in very simple used conditions (room temperature, ambient pressure, no addition of toxic reagents, no filtration steps).

Keywords: Environment, Birnessite, Mn_7O_{13}, Electrodeposition, Phenothiazines.

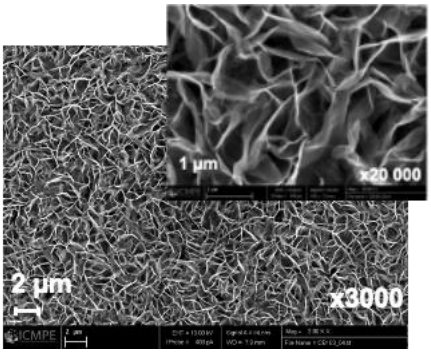

Figure 1: Typical example of nanostructured birnessite thin film electrodeposited: SEM observations.

References:

1. M. Zaied, S. Peulon et al., Appl. Catalysis B-Environ. 101 (2011) 441.
2. M. Zaied, E. Chutet, S. Peulon et al., Appl. Catalysis B-Environ. 107 (2011) 42.
3. Ndjeri, M., A. Pensel, S. Peulon et al., Colloids Surf. A, 435 (2013) 154.
4. A. Pensel, S. Peulon et al., Electrochem. Comm. 69 (2016) 19.
5. F. Tsin, A. Pensel, J. Vigneron, A.M Gonçalves, S. Peulon et al., Appl. Surf. Sci. 525 (2020) 146555.
6. R. Choumane, S. Peulon, Colloids Surf. A, 577 (2019) 594.
7. Aemig, Q., Hélias, A., D. (2021). Water Research, 188, 116524.
8. C. Boillereau, S. Peulon, in preparation (2023).

Enhanced adsorption and Photo-Fenton degradation of 2, 4-Dichlorophenoxyacetic acid using nanomagnetite/alginate nanocomposite based on brown algae: kinetic and thermodynamic studies

Laila M. Alshandoudi
Science Department, Al Rustaq College of Education, University of Technology and Applied Sciences, Al Rustaq, Sultanate of Oman
Corresponding author: lailaj.rus@cas.edu.om

Abstract
Three solid nanomaterials namely; nanomagnetite (NG), alginate (AG), and nanomagnetite/alginate nanocomposite (NGA) were prepared based on brown algae. The synthetized solid adsorbents were investigated using different physicochemical techniques such as TGA, XRD, nitrogen adsorption/desorption studies, SEM, TEM, zeta potential, ATR-FTIR, and DRS. The fabricated composite beads (NGA) exhibited advanced textural and chemical structure as 540 m^2/g as specific surface area, particle size of 85 nm, pH_{PZC} 7.3, and energy band gap of 2.1 eV. The prepared nanomagnetite/alginate nanocomposite contains different chemical functional groups in comparison with the other two solid materials due to the incorporation of nanomagnetite particles into the matrix of alginate biopolymer. Adsorption and Photo-Fenton oxidation degradation of 2,4-D (2,4-Dichlorophenoxyacetic acid) as one of the most widely used herbicide around the world were studied under different applications conditions as pH, dosage, initial 2,4-D concentration, time, and temperature. Nanomagnetite/alginate nanocomposite (NGA) had 256.8 mg/g at 35 ^oC, as the maximum adsorption capacity after 15 hours of shaking time. The adsorption process was well fitted by Langmuir, Temkin, PFO, and Elovich adsorption model. Photo-Fenton degradation of 2,4-D onto the surface of nanomagnetite/alginate nanocomposite requires only 15 minutes to reach 97% degradation efficiency at 25 ^oC. Kinetics and thermodynamic investigation of 2,4-D adsorption onto the three solid adsorbents were found to be spontaneous, endothermic, and physisorption in nature. On the other hand, Photo-Fenton degradation process was found to be non-spontaneous, and endothermic. The reusability of NGA as a catalyst confirmed that only 2.1% of its catalytic activity was decreased after six cycles of applications. Comparison between adsorption and Phot-Fenton catalysis proved that the prepared composite is efficient solid adsorbent at higher pollutant concentration while at lower herbicide concentration Photo-Fenton process is the best choice method.

Keywords: Nanomagnetite; alginate; composite; adsorption; Photo-Fenton; degradation.

References:

1. Asaad. F. Hassan, Laila M. Alshandoudi, Aya M. Awad, Ahmed A. Mustafa, Ghada Esmail (2023) Synthesis of nanomagnetite/copper oxide/potassium carrageenan nanocomposite for the adsorption and Photo-Fenton degradation of Safranin-O: kinetic and thermodynamic studies, Macromolecular Research. https://doi.org/10.1007/s13233-023-00147-4
2. Roman Bulánek, Hrdina Radim, A.F. Hassan (2019) Preparation of polyvinylpyrrolidone modifed nanomagnetite for degradation of nicotine by heterogeneous Fenton process. J. Environ. Chem. Eng. 7, 102988. https://doi.org/10.1016/J.JECE.2019.102988
3. Hammouda S.B., Adhoum N., Monser L. (2015) Synthesis of magnetic alginate beads based on Fe_3O_4 nanoparticles for the removal of 3-methylindole from aqueous solution using Fenton process. J. Hazard. Mater. 294, 128–136. https://doi.org/10.1016/J.JHAZMAT.2015.03.068
4. Asaad F. Hassan, Ahmed A. Mustafa, Ghada Esmail, Aya M. Awad (2022) Adsorption and photo-fenton degradation of methylene blue using nanomagnetite/potassium carrageenan bio-

composite beads. Arab. J. Sci. Eng. https://doi.org/10.1007/s13369-022-07075-y
5. Raheb, M.S. Manlla (2021) Kinetic and thermodynamic studies of the degradation of methylene blue by photo-Fenton reaction. Heliyon. 7, e07427. https://doi.org/10.1016/J.Heliyon2021.E07427
6. Sharma, K., Raizada, P., Hosseini-Bandegharaei, A., Thakur, P., Kumar, R., Thakur, V.K., Nguyen, V.H., Pardeep S. (2020) Fabrication of efcient CuO/graphitic carbon nitride based heterogeneous Photo-Fenton like catalyst for degradation of 2, 4 dimethyl phenol. Process Saf. Environ. Prot. 142, 63–75. https://doi.org/10.1016/j.psep.2020.06.003
7. Laila M. Alshandoudi, Said R. Alkindi, Tariq Y. Alhatmi, Asaad F. Hassan (2023) Synthesis and characterization of nano zinc oxide/zinc chloride–activated carbon composite based on date palm fronds: adsorption of methylene blue, Biomass Conversion and Biorefnery, https://doi.org/10.1007/s13399-023-03815-8.

A new approach towards the realization of specific and label-free biological sensing based on field-effect devices

Soumadri Samanta[1], Vinay S. Tiwari[2], Sumesh Sadhujan[3], Sherina Harilal[3,] Avital Eisenberg-Lerner[5], Ziv Rotfogel[5,6], Evgeny Pikhay[4], Ruth Shima-Edelstein[4], Doron Greental[4], Muhammad Y. Bashouti[3,9], Barak Akabayov[2], Izhar Ron[1], Yakov Roizin[4], Offer Erez[7,8], Gil Shalev[1,9]*

[1] School of Electrical Engineering, Ben-Gurion University of the Negev, Israel
[2]Department of Chemistry, Ben-Gurion University of the Negev, Beer-Sheva, Israel
[3]Department of Solar Energy and Environmental Physics, Swiss Institute for Dryland Environmental and Energy Research, Ben-Gurion University of the Negev, Israel
[4] Tower Semiconductor, PO Box 619, Migdal Haemek, Israel
[5] Ophthalmology Research Laboratory, Kaplan Medical Center, Rehovot, Israel
[6] Faculty of Medicine, The Hebrew University of Jerusalem, Jerusalem, Israel.
[7]Department of obstetrics and Gynecology Soroka University Medical Center, School of Medicine, Ben Gurion University of the Negev, Beer Sheva, Israel.
[8]Department of Obstetrics and Gynecology, Wayne State University, Detroit, MI, USA
[9] The Ilse-Katz Institute for Nanoscale Science and Technology, Ben-Gurion Uni. of the Negev, Israel

Abstract:
Specific and label-free detection of biological interactions is paramount to a plethora of technological applications. The Biologically-modified field-effect transistor (BioFET) is a promising sensing platform due to its inherent signal amplification, low power and miniaturization[1,2]. We report low-cost Meta-Nano-Channel BioFET (MNC BioFET) which provides means to electrostatically control the size, shape and location of the conducting channel such as to enhance the coupling between the locally-occurring electrostatics of the biological interactions and the electrodynamics of the underlying conducting channel. Moreover, it provides means to electrostatically control the Debye screening length at the sensing area to increase the readout signal. The MNC BioFET is fabricated in a large-scale silicon chip foundry which ensures robustness and stability, optimal noise levels and signal amplification, repeatability, and ultimate miniaturization with the potential for high-end multiplexing in ultra-small samples. We present results for specific and label-free sensing of alpha fetoprotein (AFP) with the MNC BioFET in ultra-small 0.5 µL drops of 1:100 diluted serum[3]. AFP is a biomarker for preeclamsia. Limit of the detection of 1 fg/ml and a dynamic range of 8 order of magnitude is presented. The dependency of the sensor signal on the channel configuration is also demonstrated. Recent data for sensing of PSA, botulinum, estriol and ferritin will be presented.

Keywords: specific sensing, label-free sensing, field-effect biosensing, BioFET, sensing of antibody-antigen interactions, real-time sensing.

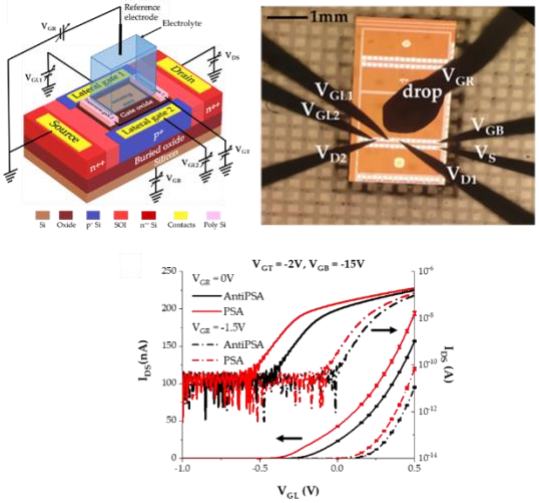

Figure 1: The MNC Biosensor and the MNC biochip. I-Vs demonstrating sensing of PSA.

References:

1. I. M. Bhattacharyya, I. Ron, A. Chauhan, E. Pikhay, D. Greental, N. Mizrahi, Y. Roizin, G. Shalev, *Nanoscale* **2022**, *14*, 2837.
2. I. M. Bhattacharyya, I. Ron, R. Shima-Edelstein, E. Pikhay, Y. Roizin, G. Shalev, *Adv. Electron. Mater.* **2022**, 2200399.
3. S. Samanta, V. S. Tiwari, S. Sadhujan, S. Harilal, A. Eisenberg-Lerner, Z. Rotfogel, E. Pikhay, R. Shima-Edelstein, D. Greental, M. Bashouti, B. Akabayov, I. Ron, Y. Roizin, O. Erez, G. Shalev, *Submitted*

Posters Session

Targeted synthesis and tailoring of gold nanorods

David G. Schauer*, Jona Bredehoeft, Hans Jakob Wörner
Department of Chemistry and Applied Biosciences, Laboratory of Physical Chemistry (LPC),
ETH Zurich, Vladimir-Prelog-Weg 2 / HCI E 241, 8049 Zurich, Switzerland

Abstract:
Metal nanoparticles (MNPs) are used in a wide range of everyday applications, e.g. in biomedicine for individual cell targeting, in pharmacy as vectors for CoViD-19 rapid tests, or also in sun lotions as a blockade against cancer-causing UV radiation. In all these applications, the size and shape of the individual MNPs is extremely crucial. In MNPs which are magnitudes smaller than the wavelengths of the incident light, the conduction electrons start oscillating when the surface of these MNPs is penetrated by electromagnetic radiation. The resonance frequency of these oscillations, also known as localized surface plasmon resonance (LSPR), can be influenced by the size of the MNPs. These oscillations create a dipole moment that interferes destructively with the incident light, which gives rise to absorbance at certain wavelengths. Therefore a correlation exists between the absorption maximum of MNP solutions and the size of the MNPs [1].

The gold nanorods (GNRs) for this work were synthesized using a seed-mediated growth method taken from Leng et al. (Ref. [2]). As figure 1 illustrates, a variety of GNRs were synthesized with different pH, volume of the chemicals used and growth time. A clear trend between the absorption wavelength and the pH was observed. At growth times longer than 1 h, at a pH > 5 the GNRs absorb at larger wavelengths (longer rods) and with an increase of the pH (~ 5 – 7.5) the absorption peak corresponding to the length of the rods undergo a blue shift (shorter rods). Adjusting both a higher volume and a growth time shorter than 1 h, this trend was no longer present. At a lower pH the absorption peaks indicating the lengths of the rods were blue shifted. As soon as the pH was set to a more basic value (~ 6.5), an overlap with the trend for GNRs with a growth time > 1 h was observed.

In order to carry out a targeted synthesis and tailoring of GNRs of any length, the pH value in relation to the volume and the growth time must be known and adjusted accordingly. This work therefore demonstrates a unprecedented level of detail on the controlled growth of gold nanoparticles (GNPs), which opens promising applications in nanoscience.

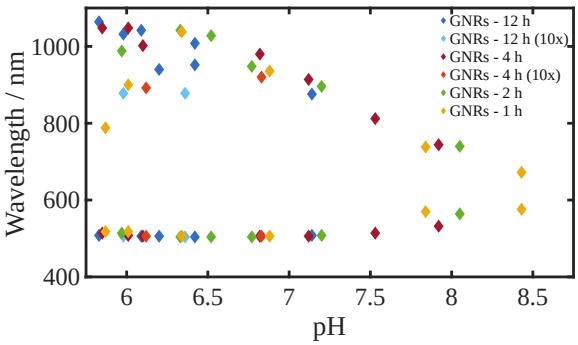

Figure 1: GNRs show two absorption maxima (diameter, length) in the Vis/NIR spectrum. The colored diamonds at the bottom (shorter wavelengths) indicate the absorption peaks for the diameter and their vertical correlating diamonds at longer wavelength show the absorption peaks of the lengths of different GNRs in respect to their pH. Reaching higher pH values (> 7.5) the absorption peaks corresponding to the diameter (shorter wavelengths) also undergo a shift towards longer wavelengths (red shift).

Keywords: gold nanorods, GNRs, gold nanoparticles, GNPs, metal nanoparticles, nanophotonics, localized surface plasmons, nanoparticle synthesis, pH-controlled, growth time, seed-mediated growth

References:

1. Amendola, V.; Pilot, R.; Frasconi, M.; Maragò, O. M.; Iatì, M. A. Surface Plasmon Resonance in Gold Nanoparticles: A Review. *J. Phys. Condens. Matter* **2017**, *29* (20), 203002.
2. Leng, Y.; Yin, X.; Hu, F.; Zou, Y.; Xing, X.; Li, B.; Guo, Y.; Ye, L.; Lu, Z. High-Yield Synthesis and Fine-Tuning Aspect Ratio of (200) Faceted Gold Nanorods by the PH-Adjusting Method. *RSC Adv.* **2017**, *7* (41), 25469–25474.

High-Speed Die Attachment by Transient Liquid Phase Bonding Using a Preform of 5 µm Cu@Sn Core-Shell Particles for High-Temperature Applications

Yeongjung Kim, Byeong Jo Han, Jong-Hyun Lee *
Department of Materials Science & Engineering, University Seoul National University of Science and Technology, Seoul 01811, Republic of Korea

Abstract:
A Sn-finish die was attached on a Sn-finish substrate through transient liquid phase (TLP) bonding at 250 °C using a preform material for attaining a bond-line which do not melt or can maintain long-term mechanical durability even at the high temperature such as 300 °C for high-temperature applications, unlike current solder joints. The preform thickness was 200 µm and consisted of Sn-coated Cu (Cu@Sn) particles. To achieve the attachment at higher speed, the particle size was decreased to average 5 µm and the Sn coating content was optimized with 30 wt%; thus, the average thickness of Sn shell was approximately 600 nm. The preform was fabricated by pressing the particles under 4 MPa and edge-grinding. The prepared 3 × 3 mm^2 preform was placed on a dummy Cu substrate with 3.18 µm thick Sn finish, and a 3 × 3 mm^2 dummy Cu chip having the identical Sn finish at bottom was aligned and placed on the preform. The attachment was performed for 5 min under 2 MPa compression at 250 °C in air. Consequently, the Sn shells disappeared by interaction with the core Cu and the fabricated bond-line presented the sufficient shear strength of 26.67 MPa by *in situ* sintering between formed Cu-Sn intermetallic compound (IMC) phases (Figure 1). Therefore, the die attachment speed by TLP bonding was outstandingly faster than that by similar bonding using 30 µm Cu@Sn particles, which can bring about a substantial effect in the improvement of production for industrial applications.

Keywords: die attachment, transient liquid phase bonding, preform, Sn-coated Cu particle, core-shell particle, intermetallic compound, shear strength.

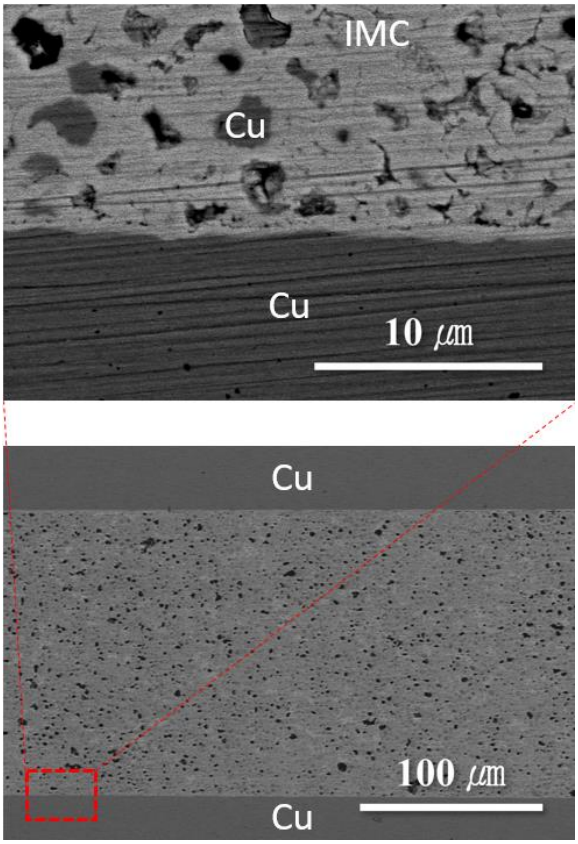

Figure 1: Cross-sectional and enlarged interfacial BSE images showing the bond-line between a Sn-finished die and substrate TLP-bonded for 5 min under 2 MPa at 250 °C using a 200 µm-thick preform of 5 µm Cu@Sn particles. Note the bond-line were totally consisted of high-melting-point phases by the rapid transformation of Sn shells into IMC.

References:

1. Hu, T., Chen, H., Li, M. (2016) Die attach materials with high remelting temperatures created by bonding Cu@Sn microparticles at lower temperatures, *Mater. Des.*, 108, 383-390.
2. Chen, H., Hu, T., Li, M., Zhao Z. (2017) Cu@Sn Core–shell structure powder preform for high-temperature applications based on transient liquid phase bonding, *IEEE Trans. Power Electron.*, 32, 441-451.

Analysis of B-rich B-Te Ovonic Threshold Switching Materials and Devices with Various Compositions

Hoedon Kwon[1], Kwangsik Jeong[3], Yeonwoo Seong[1], Hyoungsub Kim[4] and Mann–Ho Cho[1,2*]
[1] Department of Physics, Yonsei University, Seoul, 03722, Korea
[2] Department of System Semiconductor Engineering, Yonsei University, Seoul 03722, Rep. of Korea
[3] Division of Physics and Semiconductor Science, Dongguk University, Seoul 04620, Rep. of Korea
[4] School of Advanced Materials Science & Engineering, Sungkyunkwan University, Suwon 16419, Rep. of Korea

Abstract:
In manufacturing high-density multi-parallel structure memory devices such as 3D cross-point of Intel, the existence of sneak current through an unwanted path causes deterioration of information reliability. In order to prevent sneak current, selector device that can be switched by voltage is required. Among the selector materials of various material groups, the chalcogenide-based Ovonic threshold switching(OTS) materials have many advantages such as high speed, high selectivity, and bidirectional operation, therefore various OTS materials have been reported.

Te-based OTS materials are characterized by low-voltage operation and fast operation speed. However Te-based OTS materials have lower thermal and endurance because of lower crystallization temperature than S-based or Se-based OTS materials. In order to overcome this disadvantages, Te-based OTS materials were used by doping elements[1] or by configuring complex compositions. Unlike other two-component Te-based OTS materials, Boron telluride has been reported to have high thermal and electrical stability due to strong B-Te bonds and stable amorphous state caused by large size difference between boron and tellurium[2].

In this study, B-rich B-Te OTS devices with various composition ratios were fabricated and their electrical characteristics were confirmed by I-V measurement. The XPS analysis was conducted to investigate the stoichiometric characteristics linked to electrical properties. In addition, UV-vis-NIR spectroscopy analysis was utilized to confirm band structures of B_xTe. When composition of boron in B_xTe is increased, it is more insulating at off state and more thermally stable. Through optimization of the composition, it was confirmed that the off current density was very low compared to previously reported Te-based OTS materials. we also reported which band characteristics are linked to the electrical characteristics of OTS and presented the possible model similar to the circuit breaker model in RRAM that can explain why B-Te device has very low off current density.

Keywords: Ovonic threshold switching, selector, chalcogenide, amorphous material, boron telluride,

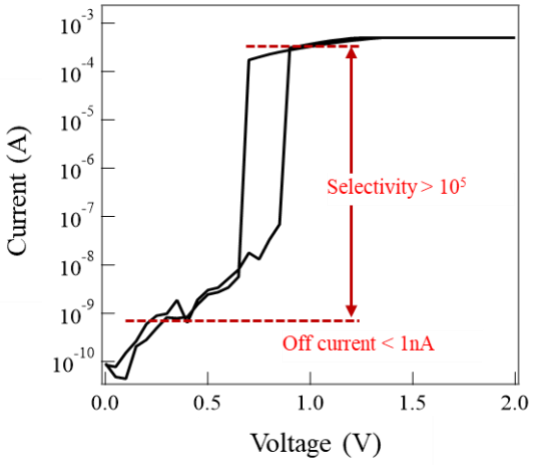

Figure 1: DC I-V characteristic of $B_{1.84}Te$ OTS device: high selectivity (> 10^5), low off current (< 1nA) and low threshold voltage (~ 1V)

References:

1. Wang, L., Cai, W., He, D., Lin, Q., Wan, D., Tong, H., & Miao, X. (2021). Performance Improvement of GeTe x-Based Ovonic Threshold Switching Selector by C Doping. *IEEE Electron Device Letters*, 42(5), 688-691.
2. Yoo, J., Kim, S. H., Chekol, S. A., Park, J., Sung, C., Song, J., Lee, D., & Hwang, H. (2019). 3D stackable and scalable binary ovonic threshold switch devices with excellent thermal stability and low leakage current for high-density cross-point memory applications. *Advanced Electronic Materials*, 5(7), 1900196.

The Effects of Gold Nanorods with Wavelength Irradiation

Tatiana Román [1*], Eden Morales-Narváez [1], Yunuen Montelogo [2]
[1] Centro de Investigaciones en Óptica, A.C. - CIO, León, Gto. México.
[2] Department of Engineering Science, University of Oxford, Oxford, OX1 3PJ UK

Abstract:
Metallic nanoparticles have useful applications in catalysis, optics, sensing, etc. In the same way, gold nanorods (AuNRs) have been found to have unique optical and photothermal properties opening up new possible applications. For example, the narrow longitudinal surface plasmon resonance (LSPR) linewidth of a gold nanorod, combined with the dipolar optical response allows only a small subpopulation of nanorods in the laser-irradiated region to be addressed optically.
By irradiating with a laser light the absorption of a laser pulse induces a temperature rise in the selected nanorods. For a relatively high laser pulse energy, the selected nanorods are heated above the melting temperature threshold and transform their shape into shorter rods or spherical particles, i.e., polarization-dependent bleaching of the irradiated light occurs (Figure 1). This results in a subpopulation of nanorods with a given aspect ratio and orientation.
In this work we seek to study the behavior of this selection of nanorods immersed in a polymeric material before and after being irradiated. Allowing to obtain different materials where each one obtains a variant of appearance and orientation of the nanorods to observe and analyze the change of properties that each of these can have.

Keywords: gold nanorods, photothermal, optical response, laser-irradiated, absorption, wavelengths.

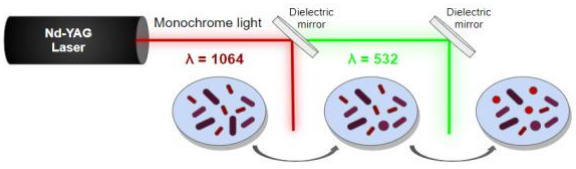

Figure 1: Experimental setup of the irradiation process with 1064 nm and 532 nm polarized laser light of Au nanorods immersed in nanocellulose.

References:

1. Babak N. and Mostafa A. (2003). "Preparation and Growth Mechanism of Gold Nanorods (NRs) Using Seed-Mediated Growth Method". Chem. Mater., 15, 1957-1962.
2. Peter Zijlstra, James W. M. Chon & Min Gu (2009). "Five-dimensional optical recording mediated by surface plasmons in gold nanorods". Nature, Vol 459.
3. Xu Ouyang, Yi Xu, Mincong Xian, Ziwei Feng, Linwei Zhu, Yaoyu Cao, Sheng Lan, Bai-Ou Guan, Cheng-Wei Qiu, Min Gu and Xiangping Li, (2021). "Synthetic helical dichroism for six-dimensional optical orbital angular momentum multiplexing". Nature Photonics, VOL 15, 901–907.

Effect of ZnO particle size on the activity in the photoreduction of CO_2

I. Pełech, A.W. Morawski, K. Ćmielewska, E. Kusiak-Nejman, U. Narkiewicz
Department of Inorganic Chemical Technology and Environment Engineering, Faculty of Chemical Technology and Engineering, West Pomeranian University of Technology in Szczecin, Pułaskiego 10, 70-322 Szczecin, Poland

Abstract:
Combustion of fossil fuels results in emission of carbon dioxide, the major anthropogenic factor related to climate change, affecting the healthy functioning of the biosphere. The existing post-combustion carbon capture technologies are energy demanding and not enough environmentally viable. The capture of carbon dioxide is a good idea, but there are much more prospective technologies (e.g. CCU, carbon capture and utilization), being a real breakthrough enabling to transform carbon dioxide into useful products (fuels or other chemicals). These technologies are still at the very initial technology readiness level and their efficiency is low, but an effort to develop them is necessary to close the carbon cycle, to moderate climate change and to decrease the exploitation of fossil fuels.
In this work, commercially available ZnO particles with different size and ZnO/carbon composites were used in the photoreduction of carbon dioxide. In order to prepare ZnO/carbon composites, carbon spheres obtained from resorcinol and formaldehyde were stirred with zinc oxide. Afterwards, the obtained mixture was transferred into a microwave-assisted solvothermal reactor, and treated for 15 min under a reaction pressure of 20 atm. Finally, the obtained composites were dried.
The photoreduction of CO_2 was carried out in two types of system: a liquid phase and a gas phase. In both cases, the processes were performed in a bottle-shaped glass reactor equipped with a quartz cooler constantly supplied with fresh water. In the cooler a medium-pressure mercury lamp TQ 150 Z3 (Heraeus, Germany) was set. Its power was 150 W and it was emitting UV/Vis light (mostly UV-A and UV-C). The reactor was placed in the thermostatic chamber in order to cut off any light sources and to ensure a stable temperature which was 20 °C. Before the process, the system was rinsed with pure CO_2 for 16 hours. Then, it was closed and the lamp was turned on. The gas phase was constantly stirred with the pump, and the liquid phase was mixed with a magnetic stirrer.
In the liquid phase processes the tested material was placed in the reactor in a form of suspension of 200 mg in 500 cm^3 of 0.2M NaOH aqueous solution. In turn, in the gas phase processes, the sample was first applied on glass fiber (FF 45 VLIES 50; 40 g/m^2) and then placed in the reactor. 10 cm^3 of distilled water was at the bottom of the reactor. It was necessary to generate hydrogen needed in the photoreduction process.
The processes were run for 6 hours and the gas samples were taken for analysis every 1 hour. The composition of the gas phase was analyzed with a Master GC gas chromatograph (DANI Instruments, Italy), equipped with a 4 m Shincarbon ST 100/120 micropacked column. The detectors were TCD and FID with the methanizer. Argon was the carrier gas. The content of individual components in the gas phase in subsequent measurements was calculated based on the calibration curve. The amount of hydrogen, carbon monoxide and methane produced during the processes was determined.
It was found that the smallest ZnO particles (26 nm) were characterized by the highest activity, regardless of type of the system: a liquid phase or a gas phase. For the materials with the addition of carbon spheres, higher activity was observed in the case of composites with addition of larger zinc oxide particles (5 μm).

Keywords: photoreduction, photocatalyst, zinc oxide, carbon dioxide, particle size, activity.

Acknowledgement:

The research leading to these results received funding from the Norway Grants 2014–2021 via the National Centre for Research and Development under the grant number NOR/POLNORCCS/PhotoRed/0007/2019-00.

Nitrates on Ceria: Effects of Morphology and Zr Doping

E. Ivanova[1*], M. Mihaylov[1], K. Chakarova[1], H. Aleksandrov[2], P. Petkov[2],
G. Vayssilov[2], K. Hadjiivanov[1]
[1]Institute of General and Inorganic Chemistry, Bulgarian Academy of Sciences, Sofia, Bulgaria
[2]Faculty of Chemistry, University of Sofia, Sofia, Bulgaria

Abstract:
Ceria (CeO_2) is a common catalyst component for DeNOx reactions. Surface nitrates act as important intermediates and their reactivity depends on their structure. Therefore, knowledge of the nitrate structure is essential for the design of new efficient DeNOx catalysts.
FTIR spectroscopy is one of the most convenient techniques for this purpose. However, the analysis of literature data shows that there are a number of problems in this respect. Therfore, we proposed a new classification of nitrates and a revision of the band assignments based on a comparison of experimental spectra with DFT-simulated spectra of modeled structures.
In this work, we report the influence of CeO_2 morphology on the type of surface nitrate species. For this purpose, samples with different crystallite shapes, nanopolyhedra, nanocubes and nanorods were hydrothermally synthesized. In the three cases different facets predominate on the surface, respectively (111), (100) and (110). In addition, the effect of Zr incorporation into the CeO_2 lattice was also studied by using mixed CeO_2-ZrO_2 oxides (with ZrO_2 content of 25 and 50%) obtained by co-precipitation.
Nitrates on the surface were obtained by coadsorption of NO and O_2 at room temperature on the samples previously activated in O_2 at 500°C and evacuated at the same temperature. Then, their stability was foolwed by FTIR under vacuum and increasing temperature. Isotopically labeled molecules, ^{15}NO and $^{18}O_2$, were also used to strengthen the IR band attributions.
At least five types of nitrate structures were identified, labeled A–E in descending order of their highest frequency (Figure 1). Note that nitrates are characterized by a set of three bands in the range 1700-900 cm^{-1}. Their stability increases in the same order, with the exception of C type, which are more stable than D type. The most stable nitrates, E type, are bonded through their three oxygen atoms, but most strongly through one of them. All other nitrates are linked by two oxygens that are both bridging and chelating, but differ (i) in the number of cerium ions to which they are linked and (ii) in their geometry.
The (100) facet exposed on the nanocubes was found to favor the formation of highly symmetric nitrates bonded to three oxygen atoms (E type). Compared to pure CeO_2, an overall decrease in nitrate concentration is observed on the mixed CeO_2-ZrO_2 oxides, and this is most pronounced for E type nitrates. In accordance with the theoretical studies, new nitrate structures with the participation of Zr are also observed.

Keywords: ceria, ceria-zirconia, catalysis, DeNOx, DFT, FTIR spectroscopy, nitrogen oxides, surface nitrates.

Acknowledgements: The authors gratefully acknowledge the financial support by the projects TwinTeam Д01-272 and Adonis КП-06-ДВ-16.

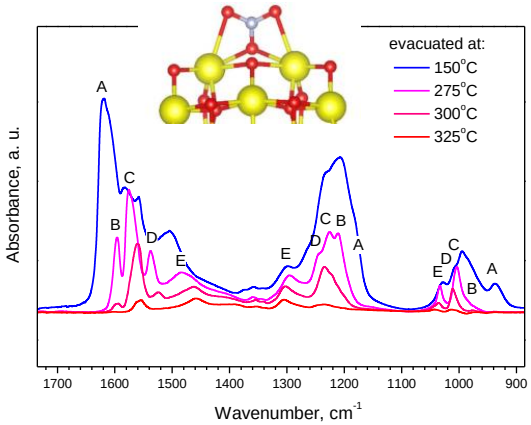

Figure 1: FTIR spectra of surface nitrates on CeO_2, formed after coadsorption of NO and O_2 and destruction upon treatment in vacuum and increasing temperature. Figure also shows the DFT-modelled structure of the E type nitartes.

References:

1. Mihaylov, M.Y., Zdravkova, V.R., Ivanova, E.Z., Aleksandrov, H.A., Petkov, P.St., Vayssilov, G.N., Hadjiivanov, K.I. (2021), Infrared spectra of surface nitrates: Revision of the current opinions based on the case study of ceria, *J. Catal.*, 394, 245-258.

CO Adsorption on Ni-MFI Zeolite

M. Mihaylov*, E. Ivanova, N. Drenchev, K. Hadjiivanov
Institute of General and Inorganic Chemistry, Bulgarian Academy of Sciences, Sofia, Bulgaria

Abstract:
Studies of CO adsorption are important for several reasons. One is related to the development of technologies for the separation of CO from other gases such as CO_2, CH_4, H_2 and N_2, which is important for both environmental protection and chemical synthesis. In particular, adsorption is a promising method that plays an essential role in CO removal for fuel cells and hydrogen storage. Another reason for conducting such studies is the use of CO as a probe molecule for characterizing the solid surfaces.
Ni-MFI was chosen as adsorbent because the MFI zeolte ensures atomic dispersion of nickel and stabilizes the nickel cations in a low coordination and valence state, which favors CO adsorption. Ni-MFI was obtained from the starting H-MFI zeolite by conventional ion exchange from aqueous Ni^{2+} solution.
CO adsorption on Ni-MFI was investigated by means of FTIR spectroscopy, TPD and breakthrough measurements. Prior to adsorption measurements, the sample was activated in O_2 at 400°C or reduced with CO at 300°C, then treated in vacuum or inert gas flow at 500°C.
FTIR spectroscopy gives unique molecular level insight into the adsorption process. In accordance with previous reports, it was found that on the O_2-activated sample, CO is adsorbed relatively firmly in the form of two types of Ni^{2+}-CO complexes. At low temperatures, $Ni^{2+}(CO)_2$ geminal species are formed, which proves the high coordination unsaturation of the cation sites. After reduction of the sample with CO, new Ni^+ sites are generated, which adsorb CO more strongly and can accommodate up to three CO molecules at low temperatures. This is explained by the existence of additional π-bonding to Ni^+ sites, their larger radius and lower coordination to the zeolite lattice compared to Ni^{2+} ions.
TPD gives information on chemisorption energetics. The TPD curve of O_2-activated Ni-MFI contains a complex feature with three components at 107, 160, and 185°C, which confirms heterogeneity of the Ni^{2+} centers. The TPD curve of the CO-reduced sample shows a new maximum at about 370°C, related to the desorption of CO from Ni^+ sites. Their amount was estimated to be about 20% of all active centers. An increase in the amount of desorbed CO is also observed, which can be associated with reduction of some ccordinatively saturated Ni^{3+} or Ni^{2+} species or increase in nickel dispersion.
Finally, CO breakthrough curves in the presence of hydrogen were measured, which gives an idea of the performance of the adsorbent in conditions close to the real ones. The full adsorption capacity of O_2-activated Ni-ZSM-5 was measured to be 3.8 $mL.g^{-1}$, which after CO reduction increased to 9.0 $mL.g^{-1}$. The breakthrough curves are steep, indicating fast kinetics leading to high bed utilization efficiency and high working capacity. Thus, Ni-ZSM-5 shows promising behavior as an adsorbent for removing CO impurities and producing pure hydrogen.

Keywords: adsorption, breakthrough curve, carbon monoxide, gas separation, hydrogen, FTIR spectroscopy, probe molecules, TPD, zeolites.

Acknowledgements: The authors gratefully acknowledge the financial support by the projects TwinTeam Д01-272 and КП-06-Н59/5.

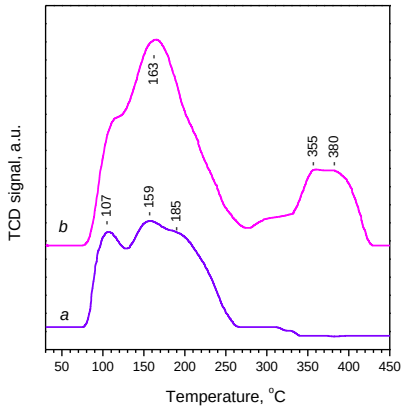

Figure 1: CO-TPD curves of O_2-activated (a) and CO-reduced Ni-MFI (b).

References:

1. Mihaylov, M., Ivanova, E., Zdravkova, V., Andonova S., Drenchev N., Chakarova K., Kefirov, R., Kukeva, R., Stoyanova, R., Hadjiivanov, K. (2022), Purification of Hydrogen from CO with Cu/ZSM-5 Adsorbents, *Molecules*, 27, 96.

Fabrication of highly permselective, mechanically robust block copolymer/ionic liquid membranes for CO_2 separation

Young Jun Kim [1], Jong Hak Kim [1,*]
[1] Department of Chemical and Biomolecular Engineering, Yonsei University, Seoul, South Korea

Abstract:
We fabricated crystalline elastomeric polymer/ionic liquid membranes by using an amphiphilic crystalline block copolymer, poly(ethylene glycol) monomethyl ether-*block*-poly(acrylonitrile) (mPEG-*b*-PAN). The copolymer was synthesized *via* one-pot free-radical polymerization under mild conditions (in water at 50 °C). The aggregation of block copolymer within the ionic liquid environment resulted in a microphase-separated, interconnected elastomeric structure where the PAN crystallites acted as crosslinking junctions. The distinctive crystalline network could retain high IL loading up to 300 wt% while maintaining outstanding mechanical strength. The mPEG-*b*-PAN/IL membrane with 250 % IL loading exhibited the highest CO_2 separation performance with a CO_2 permeability of 456.4 barrer, CO_2/N_2 selectivity of 61.4, CO_2/CH_4 selectivity of 18.1, CO_2/H_2 selectivity of 12.3. Esepecially, the CO_2/N_2 separation performance exceeds the Robeson upper bound (2008) and reached close to the upper bound (2019). Both the mechanical strength and gas separation performance of mPEG-*b*-PAN/IL membranes outperformed those of H-PAN and other membranes with ILs, indicating that a pivotal role of crystalline network formed by the strong interaction of mPEG-*b*-PAN block copolymer with IL.

Keywords: block copolymer, ionic liquid, CO_2 separation, crosslinking, crystalline network

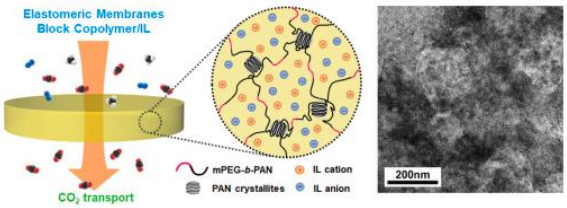

Figure 1: Schematic illustration of crystalline crosslinked network of mPEG-*b*-PAN/IL elastomeric membrane.

References:

1. H..J. Min, Y.J. Kim, M. Kang, C.H. Seo, J.H. Kim, J.H. Kim, Crystalline Elstomeric Block Copolymer/Ionic Liquid Membranes with Enhanced Mechanical Strength and Gas Sepation Properties, *J. Membr. Sci.*, 660 (2022), 120837.
2. T.P. Lodge, A unique platform for materials design, Science 321 (2008) 50-51.

Comparing submicron-thick mixed-matrix membranes with metal organic frameworks of MIL-140C and UiO-67 for CO_2 separation

Hyuk Jin Roh, Miso Kang, and Jong Hak Kim
Department of Chemical and Biomolecular Engineering, Yonsei University, Seoul, South Korea

Abstract:
Herein, we report a method of fabricating high-performance thin-film mixed-matrix membranes (MMMs) prepared from two types of zirconium-based metal-organic frameworks (MOFs), MIL-140C and UiO-67, dispersed in a polymer matrix for CO_2 separation. A poly(glycidyl methacrylate-co-poly(oxyethylene methacrylate) (PGO) copolymer, synthesized via one-pot free-radical polymerization, was used as a matrix to enhance interfacial contact with MOF fillers through its high adhesive property, successively producing a 600 nm-thick defect-free MMMs with uniform dispersion. The degree of polymer infiltration was more favorable for UiO-67 due to its large, 3D cage-like pores compared to MIL-140C containing small, 1D channel-like pores, presenting different CO_2 separation performances. All-embracing, the MMMs with MIL-140C exhibited better separation performance than those with UiO-67 owing to the less intensive polymer infiltration and structural advantages like high aspect ratio. The MMMs with 20% of MIL-140C loading showed the highest separation performance with CO_2 permeance of 1768 GPU and CO_2/N_2 selectivity of 38, exceeding the target area for practical application in the post-combustion CO_2 capture process.

Keywords: carbon dioxide, copolymer matrix, thin film, mixed-matrix membranes, metal-organic frameworks.

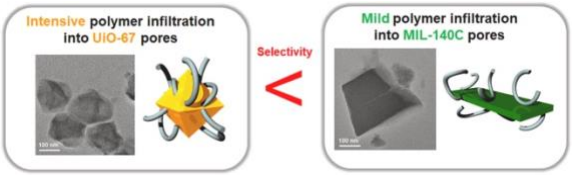

Figure 1: Figure comparing degree of polymer infiltration of UiO-67 and MIL-140C leading to different CO_2/N_2 selectivity performance.

References:

1. Kang, M., Kim, T. H., Han, H. H., Min, H. J., Bae, Y. S., & Kim, J. H. (2022). Submicron-thick, mixed-matrix membranes with metal-organic frameworks for CO2 separation: MIL-140C vs. UiO-67. *Journal of Membrane Science*, *659*.

Structure-Property Relationship of Aramid Nanofiber-Reinforced Thermotropic Liquid Crystalline Polyester Nanocomposites

Tae-Gyeong Eom, Young-Gi Song, Seok-Ju Kim, Minyoung Seo, Jin-Hyeok Park, and Young Gyu Jeong*
Department of Advanced Organic Materials Engineering, Chungnam National University, Daejeon, Republic of Korea, *ygjeong@cnu.ac.kr

Abstract:
We conducted a study to investigate the influence of aramid nanofibers (ANFs) on the melt-rheological behavior, thermal transition, thermal stability, and mechanical durability of thermotropic liquid crystal polyesters (TLCPs). For this purpose, ANFs were derived from short aramid microfiber using a deprotonation method. By using different ANF loading contents ranging from 3-15 wt%, we produced TLCP matrix nanocomposites through masterbatch-based melt-compounding and injection-molding. The SEM images and FT-IR spectra demonstrate that the ANFs are dispersed in the TLCP matrix with a microfibrillar structure through good interfacial adhesion caused by specific intermolecular interactions between the TLCP and ANFs. As a result, the complex viscosity, shear storage/loss moduli, and thermal transition (melt-crystallization, glass transition, and melting) temperatures of the nanocomposites increased with increasing ANF filler content. However, the melt-crystallization and melting enthalpies increased only at low ANF loading contents of 3-5 wt%. At high ANF contents of 7-15wt%, the enthalpies decreased owing to the partial aggregation of ANF fillers. The thermogravimetric analysis prove that the thermal stability of TLCP/ANF nanocomposites improves when the ANF filler is introduced. To examine the long-term durability of mechanical properties of ANF/TLCP nanocomposites, the elastic storage moduli were measured as functions of temperature and frequency by adopting the stepped isothermal method (SIM) with the assumption that the strain is a thermal activation process. The dynamic mechanical analysis based on the SIM shows that the addition of 5 wt% ANF to the TLCP leads to an approximately 142% improvement in elastic moduli and long-term mechanical durability at elevated temperatures.

Keywords: Aramid nanofiber, Thermotropic liquid crystalline polyester, Nanocomposites, Microstructure, Thermal property, Mechanical property, Stepped isothermal method, Structure-property relationship.

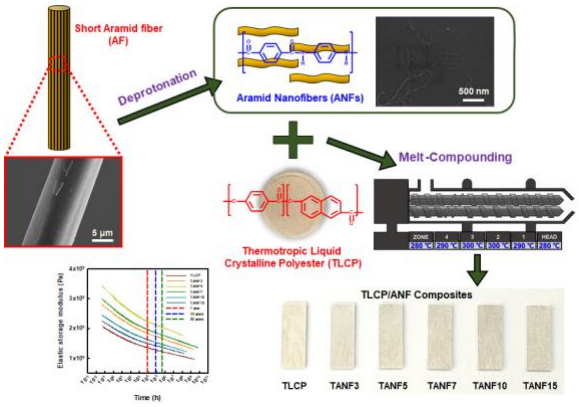

Figure 1. Scheme illustrating the fabrication and long-mechanical property analysis of aramid nanofiber-reinforced thermotropic liquid crystalline polyester nanocomposites via masterbatch melt-compounding and injection-molding.

References:

1. Eom, T.-G.; Song, Y.-G.; Seo, M.; Kim, S.-J.; Park, J.-H.; Jeon, G.-W.; Jeong, Y.-G. (2023) Short aramid fiber-reinforced thermotropic liquid crystalline polyester composites: fabrication, thermal and mechanical properties, *J. Reinf. Plast. Compos.*, In Press.
2. Jeon, H.-B.; Jeon, G.-W.; Kim, S.-Y.; Gang, H.-E.; Park, G.-T.; Jeong, Y.-G. (2022), Enhanced thermal stability and long-term mechanical durability at elevated temperatures of thermotropic liquid crystal polyester/glass fiber composites, *Mech. Adv. Mater. Struc.*, 29, 6060-6069.

Synthesis and characterization of silica/phytic acid binary nanofillers

M. Wysokowski*, J. Stachowiak, P. Bartczak
[1] Faculty of Chemical Technology, Poznan University of Technology, Poznan, Poland,
e-mail: marcin.wysokowski@put.poznan.pl

Abstract:
Phytic acid (PA) is a naturally derived material from legume seeds, cereal grains, and beans. Resulting from the unique properties, such as nontoxic, biocompatible, and green to the environment, PA has been attracted increasing interest forsustainable materials science and design[1,2]. In this study, we investigate the synthesis silica/phytic acid binary nanofillers. Sol-gel chemistry has emerged as a versatile method for synthesizing nanometric hybrid materials with controlled size, shape, and surface properties[3]. Therefore, the sol-gel process was used to synthesize silica nanoparticles with varying concentrations of phytic acid as a co-precursor. The influence of phytic acid on the structural and chemical properties of the resulting nanoparticles was investigated by means of ^{29}Si, and ^{31}P NMR spectroscopy, which are a powerful analytical tool for probing the atomic-scale structure of materials and to study the structural changes in the silica matrix and the coordination environment of phosphorus atoms in phytic acid, respectively.
The findings contribute to the understanding of the fundamental aspects of sol-gel chemistry that lies beyon silica-phytic acid materials formation. Moreover, this study provides important information for the design and development of sustainable functional fillers fo polymer materials.

Keywords: sol-gel silica, phytic acid, silica-phytic acid hybrids, nuclear magnetic resonance, binary nanofillers

References:

1. Gwóźdź, M., Brzęczek-Szafran, A. (2022) Carbon-Based Electrocatalyst Design with Phytic Acid—A Versatile Biomass-Derived Modifier of Functional Materials. *Int. J. Mol. Sci.*, 23, 11282
2. Wang, D., Wang, Y., Li, T., Zhang, S., Ma, P., Shi, D., Chen, M., Dong, W. (2020) A Bio-Based Flame-Retardant Starch Based on Phytic Acid. *ACS Sus. Chem. Eng.* 8 (27), 10265–10274.
3. Warren, S. C., Perkins, M. R., Adams, A. M., Kamperman, M., Burns, A. A., Arora, H., Herz, E., Suteewong, T., Sai, H., Li, Z., Werner, J., Song, J., Werner-Zwanziger, U., Zwanziger, J. W.; Grätzel, M., Disalvo, F. J., Wiesner, U. A (2012) Silica Sol-Gel Design Strategy for Nanostructured Metallic Materials. *Nat. Mat.* 11, 460–467
4. Feinle, A., Elsaesser, M.S., Hüsing, N. (2016) Sol–gel synthesis of monolithic materials withhierarchical porosity. *Chem. Soc. Rev.* 45, 3377-3399

Polymer Based Nanocomposites filled with Graphitic Materials and Metalic Oxides Applied to X-ray Shielding in Interventional Radiology Procedures

L. O. Faria [1,2,*], L. A. Silva [1]
[1] Centro de Desenvolvimento da Tecnologia Nuclear, Serviço de Nanotecnologia, Belo Horizonte, Brazil
[2] Depto. Engenharia Nuclear, State University of Minas Gerais, Belo Horizonte, Brazil

Abstract: Interventional radiology procedures involves long periods of direct X-rays beam pointing to the same skin region, increasing the probability of future skin cancer. Thus, the development of new polymer-based nanocomposites containing elements with good radiation attenuation properties, such as Bi and Zr and others, have been performed elsewhere. On the other hand, graphitic materials such carbon-nanotubes (CNTs) and graphene have been recently reported to enhance the X-ray attenuation efficiency of some nanocomposites. In this work, we investigate the X-ray attenuation properties of polymer-based nanocomposites filled with nanoparticles of metallic oxides (Bi_2O_3 and ZrO_2) and some Graphitic materials, i.e. Graphene Oxide (GO) or Carbon Nanotubes (CNT and MWCNT). For comparison purposes, all produced nanocomposites (Figure 1) were exposed to a monochromated photon beam (E = 6.9 keV), generated by a commercial-like X-ray Co-Tube. The low molecular weight poly(vinylidene fluoride) homopolymer [PVDF] was used as the polymeric matrix. The containing OG nanocomposite samples produced for our investigation were PVDF/OG,PVDF/GO/Bi_2O_3 and also PVDF/GO/ZrO_2. On the other hand, the samples containing CNT or MWCNT were PVDF/MWCNT/ZrO_2 and PVDF/CNT/ZrO_2 nanocomposites (100 µm thick).
The higher X-ray shielding was observed for the PVDF/MWCNT/ZrO_2 sample (31,3%). However, all nanocomposites filled with only 4.0% of GO showed similar shielding capacity, as can be seen in Figure 1(b). The results reveal that the polymer based nanocomposites filled with graphitic materials and metalic oxides are good candidates to be further investigated for application in X-ray shielding in interventional radiology.

a)

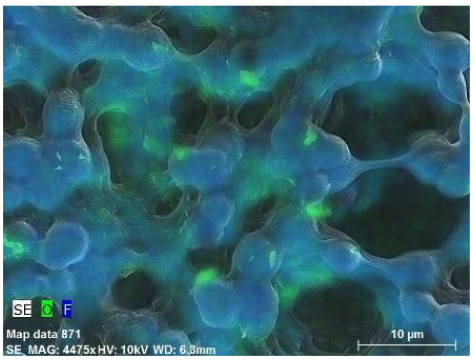

b)

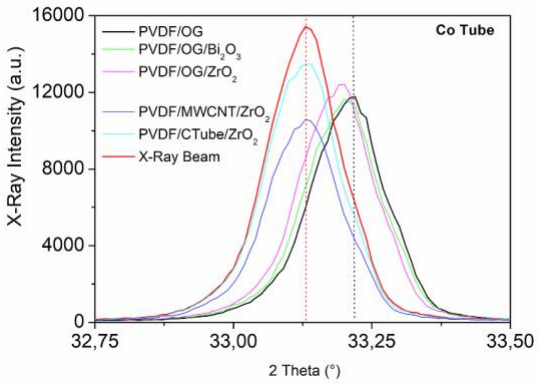

Figure 1: SEM-EDS Micrograph of PVDF/GO nanocomposite filled with 4.0% of GO. The Oxygen atoms are identified with green color (GO) while Fluorine atoms are in blue color (PVDF), showing graphene-containing structures bond to the surfaces of the PVDF crystalline spherulites (a) and the X-ray attenuation curves for all nanocomposite samples (b).

References:

1. Nambiar, S.; Yeon, J. Polymer-composite materials for radiation protection**.** ACS Appl. Mater. Interface**s,** v. 4**,** p. 5717-5726, 2012.

2. Viegas, J.; et. al. Increased X-rays attenuation efficiency of graphene-based nanocomposite. Ind. Eng. Chem. Res., 56(41)2017.

Vanadium aluminum carbide nanoparticles as a storable absorber to generate mode-locked pulses from Yb fiber laser

FAY F. RIDHA[1,2], AND ABDUL HADI AL-JANABI[1].

[1]Institute of Laser for Postgraduate Studies, University of Baghdad, Baghdad, Iraq
[2] College of Medical Techniques. Al-Farahidi University. Baghdad, Iraq

Abstract:
Nanomaterials found a potential applications in the field of photonics . Some nanomaterials which exhibit a unique nonlinear properties can be used a modulator in laser systems .On the other hand, ultra-short laser pulses generation with a switchable operation from a very small quantum defect Ytterbium-doped fiber (YDF) is of much interest. We demonstrated for the first time to the best of the authors' knowledge a stable mode-locked laser operation as well as a nanosecond dark mode-locked laser pulses by inserting a novel vanadium aluminum carbide nanomaterial (V2AlC) saturable absorber inside a Yb-doped fiber ring cavity. A 4.9 ps mode-locked pulses have been achieved at a pump power of about 84 mW at central wavelength 1065.2 nm with a 3 dB bandwidth of 0.87 nm and signal-to-noise ratio (SNR) of about 60.3 dB. The characterization of the V2AlC nanomaterial was also investigated that including scanning electron microscopy (SEM), energy-dispersive x-ray (EDX), atomic force microscopy (AFM) , x-ray diffraction (XRD) and Raman spectroscopy. The morphology and crystalline structure of MAX phase (V2ALC) nanoparticles were characterized by SEM as shown in Fig. (1a). The image obviously shows particles with a nearly tubular shape. As well from the Raman spectroscopy at 3765 cm^{-1} and 4260 $cm^{-1}$the intense phonons were realized and wich are related to the vibration of –OH and/or $–H_2$. V_2AlC have eleven active modes peaks as shown in Fig (1b). Also the nonlinear parameter which is the modulation depth was also measured using twin detector technique which was about 19.7% as shown in Fig (2 a,b).

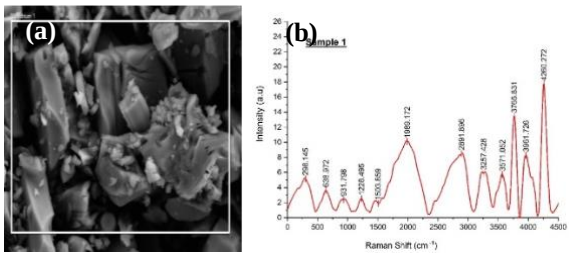

Fig. (1). Characterization of MAX phase(V2AlC). (a) SEM capture. (b) Raman Shift of MAX phase.

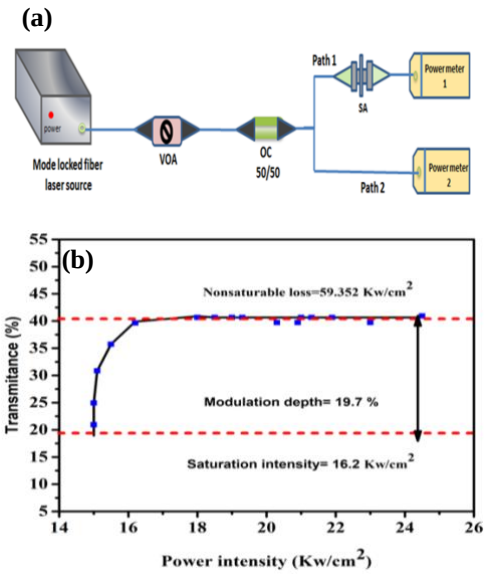

Fig .(2). (a) The experimental set up of twin detectors. **(b)** Nonlinear optical transmission of V2AlC-NF.

Keywords: Nanomaterial,Fiber laser, Raman spectroscopy, Max phase, modulation depth

References:

1. T. Wang, W. Zhang, J. Wang, J. Wu, T. Hou, P. Ma, R. Su, Y. Ma, J. Peng, L. Zhan, Bright/dark switchable mode-locked fiber laser based on black phosphorus, Opt. Laser Technol. 123 (2020) 105948.
2. H. Ahmad, N.F. Azmy, N. Yusoff, S.A. Reduan, S.N. Aidit, L. Bayang, M.Z. Samion, MoTe2-PVA as saturable absorber for passively Q-switched thulium-doped fluoride and erbium-doped fiber laser, Optik (Stuttg). 243 (2021) 167157.

Iron(III)-Polyphenol Nanocoating for Black Hair-Dyeing

Eunhye K. Kang and Insung S. Choi*
Center for Cell-Encapsulation Research, KAIST, Daejeon, Korea

Abstract:
The nanocomplex of iron(III) and polyphenols has been widely used throughout human history. For example, the use of iron gall ink dates back to the Middle Ages in Europe, where oak galls were the source of polyphenols (i.e., gallic acid and tannic acid), and green vitriol (iron(II) sulfate, $FeSO_4$) was a source of iron(III). A similar, if not the same, formulation was used in Japan and some Southeast Asian countries, such as the Philippines and Vietnam, for teeth black-dyeing. This tradition is called "ohaguro" in Japan. The blackening in the iron gall ink is made by the air oxidation of iron(II) to iron(III) ions and subsequent nanoassembly of the iron(III)-polyphenol complex. We recently reported that the iron(II)-polyphenol complex could be used as a reaction precursor for fluidic-interface engineering, inspired by the iron gall ink.[1] The iron(II)-polyphenol complex is soluble in water, and its oxidation rate can be controlled chemically during the formation of the iron(III)-polyphenol nanonanostructure. Our work has extended the study of iron-gall-ink-inspired iron(II)-poly-phenol species to the cosmetic field, with a focus on hair black-dyeing (Figure 1).[2,3] Our formulation uses only approved cosmetic ingredients and does not require any harmful oxidizing agents, such as hydrogen peroxide, making it highly impactful in the hair cosmetic industry.

Keywords: iron, polyphenols, gallic acid, iron gall ink, hair dyeing, cosmetics, nanocoating.

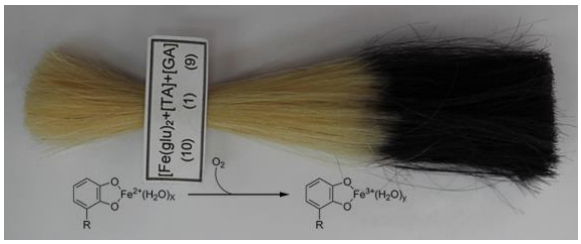

Figure 1: Optical image of a blond-hair sample that has been dyed with iron(II)-polyphenol complex. The iron(II)-polyphenol complex is air-oxidized to a blackish iron(III)-polyphenol nanostructure.

References:

1. Lee, H., Kim, W. I., Youn, W., Park, T., Lee, S., Kim, T.-S., Mano, J. F., Choi, I. S. (2018) Iron gall ink revisited: in situ oxidation of Fe(II)-tannin complex for fluidic-interface engineering, *Adv. Mater.*, 30, 1805091.
2. Han, S. Y., Hong, S.-P., Kang, E. K., Kim, B. J., Lee, H., Kim, W. I., Choi, I. S. (2019) Iron gall ink revisited: natural formation for black hair-dyeing, *Cosmetics*, 6, 23.
3. Han, S. Y., Kang, E. K., Choi, I. S. (2021) Iron Gall Ink Revisited: A Surfactant-Free Emulsion Technology for Black Hair-Dyeing Formulation, *Cosmetics*, *8*, 9.

A study of cardanol-based phosphoric flame retardant to improve the flame retardancy of epoxy material

Do-Hyun Kim
Department of fire Safety Research, Korea Institute of Civil Engineering and Building Technology, Hwaesong-si, Gyeonggi-do 18544, South Korea

Abstract:
Epoxy resin, a significant thermosetting polymer possessing outstanding chemical resistance, electrical insulation properties, and mechanical properties has versatile applications, including coating, insulation material, construction material, and paint. The epoxy adhesive has been widely applied in various applications, from automobile to building materials, owing to its excellent adhesion properties. However, epoxy adhesives are vulnerable to flame, thereby restricting their application in the industrial sector. To improve epoxy adhesive's capability to resist flame, phosphorus-containing flame retardants have been used. This study, Improves epoxy adhesive properties of flame retardancy and enhances eco-friendly using renewable resources that cardanol. As a result, this study figure out improved flame retardancy and adhesive properties of the epoxy adhesive composites.

Keywords: Cardanol; Flame retardant; Epoxy; Adhesive

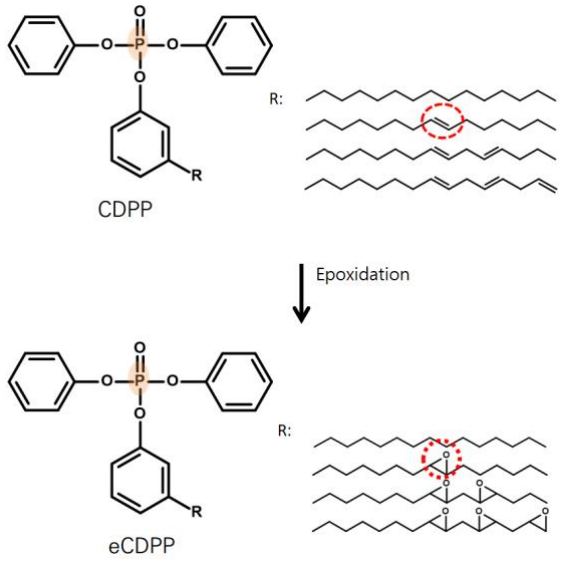

Figure 1: Synthesis of eCDPP

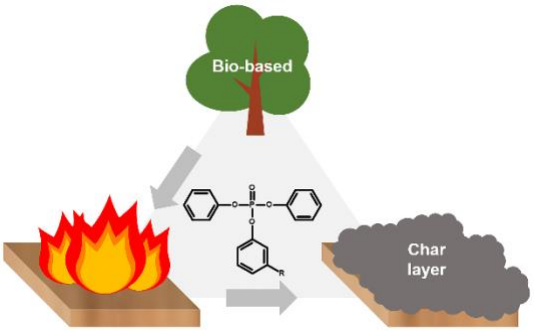

Figure 2: Machanism of eCDPP

References:

1. Do-Hyun Kim, etc, (2022), Phosphorus flame retartdant and epoxy adhesive cposotion comprising the same, *South Korea patent, No. 10-2022-0169154.*

Optimizing Ge film adhesion on polycarbonate: unraveling the impact of O_2/Ar plasma exposure

J. Peralta, J. Esteve*, A.Lousa
Department of Applied Physics, University of Barcelona, E08023 Barcelona, Spain

Abstract:
The importance of adhesion between metallic coatings and polymers cannot be overstated. It plays a crucial role in minimizing the risk of delamination, resulting in long-lasting integrity and reliable performance across a wide range of applications. In this study, polycarbonate was subjected to plasma exposure in 50:50 O_2/Ar atmospheres to modify its surface chemistry, aiming to enhance the adhesion of subsequent Ge sputtered films. The influence of the energy of the ions on wettability, chemical activation, and coating adhesion was investigated. Through a combination of XPS and FTIR analysis, it was determined that ion bombardment and UV radiation played distinct roles. Ion bombardment introduces polar functional groups on the surface of the polymer, while UV radiation breaks down these same groups within the polymer's volume, leading to degradation and delamination of the films. Although the underlying surface and volume transformations are complex, identifying the balance between these phenomena is crucial to optimize the adhesion of Ge films onto polycarbonate.

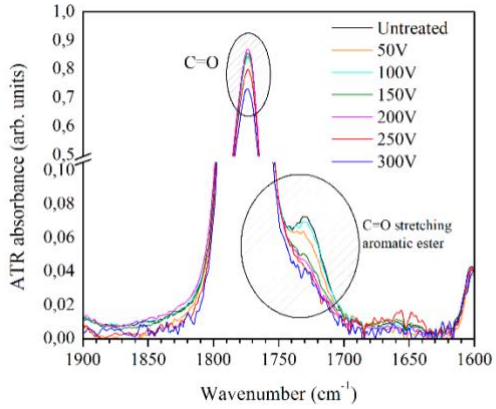

Figure 1: FTIR-ATR spectra of the carbonyl group for the different plasma conditions, showing the evolution of the $C = O$ related vibrational modes.

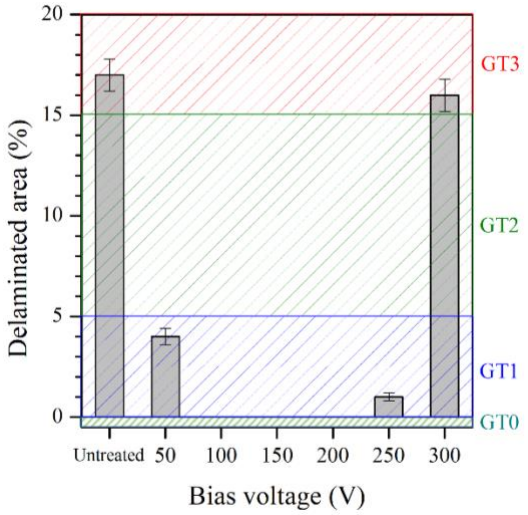

Figure 2: Delamination area of the Ge films from the PC substrate versus negative bias voltage showing an optimal range between 100 and 200 V.

Keywords: Plasma modified PC, Superhydrophilicity, Germanium films, adhesion, XPS, FTIR-ATR

References:

1. Kim, N. (2017) Recent progress of functional coating material and technologies for polycarbonate, *J. Coatings Technol. Res*, 14, 21-34.
2. Hora, J., Hall, C., Evans, D., Charrault, E. (2018) Inorganic thin film deposition and application on organic polymer substrates, *Adv. Eng. Mater.*, 20, 1-18.

Synthesis of Ag/Fe2O3 nanocomposite from essential oil of ginger via green method and its bactericidal activity

Fatimah A. M. Al-Zahrani [1], Nourah A. AL Zahrani [2], Sameera N. Al Ghamdi [3],· Long Lin [4], Salem S. Salem [5], Reda M. El Shishtawy[6,7]

[1]Chemistry Department, Faculty of Science, King Khalid University, Abha 61413, Saudi Arabia

[2] Chemistry Department, Faculty of Science, University of Jeddah, Jeddah, Saudi Arabia

[3] Chemistry Department, Faculty of Science, Al-Baha University, Al-Baha 1988, Saudi Arabia

[4] Colour Science, School of Chemistry, University of Leeds, Woodhouse Lane, Leeds LS2 9JT, UK

[5] Botany and Microbiology Department, Faculty of Science, Al-Azhar University, Cairo 11884, Egypt

[6] Chemistry Department, Faculty of Science, King Abdulaziz University, Jeddah 21589, Saudi Arabia

7 Dyeing, Printing and Textile Auxiliaries Department, Textile Research Division, National Research Centre, Dokki, Cairo, Egypt

Abstract:

Abstract Bio-synthesized nanoparticles (NPs) having reduced chemical toxicity have been focused globally and become essential component of nanotechnology recently. In the study reported here, silver/iron oxide nanocomposite (Ag/Fe2O3) was bio synthesized from ginger oil via a green, economic, and eco-friendly strategy. The biosynthesized Ag/Fe2O3 were character ized using ultraviolet visible (UV– Vis), Fourier transform infrared (FTIR), X-ray difraction (XRD), transmission electron microscope (TEM), dynamic light scattering (DLS), and scanning electron microscope/energy-dispersive X-ray (SEM–EDX) analysis. The particulates showed a spherical-morphology and had sizes between 44 and 200 nm. Ag/Fe2O3 FTIR analysis revealed functional groups that were analogous to organic metabolites, which reduced and stabilized the nanocomposite. Antimicrobial efcacy of the biosynthesized Ag/Fe2O3 against bacterial pathogens was assessed. In addition, Ag/Fe2O3 exhibited broad spectrum activities against Staphylococcus aureus, Bacillus subtilis, Escherichia coli, and Pseudomonas aeruginosa with inhibition zones 22.6±1.15, 21.1±1.44, 18±1 and 17.4±2.67 mm, respectively. The Ag/Fe2O3 showed promising antibacterial action against human bacterial pathogens, making them useful in the medical feld

Keywords: Ginger oil · Nanoparticles · Green synthesis · Antimicrobial activity · Human bacterial pathogens

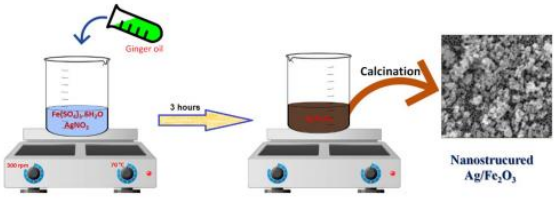

Figure 1: Schematic illustration of the Ag/Fe2O3 biosynthesized using ginger oil.

References:

1. 1. Hamad A, Khashan KS, Hadi A (2020) Silver nanoparticles and silver ions as potential antibacterial agents. J Inorg Organomet Polym Mater 30(12):4811–4828. https://doi.org/10.1007/ s10904-020-01744-x
2. 2. Salem SS, EL-Belely EF, Niedbała G, Alnoman MM, Hassan SE-D, Eid AM, Shaheen TI, Elkelish A, Fouda A (2020) Bactericidal and in-vitro cytotoxic efcacy of silver nanoparticles (Ag-NPs) fabricated by endophytic actinomycetes and their use as coating for the textile fabrics. Nanomaterials 10(10):2082. https://doi.org/10.3390/nano10102082
3. Alsharif SM, Salem SS, Abdel-Rahman MA, Fouda A, Eid AM, El-Din Hassan S, Awad MA, Mohamed AA (2020) Multifunctional properties of spherical silver nanoparticles fabricated by diferent microbial taxa. Heliyon 6(5):e03943. https://doi.org/10.1016/j.heliyon.2020.e03943

Organic-Inorganic Hybridgel: new food packaging material

Franziska Trodtfeld[1,2,*], Dr. Tina Tölke[1], PD Dr. Cornelia Wiegand[2]
[1] INNOVENT e.V., Jena ,Germany
[2] University Hospital Jena, Department of Dermatology, Friedrich-Schiller-University Jena, Germany

Abstract:
The food packaging industry strives to improve its packaging to achieve the highest durability and strength for the shelf life of the product. In view of environmental concerns, efforts are being made to reduce packaging waste, with increased use of biodegradable polymers and networks. These organic packaging materials must maintain their mechanical and barrier properties during storage and function properly before disposal. The barrier properties of organic packaging materials are not yet as effective as those of existing packaging materials. The addition of silica to biodegradable polymers makes the packaging materials more water resistant, improves their mechanical and thermal properties, and also increases their shelf life[1]. Silica-based materials are highly versatile and flexible and can be designed to meet specific applications. An organic-inorganic hybrid gel was developed as a packaging material using natural polymers such as amino acids proline, glutamic acid and monosaccharides. The organic compounds were crosslinked with nanometer aggregates of tetraorthosilicate, which was hydrolyzed and condensed in the organic compound solution. Polymeric nanocomposites on a polymerized matrix were prepared by this in situ synthesis of inorganic particles[2]. The silica particle form aggregates which act as network crosslinkers and improve the strength and stability of this polymer nanocomposite hydrogel. Rheological analysis of the material showed that the gel point of the material depends on the amount of silica in the organic matter, which makes the material highly adaptable for specific packaging purposes. The material was characterized and the barrier functions were investigated with regard to food requirements. Since the intended application is food packaging, biocompatibility was evaluated using selected biotests for cytotoxicity and allergenic potential to ensure consumer safety in case of skin contact. This material is an approach how packaging materials based on natural polymers could be developed and demonstrates their difficulties and research challenges.

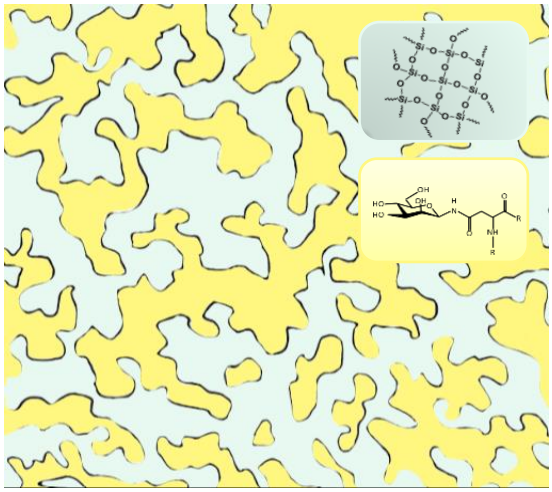

Keywords: food safety, food packaging, polymer nanocomposites , sol-gel technique, biodegradable, biocompatibility

Figure 1: Figure illustrating the proposed network of the material formation. The silica particle forming aggregates that crosslink the accumulates of organic material.

References:

1. Chadha, U., Bhardwaj, P., Selvaraj, S. K., Arasu, K., Praveena, S., Pavan, A., ... & Paramasivam, V. (2022). Current trends and future perspectives of nanomaterials in food packaging application. *Journal of Nanomaterials*, *2022*, 1-32.
2. Rane, A. V., Kanny, K., Abitha, V. K., & Thomas, S. (2018). Methods for synthesis of nanoparticles and fabrication of nanocomposites. In *Synthesis of inorganic nanomaterials* (pp. 121-139). Woodhead publishing.

Molecular dynamics study of self-diffusion pathways in alkali metals

Yevgeniya Kondratyeva[1], Artem V. Sergeev [1]
[1] N.N. Semenov Federal Research Center for Chemical Physics, Lab of Electrochemical Energy Conversion, 119991 Moscow, Russia

Abstract:
Alkali metals are promising anode materials in rechargeable batteries due to their high theoretical specific capacity (1165mAh/g for Na and 3860mAh/g for Li). However, there are some problems with simply using alkali metals as anodes. The main obstruction is formation and growth of metal deposits (dendrites, whiskers) on the electrode surface during charge stage. A lot of the growth mechanisms were proposed by now. And the latest researches pay attention to mechanical stress relaxation and masstrasfer feeding the root of the whisker. Experimental research of these processes at microscopic scale in alkali metals is especially difficult due to their chemical activity. There are some computational methods for modelling such systems. In our research we have used Molecular Dynamics (LAMMPS package) as main modeling tool. Also, the modified embedded atom method potentials (2NN-MEAM) [1] were chosen for primary simulations, later we trained Machine Learning Interatomic Potentials (MLIP) [2]. We have compared results obtained by using different potentials. Using these tools, various diffusion ways in lithium and sodium solid phases were simulated: movement of point defects in metal bulks and grain boundary diffusion. The most interesting result was received for temperature dependence of interstitial atom diffusion (Figure 1). During heating the rotation frequency increases and affects the self-interstitial atom diffusion.
This study shows the possibilities of studying reactive metals through MD-simulation and provide quantitative estimation of solid-state self-diffusion rate and its temperature dependance. The work was supported by the Russian Science Foundation grant №22–13–00427.

Keywords: lithium anode, sodium anode, diffusion coefficient, Molecular Dynamics, Machine Learning Interatomic Potentials.

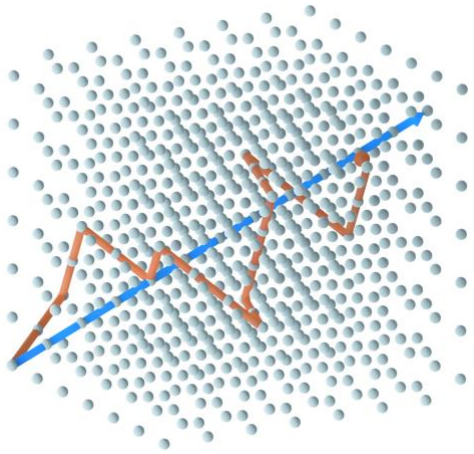

Figure 1: Figure illustrating the difference of self-interstitial atom diffusion ways at low (the blue pointer) and high (the red pointer) temperature.

References:

1. W.S. Ko, J.B. Jeon, Interatomic potential that describes martensitic phase transformations in pure lithium, Comput. Mater. Sci. 129 (2017) 202–210.
2. E. V Podryabinkin, A. V Shapeev, Active learning of linearly parametrized interatomic potentials, Comput. Mater. Sci. 140 (2017) 171–180.

Autophagy enhancer–Trehalose coated implant is available for the inflammed and infected bone

Song-Yeon Park[1], Kyung-Joo Seong[1], Shintae Kim[1], Min-Suk Kook[2], Min-Young Park[1], Ho-Jun Song[3], Suk-Gyun Park[4], Ji-Yeon Jung[1] and Won-Jae Kim[1]
[1] Dental Science Research Institute, [2] Stem cell Secretome Research Center, [3] Hard-tissue Biointerface Research Center, [4] Department of Oral Physiology, School of Dentistry, Chonnam National University, Gwangju 61186, Republic of Korea,
e-mail : wjkim@jnu.ac.kr

Abstract
Bone inflammation and infection are major causes in dental implant failure. However, strategies reducing bone inflammation and infection have been not established yet. Autophagy is known to regulate inflammation and infection. This study is aimed to investigate that Autophagy enhancer trehalose-coated implant has benefit for inflamed and bacterial infected bone and its underlying mechanism. LPS or P. gingivalis did not affect osteogenic differentiation from MC3T3-E1 but inhibited osteogenic differentiation of MC3T3-E1 by up-regulating expression and release of inflammatory cytokines from macrophage under MC3T3-E1 and Raw264.7 co-culture. Trehalose rescued LPS or P. gingivalis-reduced osteogenic differentiation of MC3T3-E1 through reducing expression and release of inflammatory cytokine production such as IL-1β and IL-6 from macrophage. Trehalose up-regulated LC3-II via AMPK pathway but not TFEB pathway in Raw264.7 cell. Trehalose also increased bacterial internalization into macrophage. Trehalose-coated titanium (Ti) surface had more hydroxyapatitie structure and MC3T3-E1 osteogenic differentiation and growth are enhanced on trehalose-coated titanium surface. Besides, trehalose-coated titanium (Ti) implants in the rabbit calvarium showed an increment of new bone formation and a decrement of inflammatory responses under LPS or Porphyromonas gingivalis treatment. Herein, we demonstrate that trehalose-coated implant might be a useful for inflamed and infected bone.

Carbon composites for biomedical application

P. Tzvetkov [1*], B. Tsyntsarski [2], I Stoycheva[2], G. Georgiev [2], B. Petrova [2], E. Grigorova [1], P. Markov [1]
[1] Institute of General and Inorganic Chemistry, Bulgarian Academy of Sciences, Sofia, Bulgaria
[2] Institute of Organic Chemistry with Centre of Phytochemistry, Bulgarian Academy of Sciences, Sofia, Bulgaria

Abstract:
Nowadays there is an increase of agents harmful for human health, i.e. air and water pollution with various chemical and biological agents. There is a need to develop such facilities and materials to cope with this wide range of hazards in the air of public buildings, hospitals and even our homes. Carbon composites, containing metal nanoparticles are promising materilas in the field of water and air purification from molecules, ions, bacteria and viruses. Coal had been used in medicine and water purification in ancient India more than 2000 years ago.
Copper and silver pots, as well as metal medical instruments, were used in Persia, India, Rome and Egypt around 2500-2000 BC. The antibacterial oligodynamic effect of metals, like copper, iron, lead, mercury, zinc, aluminum, gold and silver, is well known from ancient times in surgery and water purification. This leads to release of positively charged metal cations that interact with bacteria. The antimicrobial and cytotoxic activity of metals is most probably due to their ability to inhibit enzymes and to damage cell membranes.
Nanoporous carbon materials are synthesized by hydro-pyrolysis of peach stones at 800^0C. The product was introduced to alcoholic solutions of the metal salts (nitrates of zinc and iron). 2.4 g $Zn(NO)_3.6H_2O$ were dissolved in solution containing 80 mL water and 20 ml ethanol. In other beaker 3.3 g $Fe(NO_3)_3.6H_2O$ were dissolved in the same type of solution mixture. Two portions of 10 g of nanoporous carbon were added to both solutions. The suspensions were stirred for 2 h, dried at 150ºC, and then heated up to 600ºC for 1 h in nitrogen atmosphere. The resulting materials represents carbon matrix containing metal nanoparticles (~5 wt. % metal content).
Elemental analysis was performed using a Vario Macro Cube (Elementar Analyzensysteme GmbH) analyzer to determine the content of C, H, N, S. The oxygen content was determined by the difference. The morphology study was performed using a FEI Quanta 250 FEG scanning electron microscope, in vacuum, at 10.0-15.0 kV.
X-ray diffraction analysis was performed using a Bruker D8 Advance diffractometer with CuKα radiation. The average crystallite size was calculated by Scherrer equation. XRD data (Fig. 1) imply high degree of graphitization and presence of metal and metal oxide nanoparticles. The carbon composites are characterized by moderate surface area of 600-700 m²/g and micropores and macropores prevail. After metal deposition the surface area decrease, due to incorporation of metal nanoparticles in the pores.
The obtained carbon composites are distinguished by moderate surface area and presence of metal nanoparticles included in the carbon matrix. The properties of these carbon materials imply their use as adsorbents of molecules, atoms, ions, as well as microorganisms in water and air.

Keywords: carbon materials, carbon composites, pyrolysis, nanocarbon, soprtion.

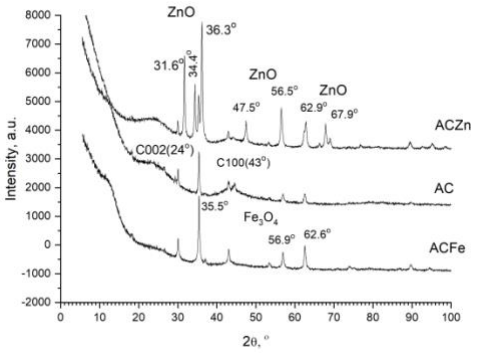

Figure 1: XRD spectra of nanoporous carbon doped with metal additives.

Acknowledgements: The authors thank to Bulgarian Ministry of Education and Science-National science fund (Project DFNI-КП-06-H27/9,08/12/2018) and part of experiments were performed with equipment included in the National Infrastructure NSI ESHER (NI SEVE) under grant agreement № DO1-161/28.07.22.

Bio-inspired formation of protein-nanoparticle complexes mimicking ocular environment

Jeong Hun Kim[1,2*], Tae Geol Lee[3]
1Fight against Angiogenesis-Related Blindness (FARB) Laboratory, Clinical Research Institute, Seoul National University Hospital, Seoul, Republic of Korea
2Department of Biomedical Sciences & Ophthalmology, Seoul National University College of Medicine, Seoul, Republic of Korea
3 Center for Nano-Bio Measurement, Korea Research Institute of Standards and Science, Daejeon, 34113, Republic of Korea

Abstract:
Nanoparticles adsorb biomolecules to form corona upon entering the biological environment. In this study, tissue-specific corona formation is provided as a way of controlling protein interaction with nanoparticles in vivo. In the vitreous, the composition of the corona was determined by the electrostatic and hydrophobic properties of the associated proteins, regardless of the material (gold and silica) or size (20- and 100-nm diameter) of the nanoparticles. To control protein adsorption, we pre-incubate 20-nm gold nanoparticles with 5 selectively enriched proteins from the corona, formed in the vitreous, to produce nanoparticle-protein complexes. Compared to bare nanoparticles, nanoparticle-protein complexes demonstrate improved binding to vascular endothelial growth factor (VEGF) in the vitreous. Furthermore, nanoparticle-protein complexes retain in vitro anti-angiogenic properties of bare nanoparticles. In particular, priming the nanoparticles (gold and silica) with tissue-specific corona proteins allows nanoparticle-protein complexes to exert better in vivo therapeutic effects by higher binding to VEGF than bare nanoparticles. These results suggest that controlled corona formation that mimics in vivo processes may be useful in the therapeutic use of nanomaterials in local environment.

Keywords: Corona; Nanomedicine; Nanoparticle; Nanoparticle-protein interaction

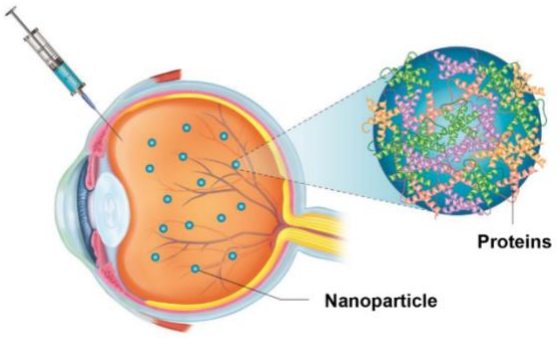

Figure 1: Figure illustrating bio-inspired formation of corona (protein-nanoparticle complexes) in vitreous cavity, where is the major place of intraocular injection of VEGF inhibitors targeting vision-threatening retinopathy including diabetic retinopathy, wet-type age-related macular degeneration and uveitis.

References:

Jo DH, Kim JH, Son JG, Dan KS, Song SH, Lee TG, Kim JH (2016) Nanoparticle-protein complexes mimicking corona formation in ocular environment, *Biomaterials*, 109, 23-31

Efficient *in vitro* and *in vivo* DNA Delivery by Multicomponent Lipid Nanoparticles

S. Renzi[1,2],E. Quagliarini[2], L. Digiacomo[2], J. Wang[3], L. Cui[3], G. Ferri[4], L. Pesce[4], V. De Lorenzi[4], G. Matteoli[4], H. Amenitsch[5], L. Masuelli[6], R. Bei[7], F. Cardarelli[4], A. Amici[3], C. Marchini[3], D. Pozzi[2], G. Caracciolo[2].

[1] Department of Anatomy, Histology, Forensic Medicine and Orthopedics, "Sapienza" University of Rome, Rome, Italy

[2] Department of Molecular Medicine, "Sapienza" University of Rome, Rome, Italy

[3]School of Biosciences and Veterinary Medicine, University of Camerino, Camerino, Italy

[4]Laboratorio NEST, Scuola Normale Superiore, Pisa, Italy

[5]Institute of Inorganic Chemistry, Graz University of Technology, Graz, Austria

[6]Department of Experimental Medicine, University of Rome "Sapienza", Rome, Italy

[7]Department of Clinical Sciences and Translational Medicine, University of Rome "Tor Vergata", Rome, Italy

Abstract:

Lipid nanoparticles (LNPs) are currently having an increasing impact in nanomedicine, as they have been designed and employed for the delivery of therapeutic agents (e.g., anticancer drugs, siRNA) and mRNA vaccines (e.g., for anti-COVID-19 vaccines). Despite these concrete advances, the encapsulation of plasmid DNA (pDNA) within LNPs and its delivery is still challenging and limited by both technological aspects and poor knowledge about the nanostructure-activity relationship. To tackle these issues, we aimed at developing innovative LNPs encapsulating DNA vaccines. First, we used a microfluidic platform to generate a library of 16 LNPs. Then, we thoroughly characterized LNPs by dynamic light scattering (DLS), microelectrophoresis, small angle X-ray scattering (SAXS), and transmission electron microscopy (TEM). 8 out of 16 LNPs exhibited suitable physical-chemical properties for gene delivery purposes and were screened for their transfection efficiency (TE) and cytotoxicity in human embryonic kidney cells (HEK-293). After the multistep screening procedure (Fig.1), the most efficient formulation (LNP15) was then successfully validated both *in vitro*, in an immortalized adult keratinocyte cell line (HaCaT) and in an epidermoid cervical cancer cell line (CaSki), and *in vivo* as a nanocarrier to deliver a cancer vaccine against the benchmark target tyrosine-kinase receptor HER2 in C57BL/6 mice. Finally, by a combination of confocal microscopy, TEM and SAXS, we were able to link the superior efficiency of LNP15 to its disordered nanostructure consisting of small-size unoriented layers of pDNA sandwiched between closely apposed lipid membranes. This feature indeed lead the massive destabilization of the LNP upon interaction with cellular lipids. Our results provide new insights into the structure−activity relationship of pDNA-loaded LNPs paving the way to the clinical translation of this gene delivery technology.

Keywords: Lipid nanoparticles, microfluidics, gene delivery, transfection efficiency, DNA vaccine.

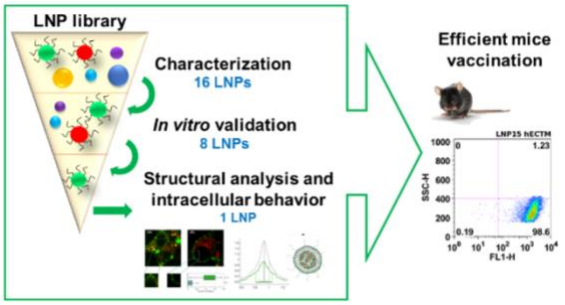

Figure 1: Cartoon of the production process of LNP library (16 LNPs) andscreening procedure for the selction of the best formulation then studied in dept (i.e. for nanostructure and biointeractions) and tested *in vivo*.

References:

1. Quagliarini E, Wang J, Renzi S, Cui L, Digiacomo L, Ferri G, Pesce L, Lorenzi V De, Matteoli G, Amenitsch H, et al. Mechanistic Insights into the Superior DNA Delivery Efficiency of Multicomponent Lipid Nanoparticles: An In Vitro and In Vivo Study. Appl Mater interfaces (2022) doi:10.1021/acsami.2c20019
2. Cui L, Renzi S, Quagliarini E, Digiacomo L, Amenitsch H, Masuelli L, Bei R, Ferri G, Cardarelli F, Wang J, et al. Efficient Delivery of DNA Using Lipid Nanoparticles. Pharmaceutics (2022) 14: doi:10.3390/pharmaceutics14081698

Magnetic levitation of nanoparticle-protein corona as an effective tool for cancer diagnosis

Erica Quagliarini[1], Luca Digiacomo[1], Damiano Caputo[2,3], Alessandro Coppola[3], Heinz Amenitsch[4], Giulio Caracciolo[1] and Daniela Pozzi[1]
[1]Department of Molecular Medicine, Sapienza University of Rome, 00161 Rome, Italy;
[2]University Campus Bio-Medico di Roma, 00128 Rome, Italy;
[3]General Surgery, Fondazione Policlinico Universitario Campus Bio-Medico, 00128 Rome, Italy;
[4]Institute of Inorganic Chemistry, Graz University of Technology, 8010 Graz, Austria;

Abstract:
Characterization of the personalized protein corona (PPC), i.e., the protein shell that coats nanoparticles once in contact with clinically relevant body fluids, has recently emerged as a detection tool for tumor onset [1]. However, the huge number of experimental steps typically required for the characterization of nanoparticles' PPC can affect the reproducibility and inter-laboratories consistency of the experimental data [2]. In fact, according to the World Health Organization (WHO), the experimental procedures for cancer screening and detection must satisfy the REASSURED (Affordable, Sensitive, Specific, User-friendly, Rapid and robust, Equipment-free and Deliverable to end-users) criteria. To comply with these requirements, herein we used an indirect PC characterization, i.e., by avoiding its isolation from NP surface, that exploits the magnetic levitation (MagLev) of PPCs derived from 15 healthy individuals and 30 oncological patients affected by four cancer types , i.e., breast cancer, prostate cancer, colorectal cancer and pancreatic ductal adenocarcinoma (PDAC). Briefly, by the use of MagLev device we analyzed levitation profiles of PPC-coated graphene oxide (GO) NPs that migrate along a magnetic field gradient in a paramagnetic medium (Figure 1). Our investigation demonstrates that sensitivity and specificity of the PPC-based MagLev tool depend on the cancer type with a global classification accuracy ranging from 70% for prostate cancer to a notable 93,3% for PDAC.

Keywords: Diagnostics, protein corona, graphene oxide, magnetic levitation

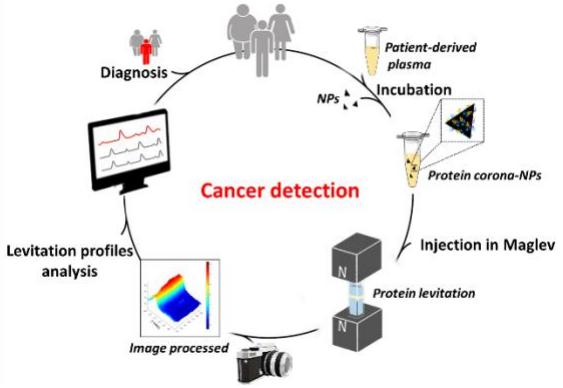

Figure 1: Experimental workflow includes (i) blood collection from healthy and oncological donors (ii) plasma isolation and incubation with graphene oxide (GO) (iii) injection of GO-protein complexes in paramagnetic solution (iv) sample inserting in Maglev device for proteins magnetic levitation (v) image acquisition and processing (vi) detection of cancer fingerprints.

References:

1. Di Santo, R., Digiacomo, L., Quagliarini, E., Capriotti, A. L., Laganà, A., Zenezini Chiozzi, R., ... & Caracciolo, G. (2020). Personalized graphene oxide-protein corona in the human plasma of pancreatic cancer patients. *Frontiers in bioengineering and biotechnology*, *8*, 491.
2. Digiacomo, L., Quagliarini, E., La Vaccara, V., Coppola, A., Coppola, R., Caputo, D., ... & Pozzi, D. (2021). Detection of Pancreatic Ductal Adenocarcinoma by Ex Vivo Magnetic Levitation of Plasma Protein-Coated Nanoparticles. *Cancers*, *13*(20), 5155.

Transdermal site-specific delivery of CD38-peptide-modified extracellular vesicles by microneedles for targeted therapy of extramedullary plasmacytoma

Yulin Cao [1#], Di Wu[2#], Qiubai Li[1*]
[1] Department of Rheumatology & Immunology, Union Hospital,Tongji Medical College, Huazhong University of Science and Technology, Wuhan, China
[2] Institute of Hematology, Union Hospital, Tongji Medical College, Huazhong University of Science and Technology, Wuhan, China

Abstract:
Extramedullary plasmacytoma (EMP) is characterized by the presence of monoclonal plasma cells outside the bone marrow and accounts for up to 30% of patients with multiple myeloma (MM). EMP has exceedingly poor outcomes in the era of novel drugs with a lack of site-specific targeted functions. Due to the unique physicochemical properties of extracellular vesicles (EVs), they have been becoming a promising drug delivery vehicle for targeted therapy of cancers. Here we use EVs derived from umbilical cord mesenchymal stem cells to be modified with polyethylene glycol and functionalized with addition of CD38 peptide for active targeting of EMP cells with CD38, a typical marker and therapy target of MM cells. Compared with native EVs, significantly more CD38-peptide-modified EVs were taken up by MM cells than CD38 negative cells. When loaded with doxorubicin, these modified EVs also significantly reduced MM cells more than native EVs in vitro. Dynamic distribution analysis following intravenous injection showed that these CD38-peptide-modified EVs are mostly intercepted in the lung and rarely arrived at the tumor site. Thus, we developed microneedle (MN), a novel noninvasive subcutaneous drug delivery method, as an active delivery system of our engineered EVs to the EMP site. These EVs reached the EMP site, were selectively taken up by the tumor cells and significantly reduced tumor burden (Figure 1). These findings highlight the attractive functions of our synergistic transdermal site-specific delivery device with our newly-engineered EVs for the active and efficient treatment of EMP and other cancers, with excellent toxicity and tolerability.

Keywords: Extramedullary plasmacytoma, CD38-peptide, extracellular vesicles, microneedle, targeting therapy.

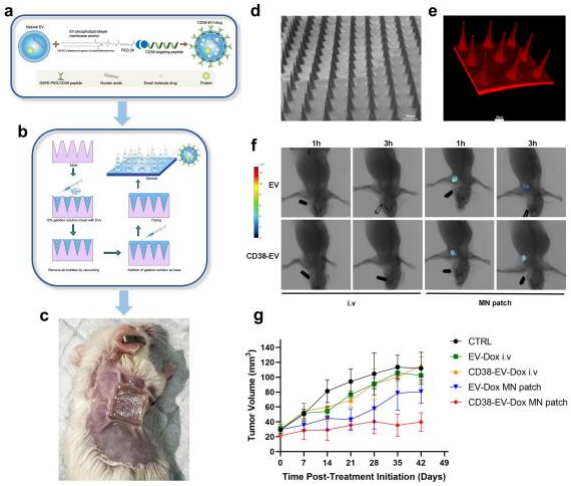

Figure 1: (a and b) Schematic illustration of the construction of CD38pep-targeted EVs loaded with drugs and the fabrication of the gelation MN patches embedded with CD38pep-targeted EVs. (c) Optical image of MNs loaded with engineered EVs to treat subcutaneous tumor implanted with multiple myeloma 8226 cell line. (d) SEM image of MN patches. (e) Scanning laser confocal image of PKH-26 staining MN patches. (f) Representative FMT images of the near-infrared fluorescence signals in tumor sites of mice at 1h and 3h from the four treatment group (DIR-EVs and DIR-CD38-EVs by intravenous injection and microneedles). (g) Tumor burden of mice treated with CD38-peptide-modified and doxorubicin-loaded EVs by i.v and MN patch.

References:

1. Rosiñol, L, et al. "Expert review on soft-tissue plasmacytomas in multiple myeloma: definition, disease assessment and treatment considerations." BRIT J HAEMATOL vol. 194, (2021): doi: 10.1111/bjh.17338
2. Di Rocco, G, et al. "Exosomes and other extracellular vesicles-mediated microRNA delivery for cancer therapy" TRANSL CANCER RES vol. 6, (2023): doi: 10.21037/tcr.2017.09.29

A role of Bi_2Se_3 topological insulator as electrodes in high-performance WSe_2 photodetector

Dajung Kim[1], Jimin Chae[1, †], Seok-Bo Hong[1], Jonghoon Kim[1], Gihyeon Kwon[1], Hoedon Kwon[1], Kwangsik Jeong[3], and Mann-Ho Cho[1,2, *]

[1] Department of Physics, Yonsei University, Seoul, 03722, Korea

[2] Department of System Semiconductor Engineering, Yonsei University, Seoul 03722, Korea

[3] Division of Physics and Semiconductor Science Dongguk University, Seoul 04620, Korea

Abstract:

In the development of photodetectors, great efforts have been made to select suitable materials to have high photoresponsivity and to improve interfacial contact characteristics using heterojunctions. Among elements constituting an optical device, an electrode forming an interfacial contact with a semiconductor plays an important role in the performance of an optical device because the interface between the electrode and the semiconductor determines the charge injection efficiency. Some of common metals or noble metals used as electrode materials cause serious charge scattering due to various defects and irregular surfaces, thereby reducing charge transport efficiency. The using topological insulators (TIs) with topologically protected Dirac surface states as electrodes is one powerful alternative with strengths in reducing scattering at the interface between semiconductor and electrode. In this study, the well-known TI Bi_2Se_3 with well-ordered interface structure was used as an electrode to improve the photosensitivity of WSe_2 in order to effectively utilize TSS and clear interface. In this study, using Bi_2Se_3 as a electrode of the WSe_2 channel, the photosensitivity was 11.47 A/W in a broadband wavelength from 450 nm to 1550 nm, which is up to 104 times higher than that of the WSe_2 photodetector using Au as the electrode. This value is the highest among 2D photodetectors, much higher than previous bulk WSe_2 photodetectors without gate voltage. Analysis using photoresponse and time-resolved photoluminescence (TRPL) as a function of thickness clearly confirmed that the presence of TSS affects the photoresponse enhancement. Hot carriers contribute to improving carrier separation with high carrier transfer efficiency, which affects photocurrent generation. In addition, it was confirmed through STEM that the van der Waals gap distance at the interface of Bi_2Se_3 was longer than that of the Au electrode, suppressing the hybridization state due to chemical interaction acting as a recombination point in DFT calculation. The role of TSS in efficiently separating eletron-hole pairs and suppressing the recombination point at the interface succeeds in generating ultra-high-speed and high-efficiency photocurrent in an optical device using a TI electrode. The role of TSS based on carrier dynamics may suggest important technologies for further applications in next-generation optoelectronic devices.

Keywords: topological insulator, photo detector, interfacial contact, topological surfacace state, photo device, photoresponsivity, detectivity, EQE

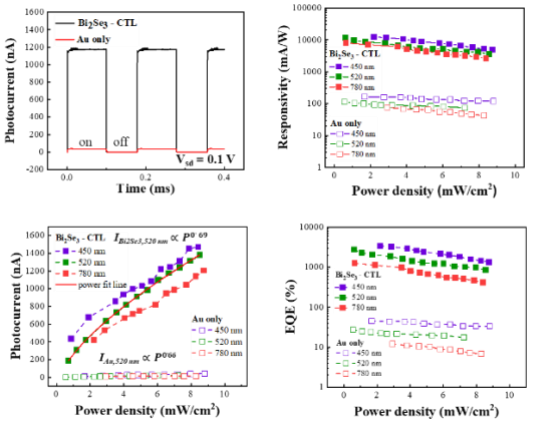

Figure 1: The phototransistor were illuminated by a laser with 520 nm wavelength (Power density = 6.24 mW/cm^2) and 0.1 ms pulse width. (red line is Au electrode device, black line is Bi_2Se_3 electrode device) Time-dependent photocurrent at V_{sd} = 0.1 V depending on power. According to power dependent photocurrent data is represented under the time-dependent photocurrent scheme about both of Au electrode and Bi_2Se_3 electrode phototransistor by wavelength. Also others are represented responsivity, EQE according to power intensity of each device.

References:

1. Jiandong Y., Zhanoqiang Z., Guowei Y., (2017) All-Layered 2D Optoelectronics: A High-performance UV-vis_NIR Broadband SnSe Photodetector with Bi2Te3

Topological Insulator Electrodes, *Advanced functional Materials*, 27,1701823
2. Mei Q., Qiuyun F., Liang Y., Wenbo P., Geng W., Zhiping Z., Wei L., (2019) A Bi_2Te_3 Topological Insulator as a New and Outstanding Counter Electrode Material for High-Efficiency and Endurable Flexible Perovskite Solar Cells, *ACS Applied Materials and Interfaces, 47868-47877*

Analysis on the Electro-Optical Properties of Quantum-Dot Light-Emitting Diodes based on Charge Transport Simulation

Y. Kim, S. Jung, J. Jo, S. Lee, J. Yang, S. Zhan, and J. M. Kim
Department of Engineering, University of Cambridge, Cambridge, United Kingdom

Abstract:
Quantum-dot light-emitting diodes (QD-LEDs) are emerging devices for next-generation displays and lighting, owing to their high color purity, color tunability, and excellent device performance. To design and optimize QD-LED devices, a quantitative understanding of charge carrier dynamics through computational charge transport simulations is required [1]. In this study, we analyzed the electro-optical properties of QD-LED devices using a computational charge transport simulation model that considers the electric field-dependent charge injection at interfaces and charge-capturing processes between quantum dots (QDs) [2, 3]. This simulation model includes all radiative and non-radiative combination processes, such as Langevin radiative recombination, Shockley-Read-Hall (SRH) recombination, and Auger recombination processes. Figure 1 illustrates the device structure used for charge transport simulations in QD-LED devices. A charge-balanced condition, in which the same densities of holes and electrons accumulate in the QD layer, is considered as an initial simulation setup. Under this charge-balanced condition, the effects of thickness, mobility, and conduction band energy level of the electron transport layer (ETL) have been investigated. Specifically, the simulation results for variations in ETL thickness are shown in Fig. 2. As illustrated in Fig. 2(a), a thicker ETL results in a weaker electric field within the QD layer due to a larger voltage drop across the ETL. This lower electric field leads to fewer charge carriers accumulating in the QD layer, as seen in Fig. 2(b). Consequently, devices with a thicker ETL exhibit lower brightness and current density (Fig. 2(c)), and the external quantum efficiency (EQE) curve peaks at a higher voltage (Fig. 2(d)). In conclusion, high-performance QD-LEDs can be achieved through device optimization based on the computational charge transport simulation employed in this study.

Keywords: QD, QD-LEDs, charge transport model, charge-capturing process, recombination process, ETL, electro-optical property.

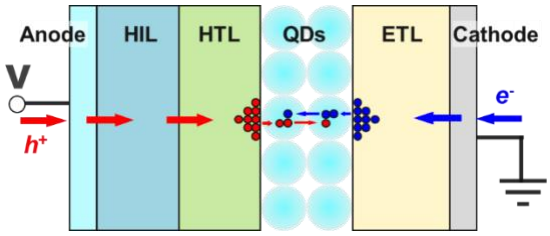

Figure 1: Schematic illustration of QD-LED device structure.

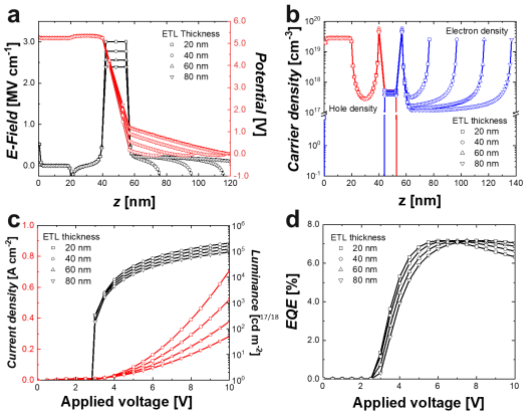

Figure 2: **a.** Simulated potential and electric field distribution across the QD-LED device for different thicknesses under the applied voltage of 6 V. **b.** Simulated distribution of hole and electron densities across QD-LED. **c.** Simulated luminance, current density curves, and **d.** EQE curves for the applied voltage.

References:

1. Kumar, B., Campbell, A. and Ruden, P. (2013) Modeling charge transport in quantum dot light emitting devices with NiO and ZnO transport layers and Si quantum dots, *J. Appl. Phys.* 114, 044507.
2. Jung, S., et al. (2021) Modelling charge transport and electro-optical characteristics of quantum dot light-emitting diodes, *npj Comp. Mat.* 7(1), 122.
3. Gao, X., and Yee, S. (1996) Hole capture cross section and emission coefficient of defect centers related to high-field-induced positive charges in SiO_2 layers, *Solid State Electron.* 39(3), 399-403.

Homogeneous Elongation of N-Doped CNTs on Nano-Fibrillated Hollow Carbon Nanofiber: Resolving Mass and Charge Imbalance in Asymmetric Supercapacitors

Taewoo Kim[1], Tae Hoon Ko[1], Kisan Chhetri[1], Hak Yong Kim[1, 2*]
[1] Department of Regional Leading Research Center, Jeonbuk National University, Jeonju, 54896 Republic of Korea
[2] Department of Organic Materials and Fiber Engineering, Jeonnbuk National University, Jeonju, 561–756 Republic of Korea

Abstract:
Manufacturing asymmetric supercapacitor (ASC) devices with a faradic cathode and a double-layer anode is a challenging task due to the large difference in capacitance values between the two electrodes, which results in a need for a significant amount of active anodic material to balance mass. To address this issue, a negative electrode with an ultrahigh capacitance is engineered. In this study, highly porous N-doped carbon nanotubes (CNTs) containing submerged Co nanoparticles are grown over nano-fibrillated electrospun hollow carbon nanofibers (HCNFs) using an in situ developed metal-organic framework (MOF)-based thermal treatment. The optimized CNT@HCNF-1.5 displays an exceptional capacitance of up to 712 F g^{-1} and excellent rate capability, which is the highest reported for any carbonaceous material so far. Using CNT@HCNF-1.5, symmetric supercapacitors (SSCs) and ASC devices are fabricated, which demonstrate exceptional performance in all aspects of SCs, including high energy density, long cycle life, and high rate capability. The SSC device has an energy density of up to 20.13 W h kg^{-1}, while the ASC device can reach up to 87.5 W h kg^{-1}, demonstrating excellent practical applicability.

Keywords: Carbon nanotubes; Hollow carbon nanofibers; Supercapacitors; Negative electrode materials

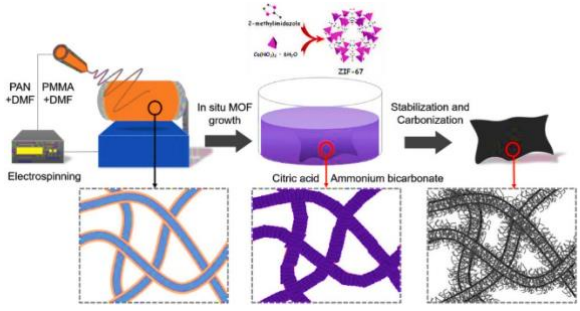

Figure 1: Figure illustrating of the fabrication technique of the CNT@HCNF-x electrode.

References:

1. Y. Zhu, S. Murali, M. D. Stoller, K. J. Ganesh, W. Cai, P. J. Ferreira, A. Pirkle, R. M. Wallace, K. A. Cychosz, M. Thommes, D. Su, E. A. Stach, R. S. Ruoff, Science 2011, 332, 1537.
2. K. Chhetri, S. Subedi, A. Muthurasu, T. H. Ko, B. Dahal, H. Y. Kim, J. Energy Storage 2022, 46, 103927.
3. N. Choudhary, C. Li, J. Moore, N. Nagaiah, L. Zhai, Y. Jung, J. Thomas, Adv. Mater. 2017, 29, 1605336.

Acknowledgments:
This work was supported by the National Research Foundation of Korea (NRF) grant funded by the Korea government (MSIT) (2019R1A5A8080326).

Cobalt Sulfide Hollow Spheres with Partial Selenium Surface Modification as an Efficient Bifunctional Oxygen Electrocatalyst for Rechargeable Zinc-Air Batteries

Tae Hoon Ko[1], Tae Woo Kim[1],Hak Yong Kim[1, 2*]
[1]Department of Nano Convergence Engineering, Jeonbuk National University, Jeonju 561-756, Republic of Korea
[2]Department of Organic Materials and Fiber Engineering, Jeonbuk National University, Jeonju 561-756, Republic of Korea
Corresponding Authors E-mail: khy@jbnu.ac.kr

Abstract:
The efficient, highly reactive, and long-lasting chemical energy conversion functions of metal-organic compound networks are envisioned as being provided by mesoporous hollow carbon nanostructures made primarily of an in situ-grown N-doped graphitic carbon matrix and embedded selenium-doped CoS_2 hollow spheres. Through the use of previously unattainable synthesis techniques, it is now possible to create a very porous conductive network at a tiny scale while simultaneously exposing abundant unsaturated reactive sites at the atomic level without compromising electrical or structural integrity. Outstanding bifunctional oxygen electrocatalysts for both oxygen reduction reaction (ORR) and oxygen evolution processes are provided by the porous framework, doping motifs, and customized structural flaws because of their inherent improved electrochemical surface area and electron transport (OER). Additionally, the outcomes of the DFT simulation demonstrate that Se doping can enhance Gn* on Co sites, increasing the inherent OER activity of Se-doped CoS_2. Due to its bifunctionality, the as-fabricated Znair battery device (Se doped MOF CoS_2 hollow spheres/Zn foil) has an appealing operating performance, outperforming the majority of previously published MOF based catalysts with a high discharge voltage of 1.20 V and a low charge voltage of 1.97 V (@ 5 mA cm^{-2}). Furthermore, a rechargeable zinc-air battery with outstanding discharge-charge performance and mechanical stability is successfully built employing this selenium-doped MOF CoS_2 hollow spherical electrode as the air cathode. This work offers a practical and universal method for building various functional linked metal-organic coordinated compounds, which may be used for a range of energy storage, conversion, and environmental applications. Examples include fuel cells and metal air batteries.

Keywords: Hollow spheres; Nanostructures,; Electrocatalysts; Mmetal-organic frameworks, and Zinc-air batteries

Phenothiazine-S,S-dioxide as a versatile compound in the synthesis of organic emitters

R. Butkute[1]*, F. Khan[2], M. Guzauskas[1], A. Dabulienė[1], M. Mahmoudi[1], D. Volyniuk[1], L. Skhirtladze[1], M. Stanitska[1], R. Misra[2], J. V. Grazulevicius[1]

[1] Department of Polymer Chemistry and Technology, Kaunas University of Technology, Kaunas, Lithuania

[2] Department of Chemistry, Indian Institute of Technology Indore, Indore, India

Abstract:

Organic electroactive compounds containing donor and acceptor moieties are recently widely studied as the components of optoelectronic devices and organic light emitting diodes in particular as well as in the different sensors [1,2]. In this presentation we report on the synthesis and properties of the derivatives phenothiazine-S,S-dioxide as potential materials for organic light emitting diodes (OLEDs) and UV sensors. The derivatives of tetraphenylethylene and the differently substituted phenothiazine-S,S-dioxides were obtained by the Suzuki cross-coupling reactions of the boronate ester of tetraphenylethylene with the appropriate bromo derivatives of phenothiazine-S,S-dioxides [3]. The compounds exhibited solid state induced emission enhancement and mechanochromic luminescence. Two compounds showed reversible switching of emission color by the virtue of conformational changes in the molecular structures. The derivatives were used as fluorescent emitters for host-free OLEDs which showed maximum external quantum efficiency of 2% and brightness of 10,000 cd/m2 [3]. Compounds exhibiting deep blue thermally activated fluorescence containing only typical electron accepting moieties with the different electron accepting abilities were obtained by simple two-step synthesis including nucleophilic substitution and oxidation with hydrogen peroxide [4]. The THF solution of the derivative of benzophenone containing phenothiazine-5,5-dioxide moieties showed green to blue emission color switching and strong fluorescence intensity enhancement by the factor of more than 60 under increase of UV excitation dose. The unusual photophysical properties of the derivative of benzophenone and phenothiazine-5,5-dioxide are attributed to the formation of different conformers.

References:

1. Steinegger A., Klimant I., Borisov S. M.. (2017) Purely Organic Dyes with Thermally Activated Delayed Fluorescence—A Versatile Class of Indicators for Optical Temperature Sensing, *Adv. Opt. Mater.*, 5, 1700372.
2. Liang X., Tu Z.-L., Zheng Y.-X. (2019), Thermally Activated Delayed Fluorescence Materials: Towards Realization of High Efficiency through Strategic Small Molecular Design, *Chem. Eur. J.*, 25, 5623 – 5642.
3. F. Khan, M. Mahmoudi, D. Volyniuk et al. (2022) Stimuli-Responsive Phenothiazine-S,S-dioxide-Based Nondoped OLEDs with Color-Changeable Electroluminescence, *J. Phys. Chem. C.*, 126, 15573−15586.
4. M. Guzauskas, E. Narbutaitis, D. Volyniuk, et al. (2021) Polymorph acceptor-based triads with photoinduced TADF for UV sensing, *Chem. Eng. J.*, 425, 131549.

Acknowledgements: This project has received funding from European Regional Development Fund (project No. 01.2.2-LMT-K-718-03-0019) under the grant agreement with the Research Council of Lithuania (LMTLT).

Modular Infrared Heater with Nanofluid Thermal Accumulation Collector - Unsteady Entropy Analysis

F. Alic
Department of Thermal and Fluid Technique, Faculty of Mechanical Engineering, University of Tuzla, Tuzla, Bosnia and Herzegovina

Abstract:
The heating of a body (heat target, HT) by thermal radiation is often accompanied by heat losses, caused by the scattering of thermal rays and by not hitting its surface. These losses occur in infrared heating of different rooms. The heat source, i.e. modular infrared heater, can change the output intensity of thermal radiation within various wavelength intervals. Although there are different combinations of modular infrared heaters with variations in power, and geometric position in relation to HT, in this paper one characteristic combination, is analyzed. By setting the HT on the surface of the nanofluid collector with nano-enhanced phase change material (N-E PCM), it enables the increase in the overall efficiency of this heating process. The nanofluid collector consists of a complex pipe element through which the nanofluid flows, and a collector inside which the thermal-accumulating N-E PCM is placed (Figure 1). According to their characteristics, infrared thermal rays heat only HT, while the heating of the ambient air through which they pass is negligible. Based on this fact, the accumulated heat inside the N-E PCM can be used for convective heating of the ambient air around the HT surface. This process reduces the convective heat dissipation from HT to the ambient air and increases the efficiency of the modular infrared heat source. Also, the accumulated heat inside the N-E PCM can be used for various technical applications. In this study, a mathematical model of the unsteady thermal entropy generation of the described heating system is established. By finding the unsteady thermal entropy, the next process of minimizing thermal irreversibility and maximizing the energy efficiency of the analyzed system is enabled. The volume fraction ratio of Al_2O_3 nanoparticles varies within the base fluid (water). Furthermore, the temperature of the infrared heaters varies as well as the volume fraction ratio of Al_2O_3 within the N-E PCM.

Keywords: infrared heater, thermal radiation, nanofluid, nano-enhanced phase change material, accumulation collector, unsteady entropy, unsteady energy efficiency.

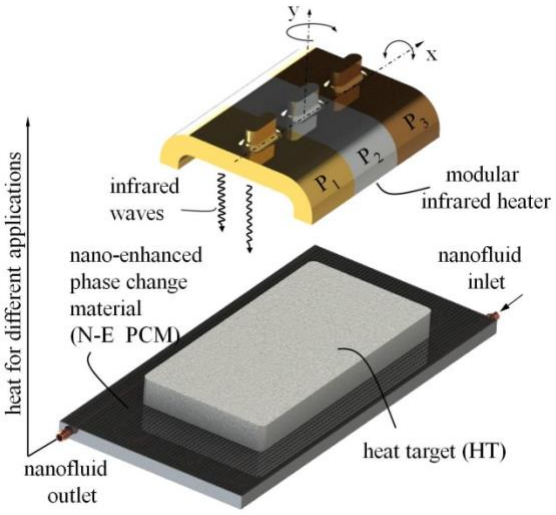

Figure 1: Figure representing modular infrared heating of the body by thermal radiation and accumulation of one part of it with the establishment of the following goals: to justify the installation of a nanofluid thermal-accumulation collector in order to minimize the dissipation of thermal energy of the heating infrared source, to determine how much the cross variation of the process variables of this heating system affects its overall thermal irreversibility and energy efficiency.

References:

1. Syeda, L.T, et al. (2020), Nanoparticles enhanced phase change materials (NePCMs)-A recent review, *Applied Thermal Engineering*, 176, 115305.
2. Alic, F. (2020), Entransy Dissipation Analysis and New Irreversibility Dimension Ratio of Nanofluid Flow Through Adaptive Heating Elements, *Energies.*, 13, 114.
3. Alic, F. (2019), The non-dimensional analysis of nanofluid irreversibility within novel adaptive process electric heaters, *Applied Thermal Engineering*., 152, 13-23.

Nanocarbons as additives to Mg-based hydrogen storage materials

E. Grigorova [1*], B. Tsyntsarski [2], P. Markov [1], P. Tzvetkov[1] and I. Stoycheva[2]
[1] Institute of General and Inorganic Chemistry, Bulgarian Academy of Sciences, Sofia, Bulgaria
[2]Institute of Organic Chemistry with Centre of Phytochemistry, Bulgarian Academy of Sciences, Sofia, Bulgaria

Abstract:
Nanoporous activated carbons are prepared by hydropyrolysis processing from precursors peach stones (PS) [1] and polyolefin wax (POW) a polyethylene production waste (Fig. 1). They are distinguished by high surface area and prevailing microporous structure. These properties determine their application as effective adsorbents for removal of organic and inorganic pollutants. Other application of these materials could be as additive for hydrogen storage materials. Carbon containing additives improve hydrogen absorption-desorption characteristics, because they hinder the oxygen back diffusion from the bulk to the surface and also prevents particles agglomeration during ball milling, which increases the accessibility of the surface for hydrogen. The obtained activated carbons and Ni or V are used as additives in the preparation of MgH_2-Ni-POW [2] and MgH_2-Ni-PS composites by ball milling under Ar. Structure and phase composition of obtained materials are monitored by XRD analyses and for MgH_2-Ni-POW after hydrogenation by TEM (TEM HR STEM JEOL JEM 2100). TEM characterization of these MgH_2- based materials is challenging, because of their sensitivity to oxidation and the high energy of the electron beam exposure, which could cause negative impact so the HRTEM and SAED are obtained by low beam current values. The SAED and HRTEM revelead that MgH_2-Ni-POW consists of mainly MgH_2, but also of Mg_2NiH_4 with orthorhombic and monoclinic structures and some traces of Mg, Ni and MgO and some graphitic structure areas. The hydrogen absorption capacity value is 5.3 wt. % at 300^0C and 1 MPa for Ni and POW containing sample and about 4 wt. % for the other one with V and PS. The nanoporous carbon derived from POW has more pronounced positive effect on absorption kinetics of MgH_2, because of its higher pore volume and specific surface area. Using nanocarbons from biomass and a polyethylene production waste in combination with Ni and V, as additives to MgH_2, lead to the production of hydrogen storage materials with high capacity and improved kinetics.

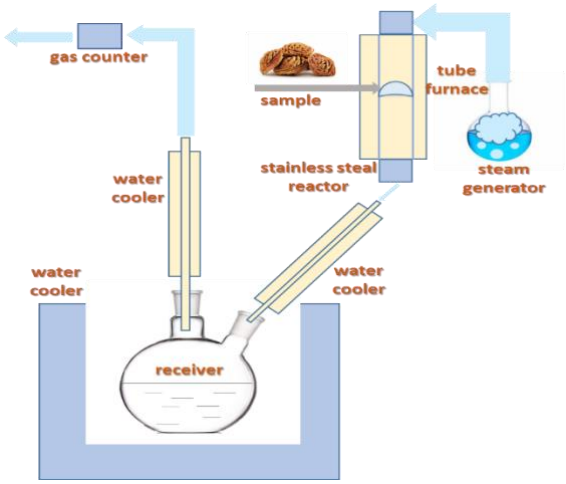

Figure 1: Figure illustrating equipment for pyrolysis and hydro-pyrolysis procedures for synthesis of nanocarbons.

Keywords: nanocarbons, sorption, hydrogen storage, Mg-based hydrides, TEM analyses.

References:

1. Tsoncheva, T., Mileva, A., Tsyntsarski, B., Paneva, D., Spassova, I. Kovacheva, D., Velinov, N., Karashanova, D., Georgieva, B., Petrov, N. (2018), Activated carbon from Bulgarian peach stones as a support of catalysts for methanol decomposition, Biomass and Bioenergy, 109, 135-146.
2. Grigorova, E., Nihtianova, D., Tsyntsarski, B., Stoycheva, I. (2020), Investigation of hydrogen storage characteristics of MgH_2 based materials with addition of Ni and activated carbon, *Inorganics*, 8, Article № 12.

Acknowledgements: The authors thank to Bulgarian Ministry of Education and Science-National science fund (Project DFNI-КП-06-H27/9,08/12/2018) and part of experiments were performed with equipment included in the National Infrastructure NSI ESHER (NI SEVE) under grant agreement № DO1-161/28.07.22.

Green Hydrogen from Sunlight via Plasmon Enhanced Photocatalysis

L. Steinmüller, T. Walter
Innovent e.V, Jena, Germany

Abstract:
The interest in hydrogen as a sustainable energy source and base chemical is increasing and solar photocatalysis for water splitting represents a promising approach to meet this demand. TiO_2 is an known photocatalyst for facilitating the hydrogen evolution reaction (HER) and several modifications are currently researched. Among others, the combination of TiO_2 with gold nanoparticles increases the catalytic activity due to the formation of a Schottky barrier as well as the plasmonic properties of the nanoparticles[1].
While extensive research on those combined photocatalysts has been done under lab conditions, solar water splitting needs to be transferred to the large scale. For this purpose, the catalyst can be applied as a functional coating on elements that can then be incorporated into water splitting devices. The present work explores the application of TiO_2 coatings using CCVD and rCCVD[2] as well as electrospinning and the resulting properties of the coatings.
Both CCVD and rCCVD give rough coatings with a high surface area, which is generally beneficial for catalytic processes. As both techniques make use of different precursors, they produce coatings of different thickness, porosity and stability. rCCVD yields thicker and more stable coatings than CCVD, but requires a more complex and costly setup. A catalytic activity of the coatings under solar irradiation has been demonstrated, especially for coatings that have been further post-annealed at 450°C. Using, electrospinning, TiO_2 particles were incorporated into polymer fibers that exhibit a catalytic activity as well.
These results suggest that rCCVD could be a suitable technique for the large-scale fabrication of TiO_2-coated surfaces. However, for all techniques introduced, a further optimization is required. In particular, the combination with gold nanoparticles on a CCVD or wet chemical route is pursued. With a stable and highly effective catalyst coating, the solar HER can be moved toward the industrial scale.

Keywords: coating, combustion chemical vapour deposition, electrospinning, physical vapour deposition, photocatalysis.

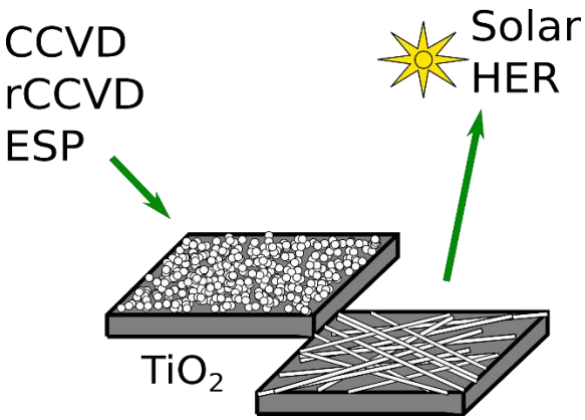

Figure 1: Schematic representation of the coatings applied with CCVD/rCCVD and electrospinning (ESP)

References:

(1) Seh, Z. W.; Liu, S.; Low, M.; Zhang, S.-Y.; Liu, Z.; Mlayah, A.; Han, M.-Y. Janus Au-TiO2 Photocatalysts with Strong Localization of Plasmonic Near-Fields for Efficient Visible-Light Hydrogen Generation. *Adv. Mater.* **2012**, *24* (17), 2310–2314. https://doi.org/10.1002/adma.201104241.
(2) Zunke, I.; Kretzschmar, B. S. M.; Heft, A.; Schmidt, J.; Schimanski, A.; Grünler, B. Flame Pyrolysis—a Cost-Effective Approach for Depositing Thin Functional Coatings at Atmospheric Pressure. In *Handbook of Modern Coating Technologies*; Aliofkhazraei, M., Nasar, A., Chipara, M., Laidani, N., De Hosson, J. Th. M., Eds.; Elsevier, 2021; pp 139–179. https://doi.org/10.1016/B978-0-444-63240-1.00006-1.

Enhancement of Electric Field Intensity by Plasmon Coupling between Ag Film and Gold Nanoparticles

J. -H. Jang [1], H. Y. Lee [1,2], J. -H. Ryu [1,2], J. -Y. Lee [1,2], S. -H. Kim [1,2], S. -L. Hwang [3], H. S. Ahn [1], Y. T. Chun [1], S. N. Yi [1,2 *]

[1] Major of Nano-Semiconductor Engineering, Korea Maritime & Ocean University, Busan, South Korea

[2] Interdisciplinary Major of Maritime AI Convergence, Korea Maritime & Ocean University, Busan, South Korea

[3] Department of ICT Convergence Engineering, Kangnam University, Yongin, South Korea

Abstract:

For the first time, Our research group fabricated a light pressure electric generator(LPEG), a device that converts the kinetic energy of radiation pressure into electrical energy using the particle nature of electromagnetic waves. In order to amplify the very low radiation pressure of the sun, the intensity of the electric field was amplified according to $P = |E|^2/c^2\mu_0$ through surface plasmon resonance(SPR) at the Ag film. In this study, we amplified the intensity of the electric field through plasmon coupling by combining gold nanoparticles(AuNPs) with LPEG.[1] AuNPs, which can act as nanoantennae, can absorb incident light and greatly enhance the strength of the electric field by combining with Ag film's propagating surface plasmon(PSP). Therefore, the amplified electric field is converted into pressure that can cause deformation of the PZT layer, which is a piezoelectric material, and electricity can be produced by the piezoelectric effect (Figure 1). We performed FDTD simulation to confirm the electric field distribution amplified through plasmon coupling at the Ag film and AuNPs interfaces, and COMSOL Multiphysics simulation was conducted to confirm the effect of the amplified electric field on the piezoelectric material. In addition, to compare with the simulation results, the piezoelectric and electrical characteristics were analyzed using a chargemeter and a solar simulator(AM 1.5G) (Figure 2). As a result, a power density of 642.7 $\mu W/cm^2$, which is 86.5% higher than the previous one, was obtained.

Keywords: light pressure, electric generator, PZT, gold nanoparticles(AuNPs), plasmon coupling, FDTD simulation, COMSOL Multiphysics, chargemeter, solar simulator

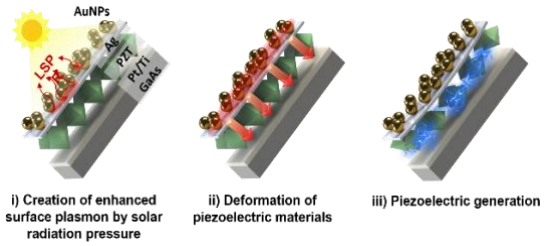

Figure 1: Mechanism schematic of LPEG coupled with AuNPs.

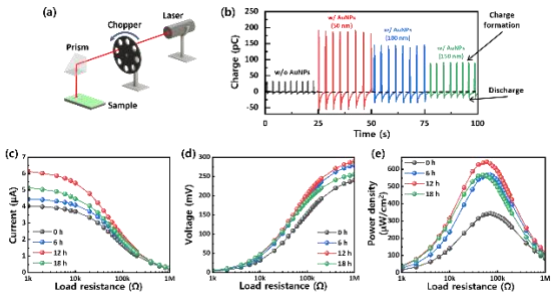

Figure 2: (a) Schematic diagram of the electrical output measurement. (b) The behavior of charge formation and discharge with different size of AuNP. Measured output (c) current, (d) voltage, and (e) calculated power density under different load resistance varying 1 kΩ to 1 MΩ for LPEG coupled with self-assembled AuNPs with various incubating times.

References:

1. H. Y. Lee, M. S. Kwak, G.-T. Hwang, H. S. Ahn, R. A. Taylor, D. H. Ha, S. N. Yi, (2023), Direct Current Piezoelectric Energy Harvesting Based on Plasmon-Enhanced Solar Radiation Pressure, *Adv. Optical Mater*, 11, 2202212

Acknowledgments

This work was supported by Korea Institute for Advancement of Technology(KIAT) grant funded by the Korea Government(MOTIE)(P0012451, The Competency Development Program for Industry Specialist)

Evaluation of quality of patterns for printed electronics by measuring printability

Chung-Hwan Kim[1 *], Ha Kyung Park[1]
[1] Chungnam National University, Daejeon, South Korea

Abstract:
Pinted electronics has been remarked as a novel technology useful to manufacture flexible devices such as flexible displays, lightings, energy devises, and wearable devices, etc. It is most important to garantee high reliability and productivity for the commercialization of the flexible electronics products. The printed electronics devices consist of various patterns by printing technologies such as inkjet, gravure, screen, etc. and consequently the performance and productivity of devices are strongly affected by the printability of printed patterns. International Electrotechnical Commission (IEC) defines printability as 'The measurements or requirements of both the qualities of printed patterns and the reproducibility of printing designs as the result of interaction of printing media, inks, substrates, and environmental conditions[1]'. As shown in this definition, printability is very important concept to measure the quality of the printed patterns and consequently to determine the performance, yield rate, and reliability of the devices. Therefore, the international standards to measure and evaluate the printability of printed patterns have been[2][3][4] or being established by TC119 which is the technical committee for printed electronics in IEC. Although the individual international standards to measure the printability of the patterns such as measurement method for pattern width, voids, waviness have been established, the integrated system to measure and evaluate the printability of the patterns has not been established. In this study, the integrated S/W to evaluate the quality of printed patterns by measuring printability of the patterns was developed based on the existing international standards(Figure 1). As the measurement objects of printability, the variation of area, dimensions, and the ratio of voids were selected. The pass or fail of patterns is dependent on the pre-set criteria which can be determined by users or customers. The developed system was applied to the actual printed patterns and it was verified that the developed system can be appropriate to measure and evaluate the printability of the printed patterns. The system will be very useful in the industrial fields to evaluate and manage the reliability and quality of the printed electronics devices at the pattern level from the view point of printability.

Keywords: prited electronics, printability, printed pattern, international standard.

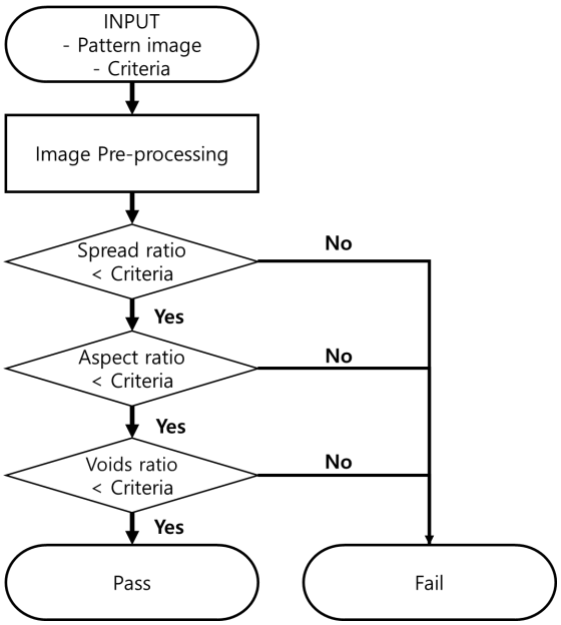

Figure 1: Figure illustrates the evaluation alrorigm of quality of printed electronics patterns by measuring printability of patterns for spread ratio, aspect ratio, and voids ratio.

References:

1. IEC, 2022, retrieved from https://www.iec.ch/dyn/www/f?p=103:22:509769971963736:::FSP_ORG_ID,FSP_LANG_ID:8679,25
2. IEC. IEC 62899-402-1:2017
3. IEC. IEC 62899-402-2:2020
4. IEC, IEC 62899-402-3:2021

Polymeric Enhanced Membranes for Photocatalytic Degradation of Organic Contaminants

A.C.W.E. Santo[1]; L.L.S. Silva[1]; A.M.F. Linhares[2]; C.P.Borges[2]; F.V. Fonseca[1]
[1] School of Chemistry, Federal University of Rio de Janeiro, Rio de Janeiro, Brazil
[2] COPPE, Federal University of Rio de Janeiro, Rio de Janeiro, Brazil

Abstract:
Recalcitrant organic contaminants is a growing challenge in the water treatment field since conventional tretaments are not suitable to remove them. Thus, the use of technologies that are capable to generate hydroxyl radicals (·OH) to promote a high efficient degradation, such as the Fenton process and Photocatalysis, are utlimost important. Other technology indicated is Membrane Separation Process (MSP), which allows the removal of such contaminants through selective membranes[1]. In order to increase the efficiency of both processes, Advanced Oxidative Process (AOP) and MSP can be combined by the impregnation of nanoparticles in polymeric membranes to build a hybrid process[1]. In this sense, the current study aims to analyzek and compare the degradation of dyes by MSP/AOP hybrid process using polymeric membrane functionalized with Fe^0 (nZVI) and TiO_2 nanoparticles. First, Drimaren Red (DR) dye was used as a model contaminant to verify the best operating conditions of this new process. In the MSP/AOP system the membrane cell allows UV-254nm radiation (24 W, 2833 $\mu W/cm^2$) onto the surface of the catalityc material through a quartz plate[2]. During the experiments, aliquots were withdrawn at specific times from the permeate for DR and flow analysis. Results showed that in the case of the nZVI membranes, the process without UV light achieved 30% of DR removal after 1 h of operation, while with the addition of UV radiation it increased significantly, reaching 43% after the same period. On the other hand, by applying TiO_2 functionalized membranes, DR removal raised to 67%, achieving 85% removal after 2 h of operation (Figure 1), indicating the high effectiveness of the hybrid process with TiO_2 nanoparticles. The permeate flux remained stable in the dark condition and nZVI membranes (0.21± 0.01 L/min), while the test with UV-254nm there was an increase from 0.14 to 0.47 L/min after 2 h, which can be explained by the attack of the radiation to the polymer chains of the membrane. In the case of membranes with TiO_2 it was noted that the flow remained the same during the experiment (~0.49 ± 0.06 L/min) proving the efficiency of these nanoparticles in protecting the surface of the membranes.

Keywords: AOP, fotocatalysis, Drimaren Red, membranes, water treatment, nanoparticle, iron, titanium.

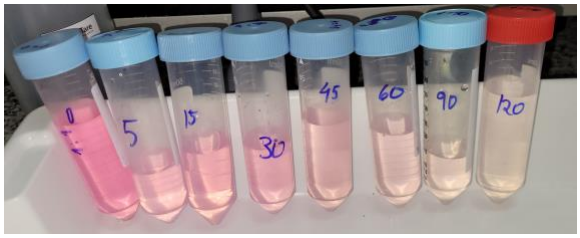

Figure 1: Figure illustrating the removal of dye by a hybrid MSP/AOP system.

References:

1. Novel materials for environmental remediation applications: Adsorption and Beyond. Oxford, Elsevier. 2023.
2. Silva L, A. Caldara J, Maria Rocco A, P. Borges C, V. Fonseca F. Evaluation ofNano Zero-Valent Iron (nZVI) Activity in Solution and Immobilized in Hydrophilic PVDF Membrane for Drimaren Red X-6BN and Bisphenol-a Removal in Water. Processes. 2019; 7(12):904.

Design of Metal-Organic Frameworks-based composites for visible-light-driven heterogeneous photocatalysis

K. Dassouki, S.Dasgupta, E. Dumas and N. Steunou
Institut Lavoisier de Versailles, UMR CNRS 8180, Université de Versailles St Quentin en Yvelines, Université Paris Saclay, 78035 Versailles, France

Abstract:
The design of highly performing and cost-effective photocatalytic platforms is highly challenging. Ti^{4+} based MOFs have sparked a great interest for (photo)catalysis due to their chemical stability and redox properties. Moreover, they represent an ideal platform for hosting catalytically active species. This project thesis deals with the design of novel photocatalysts by combining chemically stable MOFs (Ti^{4+} and Zr^{4+} MOFs) with Cu based co-catalysts. These materials were characterized by multiple advanced techniques and their catalytic properties are currently studied.

Keywords: *Ti-MOFs, Zr-MOFs, heterogeneous photocatalysis, Cu based co-catalysts.*

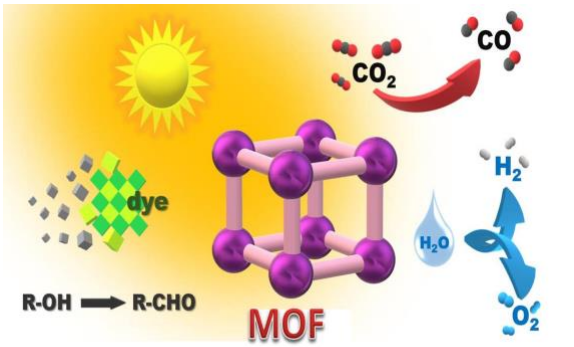

Figure 1: Schematic representation of photocatalytic reactions catalyzed by MOFs.

References:

1. Vilela, S.M.F., Salcedo-Abrairam, P., Colinet, I., Salles, F., Martijn, C. de Koning, M. C. de., Joosen, M. J. A., Serre, C., Horcajada, P., (2017) Nanometric MIL-125-NH_2 Metal-Organic Framework as a Potential Nerve Agent Antidote Carrier. *Nanomaterials*. 7, 321
2. DeStefano, M. R., Islamoglu, T., Garibay, S. J., Hupp, J. T., Farha, O. K., (2017) Room-Temperature Synthesis of UiO-66 and Thermal Modulation of Densities of Defect Sites. *Chem Mater*. 29, 1357
3. Ejsmont, A., Jankowska, A., Goscianska, J., (2022) Insight into the Photocatalytic Activity of Cobalt-Based Metal–Organic Frameworks and Their Composites. *Catalysts*. 12, 110

SETCOR
Conferences & Exhibitions